

IONIC SURFACTANT SYSTEMS FOR EOR APPLICATIONS IN HIGH-  
TEMPERATURE SHALE RESERVOIRS

A Thesis

by

OLUWATOBILOBA OLUWAFIKEMI DEBORAH ADEBISI

Submitted to the Graduate and Professional School of  
Texas A&M University  
in partial fulfillment of the requirements for the degree of

MASTER OF SCIENCE

Chair of Committee,	David Schechter
Committee Members,	Bryan Maggard
	Mark Everett
Head of Department,	Jeff Spath

December 2021

Major Subject: Petroleum Engineering

Copyright 2021 Oluwatobiloba Adebisi

## ABSTRACT

Previous experimental studies and limited field results have shown that the application of surfactants can be effective in improving recovery from unconventional liquid-rich reservoirs. Most of these studies and field applications have been conducted at temperatures below 200°F. The application of surfactants for EOR has not been evaluated at higher temperature conditions. However, many of the potential EOR candidates in the lower 48 are reservoirs that have temperatures greater than 200°F. For instance, temperatures greater than 320°F in the Eagle Ford liquid-rich window have been reported. Therefore, this study aims to design surfactant systems that are thermally stable and effective for high-temperature EOR applications in shale reservoirs.

This study provides a complete workflow for surfactant selection for high-temperature EOR applications and presents guidelines for designing surfactant systems for these high-temperature conditions. Single ionic surfactant systems, as well as novel blends of ionic surfactants, were evaluated. The behavior of the different ionic surfactant systems was investigated through contact angle (CA) and interfacial tension (IFT) measurements for a wide range of temperatures up to 350°F and pressures of up to 5000 psia. These measurements were performed with crude oil and oil-saturated rock samples obtained from a high-temperature Eagle Ford reservoir. Surfactant systems that were effective in altering wettability favorably at high-temperature conditions were further evaluated by Surfactant Assisted Spontaneous Imbibition in order to quantify their impact

on improving oil recovery. Surfactant aqueous stability, time stability, and solubility were also investigated.

CA and IFT measurements reveal that temperature has a significant impact on the effectiveness of surfactant systems. At low-temperature conditions, some ionic surfactants were effective in altering wettability favorably. However, at increased temperatures, ionic surfactants showed limitations in altering the wettability favorably above a certain temperature limit tagged the ionic surfactant temperature limit (ITL). To ensure the applicability of surfactants at high-temperature, the ITL has to be above the reservoir temperature. Means of improving the ITL, as well as designing surfactants with higher ITL, became the paramount objective. Furthermore, it was revealed that the use of higher surfactant concentration and higher salinity systems improved the ITL, thereby making surfactant systems more effective for high-temperature applications. Optimal surfactant molecular structures to improve the ITL of the surfactant system are described. Novel co-surfactants systems, which are blends of cationic and zwitterionic surfactant systems, showed the most promising results for high-temperature applications with recovery factors up to 22.6% OOIP.

This study establishes a foundation in understanding the behavior of surfactant molecules at high-temperature conditions and unlocks the potential for improving oil recovery significantly in high-temperature unconventional reservoirs.

## DEDICATION

To my family, my friends, and my loved ones.

## ACKNOWLEDGEMENTS

I would like to express my immense gratitude to my committee chair, Dr. Schechter, for his guidance and support. Thank you for taking a chance on me and giving me the opportunity to be a part of this world-class research group.

I am also grateful to ConocoPhillips for sponsoring this project and providing the resources for this work. Their interest and contribution to this research were pivotal for its success.

I am very grateful to my committee members, Dr. Maggard and Dr. Everett, for their support and contribution throughout this research.

My special gratitude to I Wayan Rakananda Saputra, who always answered my numerous questions and pointed me in the right direction. I found his insights, knowledge, and wealth of ideas invaluable during my research program.

I would like to thank Stefano Taligeferi for his contributions in ensuring the success of my experiments and research. I am also very grateful to my other colleagues in Dr. Schechter's research group for making the overall experience an interesting one.

## CONTRIBUTORS AND FUNDING SOURCES

### **Contributors**

This work was supervised by a thesis committee consisting of Professor David Schechter and Professor Maggard of the department of Petroleum Engineering and Professor Everett of the Department of Geophysics.

All work conducted for this thesis was completed by the student independently.

### **Funding Sources**

Graduate study was supported by a research assistantship from Harold Vance Department of Petroleum Engineering and Texas Engineering Experimental Station (TEES) at Texas A&M University.

The student was funded by ConocoPhillips through the period of this study.

## NOMENCLATURE

BOPD	Barrels of oil per day
Ca	Capillary number
CA	Contact angle
CT	Computed tomography
COBR	Crude oil/brine/rock
d	Days
DAC	Dimethyl Amine Chloride
DI	De-Ionized
EO	Ethylene oxide
EOR	Enhanced oil recovery
gpt	Gallon per thousand gallons
h	Hours
IFT	Interfacial tension
IOS	Internal Olefin Sulfonate
mN/m	Millinewton per meter
OOIP	Original oil in place
$P_c$	Capillary pressure
POS	Propylene oxide Sulfate
SARA	Saturates, Aromatic, Resin and Asphaltenes
SASI	Surfactant-Assisted Spontaneous Imbibition
RF	Recovery Factor

TAC	Trimethyl Amine Chloride
TOC	Total Organic Content
TDS	Total dissolved solids
ULR	Unconventional liquid-rich reservoir
USBM	U.D. Bureau of Mines
wt. %	Weight percent
°	Degrees
°F	Degrees Fahrenheit



# TABLE OF CONTENTS

	Page
ABSTRACT .....	ii
DEDICATION .....	iv
ACKNOWLEDGEMENTS .....	v
CONTRIBUTORS AND FUNDING SOURCES.....	vi
NOMENCLATURE.....	vii
TABLE OF CONTENTS .....	ix
LIST OF FIGURES.....	xi
LIST OF TABLES .....	xvi
1 INTRODUCTION.....	1
1.1 Research objectives and overview.....	6
1.2 Thesis organization.....	7
2 LITERATURE REVIEW .....	9
2.1 Wettability of a rock surface .....	9
2.1.1 Methods of estimating wettability.....	12
2.1.2 Contact Angle.....	14
2.2 Interfacial Tension.....	15
2.3 Spontaneous imbibition .....	16
2.4 Surfactants and wettability alteration .....	20
2.4.1 Types of Surfactants.....	20
2.4.2 Nonionic Surfactants and Cloud point Limitation .....	23
2.4.3 Mechanism of Surfactant Operation .....	25
2.4.4 Surfactant Concentration.....	29
2.5 Surfactant Assisted Spontaneous Imbibition (SASI).....	30
2.6 Parameters for Surfactant EOR .....	36
2.6.1 Salinity .....	36
2.6.2 Temperature .....	39
2.6.3 Co-surfactants.....	40
3 METHODOLOGY .....	44

3.1	Rock and oil properties .....	46
3.1.1	Rock Sample .....	46
3.1.2	Rock cleaning and aging .....	47
3.1.3	Oil Sample Properties.....	49
3.1.4	Oil Sample Preprocessing .....	52
3.2	Fluid system properties.....	52
3.2.1	Surfactant Properties .....	52
3.2.2	Brine Properties.....	54
3.2.3	Aqueous phase stability.....	55
3.2.4	Surfactant and rock damage .....	60
3.3	Contact angle and IFT measurements.....	62
3.3.1	LPT CA and IFT Measurements .....	62
3.3.2	HPHT CA and IFT measurements .....	64
3.4	Spontaneous Imbibition Experiments.....	66
4	TIME STABILITY OF SURFACTANT SYSTEMS.....	71
4.1	Time stability of ionic and nonionic surfactant systems .....	72
4.2	Effect of salinity on time stability .....	76
4.3	Effect of ionic surfactant head group charge.....	81
5	WETTABILITY ALTERATION AND IFT REDUCTION BY SURFACTANT	85
5.1	Contact angle results.....	85
5.1.1	Effect of preservation on rock wettability.....	85
5.1.2	Aging of rock chip samples.....	87
5.1.3	Surfactant selection study.....	91
5.1.4	LPT CA Results .....	92
5.1.5	HPHT CA Results .....	104
5.2	Interfacial tension results.....	126
5.2.1	LPT IFT results .....	126
5.2.2	HPHT IFT results .....	130
6	SPONTANEOUS IMBIBITION EXPERIMENTS .....	149
6.1	Impact of CA and IFT on Capillary Pressure ( $P_c$ ).....	150
6.2	Oil recovery from SASI experiments .....	151
6.3	CT Scan Images and Results .....	139
7	CONCLUSIONS .....	160
	REFERENCES.....	164

## LIST OF FIGURES

	Page
Figure 1: Chemical EOR Methods for unconventional reservoirs .....	4
Figure 2: Schematic of oil drop contact angle indicating (a) water-wet (b) oil-wet wettability conditions.....	15
Figure 3: Amphiphilic structure of different types of Surfactants. ....	21
Figure 4: Schematic for the suggested mechanism for the wettability alteration caused by ion-pair formation ( adapted from Standnes and Austad, 2000b).....	31
Figure 5: Workflow chart for ionic surfactant studies. ....	45
Figure 6: Mineral composition of Eagle Ford rock sample (Sample depth: 14,049ft to 14,050ft).....	47
Figure 7: Schematic of the Dean-Stark apparatus for core plug cleaning (left) and the pressurized saturation vessels and pumps (right).....	49
Figure 8: SARA composition of crude oil sample. ....	50
Figure 9: Anton-Paar DMA 4100M for measuring density. ....	51
Figure 10: Molecular structure of surfactant head groups. ....	54
Figure 11: Images of (I) clear and (II) turbid brine samples. ....	57
Figure 12: Images of unstable (I and II) and stable (III) surfactant solutions.....	58
Figure 13: Aqueous phase stability of anionic surfactants (A-1, A-2, A-3, A-4, and A-5) at 72°F at concentration 0.2 wt.% in DI, brine A, and brine 1E. (Green color represents stable mixture. Red color represents an unstable mixture).....	60
Figure 14: Rock chips retrieved from C-5 solution at a) 72°F b) 200°F.....	61
Figure 15: pH of ionic surfactants at 0.2 wt.% concentration.....	61
Figure 16: Dataphysics OCA Pro Apparatus for LPT CA and IFT measurements. ....	63
Figure 17: Images recovered from 1) CA and 2) IFT measurements. ....	64

Figure 18: Biolin Theta apparatus for HPHT CA and IFT measurements.....	66
Figure 19: Set-up for HPHT SASI experiments.....	68
Figure 20: HPHT core holder cell for spontaneous imbibition experiments. ....	68
Figure 21: Toshiba Aquilion TSX-101A CT-scan equipment.....	70
Figure 22: Time stability behavior of ionic and nonionic surfactants. CA versus time results for the base case and surfactants C-1, A-1, and N-1. ....	75
Figure 23: Timelapse of CA images showing time stability behavior in ionic and nonionic surfactants. ....	75
Figure 24: $\Delta CA_m$ ( y-axis) versus time (x-axis) for C-1 at different surfactant concentrations (0.02 wt.% - Blue color, 0.1 wt.%- Red color, and 0.2 wt.% - Green color) in varying salinity aqueous phases (Brine TDS on x-axis) (0% - DI, 0.2% - brine A, 6% -brine 1C, 12% - brine 2C, 12% - brine 3C).....	80
Figure 25: $\Delta CA_m$ ( y-axis) versus time (x-axis) for A-1 at different surfactant concentrations (0.02 wt.% - Blue color, 0.1 wt.%- Red color, and 0.2 wt.% - Green color) in varying salinity aqueous phases (Brine TDS on x-axis) (0% - DI, 0.2% - brine A). ....	83
Figure 26: $\Delta CA_m$ ( y-axis) versus time (x-axis) for C-1 (blue color) and A-1 (red color) at different surfactant concentrations (y-axis - 0.02 wt.%, 0.1 wt.%, and 0.2 wt.%) in varying salinity aqueous phases (Brine TDS on x-axis) (0% - DI, 0.2% - brine A, 6% -brine 1C, 12% - brine 2C, 12% - brine 3C).....	84
Figure 27: CA of preserved chips measured at 72°F (left) and 170°F (right) indicate water-wetness.....	87
Figure 28: Changing CA values over an aging time of 8 weeks for different sets of rock chips measured in DI and brine B at temperatures of 72°F and 170°F. ....	89
Figure 29: Standard deviation of measured contact angle values for set 1 rock chips during the aging process in DI and brine B at 72°F and 170°F. ....	91
Figure 30: Wettability alteration by ionic surfactants for rock chip sets (a) 1 and (b) 3. ....	94
Figure 31: Contact angles of surfactants C-2 and Z-1 blends in brine A at 170°F. Corresponding CA images are displayed below each bar.....	96
Figure 32: Contact angles of surfactants C-6 and Z-1 blends in brine A at 170°F. Corresponding CA images are displayed below each bar.....	97

Figure 33: Contact angles of surfactants C-1 and Z-1 blends in brine A at 170°F. Corresponding CA images are displayed below each bar.....	98
Figure 34: Co-surfactant system C-2:Z-1 at combination ratios 1:3, 3:2, and 2:3 evaluated at varying total surfactant concentrations. ....	101
Figure 35: Surfactants C-1, A-1, Z-1, and C-2:Z-1(1:3) at concentration 0.2 wt.% evaluated at varying salinity conditions.....	103
Figure 36: Contact angle results for surfactants C-1 and C-5 at 0.2 wt.% concentration in brine A at high-temperature conditions. ....	106
Figure 37: Contact angle images and values for surfactant C-5 at 0.2 wt.% concentration in brine A at high-temperature conditions. ....	107
Figure 38: Contact angle images and values for surfactant C-5 at 0.2 wt.% concentration in brine A at high-temperature conditions. ....	108
Figure 39: Contact angle results for surfactants A-1 and A-3 at concentrations 0.2wt% in brine A. CA values are initially water-wet (44.5° for A-1 and 31.6° for A-3). The system becomes oil-wet within the first 13 minutes.....	109
Figure 40: Contact angle results for co-surfactants C-2:Z-1 at combinations 3:1 and 1:3 at a total concentration of 0.2 wt.% at high-temperature conditions. ....	112
Figure 41: Contact angle images and values for co-surfactants C-2:Z-1 at combinations 3:1 and 1:3 at a total concentration of 0.2 wt.% in brine A at high-temperature conditions.....	113
Figure 42: Contact angle results for surfactants C-1 at concentrations 0.2 wt.%, 0.4 wt.%, and 0.6 wt.% evaluated at high-temperature conditions. Higher surfactant concentrations more suitable for high-temperature applications. .	115
Figure 43: Contact angle results for co-surfactants C-2:Z-1 at combination 1:3 at total concentration of 0.2 wt.% and 0.4 wt.% and combination 2:3 at total concentration of 0.4 wt.% evaluated at high-temperature conditions.....	117
Figure 44: HPHT contact angle data for C-2:Z-1_1:3 0.4 wt.% surfactant in brine A. CA observed to be water-wet up to 355°F.....	118
Figure 45: Contact angle images and values for co-surfactants C-2:Z-1 at combination 2:3 at a total concentration of 0.4 wt.% in brine A at high-temperature conditions. CA observed to be water-wet up to 333°F.....	119

Figure 46: Contact angle results for surfactant C-1 at a concentration of 0.2 wt.% in brine A (0.2% TDS), brine 1D (1% TDS), and brine 2D (2% TDS) evaluated at high-temperature conditions. .... 120

Figure 47: Contact angle results for co-surfactants C-2:Z-1 at combination 1:3 at a total concentration of 0.2 wt.% in brine A (0.2% TDS), brine 1D (1% TDS), and brine 2D(2% TDS) evaluated at high-temperature conditions. .... 122

Figure 48: Contact angle images and values for co-surfactants C-2:Z-1 at combination 1:3 at a total concentration of 0.2 wt.% evaluated at high-temperature conditions. Contact angles observed to be water-wet up to 320 °F. .... 123

Figure 49: IFT results for different ionic surfactants at varying concentrations evaluated at LPT conditions. .... 128

Figure 50: IFT results for co-surfactants C-1:Z-1 and C-2:Z-1 at different combination ratios and total concentration of 0.2 wt.%. .... 129

Figure 51: IFT Results for surfactant C-5 at concentration 0.2 wt.%, 0.4 wt%, and 0.6 wt.% evaluated in brine A at high-temperature conditions. IFT values increase with increasing temperature when surfactants are present..... 133

Figure 52: IFT Images and values (in mN/m) displayed with temperature. Results displayed for the base case and surfactant C-5 at concentrations of 0.2 wt.%,0.4 wt.%, and 0.6 wt.%. .... 134

Figure 53: IFT Results for co-surfactants C-2:Z-1 at combination ratio 1:3 at total concentration of 0.2 wt.%, 0.4 wt%, and 0.6 wt.% in brine A evaluated at high-temperature conditions. .... 136

Figure 54: IFT Images and values (in mN/m) displayed with temperature. Results displayed for base case and co-surfactants C-2:Z-1 at concentrations of 0.2 wt.%,0.4 wt.%, and 0.6 wt.%. .... 137

Figure 55: IFT results for surfactant C-1 at 0.2 wt.% in brine A (0.2% TDS), brine 1D (1% NaCl), and brine 2D(2% NaCl) at high-temperature conditions..... 139

Figure 56: IFT Images and values (in mN/m) displayed with temperature for surfactant C-1 at 0.2 wt.% in brine A, brine 1D, and brine 2D. .... 140

Figure 57: HPHT IFT results for co-surfactant blends of C-2 and Z-1 at combinations 1:3 at a total concentration of 0.2 wt.% in brine A, brine 1D, and brine 2D. 142

Figure 58: IFT images and values (in mN/m) for co-surfactant blends of C-2 and Z-1 at combinations 1:3 at a total concentration of 0.2 wt.% in brine A, brine 1D, and brine 2D. .... 143

Figure 59: IFT results for single surfactant systems C-2 and Z-1 at concentrations 0.2 wt.% and the co-surfactants C-2:Z-1 at combination ratios 1:3 and 3:1 at a total concentration of 0.2 wt.% in brine A evaluated at high-temperature conditions. .... 146

Figure 60: IFT images and values (mN/m) for single surfactant systems C-2 and Z-1 at concentrations 0.2 wt.% and co-surfactants C-2:Z-1 at combinations 1:3 and 3:1 at total concentration of 0.2 wt.%. .... 147

Figure 61:  $P_c / r$  results for the selected surfactant systems. .... 151

Figure 62: Oil recovery factors for the different surfactant systems after the SASI experiments. .... 153

Figure 63: Images of produced oil volume for the different surfactant systems at the end of 192h. .... 154

Figure 64: Effect of (a) surfactant concentration and (b) brine salinity on the recovery factor. .... 156

Figure 65: CT Images of core samples before and after imbibition experiments for different surfactant cases. .... 158

Figure 66: Subtracted, Before, and After Imbibition scans presented for (a) 2D slice across core diameter (b) 2D slice across core length. .... 159

## LIST OF TABLES

	Page
Table 1: Eagle Ford sample rock properties.....	47
Table 2: Rock cleaning and aging procedure for rock chips in contact angle study.....	48
Table 3: Polarity of crude oil fractions.....	50
Table 4: Properties of Eagle Ford oil sample.....	51
Table 5: List of ionic surfactants evaluated (C = Cationic, A = Anionic, Z = Zwitterionic, N = Nonionic).....	53
Table 6: Composition of synthetic brines. ....	55
Table 7: Dimensions and data of core samples .....	69
Table 8. Depths of core samples retrieved from Eagle Ford formation used in contact angle study.....	86
Table 9: Formulation of cationic-zwitterionic surfactant blends .....	95
Table 10: Selected surfactant systems for SASI investigation. Systems will be referenced by their tags.....	150
Table 11: Data on core samples used in SASI experiments. ( $m_{AC}$ = mass of core after cleaning, $m_{AA}$ = Mass of core sample after aging) .....	152
Table 12: Core Samples and Fluid Systems used in SASI analysis .....	153



## 1 INTRODUCTION

Oil production from unconventional liquid reservoirs (ULR) has reversed the decline in oil production in the United States over the last decade. The US Energy Information Administration forecasts that oil produced from these reservoirs will continue to be a key driver in the total crude oil production of the US (EIA, 2021). The shale plays, Eagle Ford, Bakken, Wolfcamp, Niobrara, etc., have significant amounts of oil in place. There are up to 5 billion barrels of proved reserves in Eagle Ford only (EIA, 2018). Todd and Evans (2016) estimate that these unconventional oil reservoirs contribute an additional 4 million barrels per day to the US daily oil production. As of now, production from these unconventional reservoirs accounts for 70% of the total onshore production (EIA, 2021), with a total of approximately 8 million BOPD.

As a result of unique petrophysical properties associated with the shale reservoirs, low porosity, and ultra-low permeability, the shale reservoirs are produced by multistage hydraulic fracturing in horizontal wells. This enhances the wellbore-matrix connectivity, which allows for commercial production from the reservoirs. However, primary recovery from these reservoirs remains low, with about 5% to 10% of the original oil in place (Manrique et al., 2010; Wang et al., 2015). Oil recovery in liquid-rich unconventional reservoirs of the Bakken Formation is believed to be less than 10% OOIP (Clark, 2009). The producing wells also show a steep production decline. Typically, a high production rate drops to a very low rate in the first 3-5 years (Alfarge et al., 2017). The relatively low oil recovery fractions and early production decline necessitate the need for enhanced oil

recovery processes. Since there are very large oil reserves, the application of EOR/IOR processes that may lead to even a slight increase in productivity could result in millions of barrels of additional oil production.

The infill drilling technique has been applied in the development of these reservoirs. However, this only leads to a short-term increment in the production rate. The new wells also experience a similarly steep decline as the parent wells. In some cases, the productivity of the infill wells has been observed to be significantly lower than that of the parent wells (Lindsay et al., 2018). This makes this technique uneconomic for application in unconventional reservoirs, and the results do not justify the high cost of drilling the multistage fractured horizontal wells.

More than 20 EOR techniques have been investigated for use in conventional reservoirs, and several of those methods have successful applications. However, most of these methods have limited applications in unconventional reservoirs as a result of their low porosities and permeabilities, total organic carbon (TOC) content, and mixed lithology. Alfarge et al. (2017) reviewed several laboratory experiments, simulation studies, and field pilot tests to identify best practices for improving recovery in these reservoirs. Miscible gas injection, low-salinity water flooding, and surfactant application were determined to be the most feasible EOR practices for application in unconventional reservoirs.

In the miscible gas injection method, oil recovery may be improved by several mechanisms such as diffusion, oil swelling, oil viscosity reduction, and repressurization. While CO<sub>2</sub>, Nitrogen, natural gas, or enriched gas may be used in this process,

experimental focus has been on CO<sub>2</sub> because of its unique properties, which makes it most suitable for use in unconventional reservoirs. Compared to the other gases, CO<sub>2</sub> has a lower miscibility pressure with shale oil, which makes the CO<sub>2</sub> miscible injection process applicable under a wide range of reservoir pressures (Zhang, 2016). Miscible CO<sub>2</sub> EOR application in unconventional reservoirs has been well investigated, and up to 50% OOIP recovery has been observed in some studies (Adel et al., 2018). Experiments performed by Gamadi et al. (2014) on Mancos and Eagle Ford shale cores showed that cyclic CO<sub>2</sub> injection improved recovery of shale oil from 33% to 85%, indicating that cyclic CO<sub>2</sub> injection has high recovery potential in shale reservoirs.

Low Salinity water (LSW) flooding technique has been widely investigated with regards to conventional reservoirs. Those studies established that lower salinity brines induce more water-wet tendencies (Mohanty and Chandrasekhar, 2013; AlShaikh and Mahadevan, 2016) whereas, higher salinity may lead to an increase in oil-wetness, which is unfavorable for oil recovery (Shubham et al., 2012). There is an optimum concentration of salt for maximum oil recovery, which is usually low. In one study (Alameri et al., 2014), increased water-wetness was observed with decreasing salinity, creating a condition more favorable for oil recovery; this mechanism of wettability alteration involved the interaction of Na<sup>+</sup>, Cl<sup>-</sup>, Ca<sup>2+</sup>, Mg<sup>2+</sup>, SO<sub>4</sub><sup>2-</sup> ions, and crude oil carboxylate ions (R-COO<sup>-</sup>) with the rock in the electrical double layer (EDL) near the surface of the carbonate pores.

LSW flooding has also been investigated for improving recovery in unconventional reservoirs. In this case, mechanisms of improving recovery are shale

cracking, clay swelling, changing pH, or wettability alteration (Alfarge et al., 2017). In an experimental and simulation study by Morsy et al. (2013) on improving recovery in the Eagle Ford formation, distilled water and 2% KCl brine solutions were examined. Higher oil recovery was observed from shale samples placed in distilled water (19% OOIP) compared to recovery from samples placed in 2% KCl brine (12% OOIP). The higher recovery from distilled water was concluded to be a result of cracking from shale swelling, which was not observed in the case of the 2% KCl brine solution. A similar mechanism of shale cracking was suggested by Wang et al. (2011) in experimental studies in Bakken Formation.

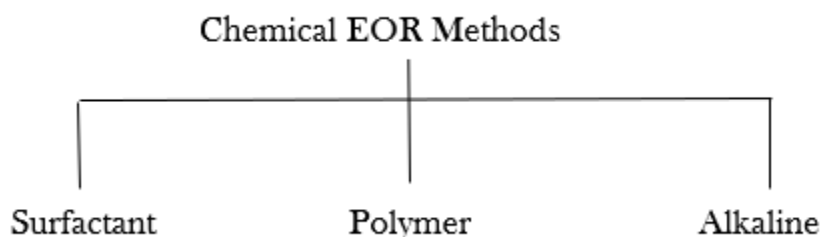


**Figure 1: Chemical EOR Methods for unconventional reservoirs**

**Figure 1** identifies some chemical EOR methods in unconventional reservoirs. Alkali-surfactant polymer (ASP) and Surfactant-Polymer flooding have also been shown to be effective in enhancing oil recovery in conventional reservoirs (Zhang et al., 2006; Felix et al., 2015). However, due to formation damage caused by alkali and related scaling issues, the surfactant-polymer has been more widely used. Scant literature exists on the applicability of alkaline and polymer techniques in unconventional reservoirs. This may be due to polymer injectivity limitations in these reservoirs, which have small pore and

pore throat sizes, and a possible lack of compatibility between alkaline chemical agents and complex mineral compositions of the reservoirs (Alfarge et al., 2017).

In the application of Chemical EOR methods, surfactants have the highest potential of improving oil recovery in these reservoirs (Alfarge et al., 2017). The cost of other EOR programs also makes surfactant applications the most attractive. Surfactants have been applied in the field to achieve different objectives. In conventional surfactant flooding, the goal is the reduction of the oil/water interfacial tension. The interfacial tension reduction causes an increase in the capillary number ( $Ca$ ), which creates favorable conditions for oil to be displaced and reduces the residual oil saturation. However, for other surfactant applications, the main goal is wettability alteration. The surfactants alter the wettability of the rock surface from original oil-wet conditions to favorable water-wet conditions, which results in a shift in the capillary pressure ( $P_c$ ) from negative to positive. Positive capillary pressure drives the spontaneous imbibition of the aqueous phase into the rock matrix, causing oil to be displaced and recovered from the rock. The capillary number ( $Ca$ ) has no effect on this method.

The impact of surfactant adsorption differs based on the primary goal of the surfactant application. In conventional surfactant flooding, adsorption is unfavorable as the method relies on lower surfactant adsorption to maximize the IFT reduction mechanism. Surfactant adsorption hinders the propagation of the surfactant molecules, resulting in surfactant loss and increasing the amount of surfactant that must be injected to maintain low interfacial tension throughout the life of the flood. In contrast, when surfactants are used for the primary purpose of wettability alteration, surfactant adsorption

is a favorable and necessary parameter. Surfactant molecules must be adsorbed on the rock surface to alter wettability, thereby increasing the capillary pressure, which drives spontaneous imbibition and improves oil recovery.

The focus of this study is the application of surfactant molecules with the primary goal of wettability alteration. Studies conducted on the application of surfactants in conventional and unconventional reservoirs determined that surfactants have the ability to alter wettability and improve oil recovery by spontaneous imbibition into the rock matrix (Standnes and Austad, 2000; Alvarez et al., 2017). Different mechanisms of operations have been described for different surfactant types. The surfactant head charge, rock surface charge, oil characteristics, salinity, etc., are important parameters in the operation of the surfactant systems. Ultimately, the goal of surfactant studies is to identify systems that promote imbibition and result in improved oil recovery. This is established by performing contact angle (CA) measurements, interfacial tension (IFT) measurements, stability tests, and surfactant-assisted spontaneous imbibition experiments (SASI) with the crude oil/brine/rock systems.

## **1.1 Research objectives and overview**

The ultimate goal of this work is to provide a complete workflow in evaluating surfactant performance in improving oil recovery in high-temperature unconventional reservoirs. The research objectives addressed in this study are described below:

1. To investigate the surfactant behavior at high-temperature conditions through contact angle and interfacial tension measurements.

2. To determine optimal surfactant molecular structures preferred for high-temperature applications.
3. Evaluate synergism between ionic co-surfactants and their applicability in surfactant EOR.
4. Understand the impact of salinity on surfactant systems for a range of temperature conditions.
5. Investigate ionic surfactant time stability behavior and its effect on the application of surfactant systems.
6. Provide a comprehensive workflow from laboratory measurements to spontaneous imbibition experiments to assess the effect of surfactant application on oil recovery in high-temperature unconventional reservoirs.

## **1.2 Thesis organization**

This thesis comprises six chapters. Chapter 1 introduces the research problem and outlines the objectives of the research study. Chapter 2 follows up with a literature review highlighting previous studies that have been conducted on subjects related to this work, along with definitions of important parameters and concepts that form the basis of the study. Chapter 3 discusses the methodologies followed for the laboratory experiments and provides information on the materials used. Chapter 4 introduces the time stability concept, as well as discussions on its effect. Chapter 5 presents contact angle and IFT results for a range of temperature conditions and investigates the impact of surfactant type, surfactant concentration, aqueous phase salinity, and surfactant solubility. Chapter 6

analyzes results from spontaneous imbibition experiments, which quantifies the actual oil recovery and presents results on oil displacement monitoring by CT-Scan imaging. Chapter 7 is the concluding chapter which highlights the key observations and takeaways from the research study.



## 2 LITERATURE REVIEW

This literature review describes the basic terminologies in wettability alteration and surfactant application studies, such as contact angle, interfacial tension, and spontaneous imbibition. An overview of studies previously conducted on surfactant application and their role in improving oil recovery is presented. Surfactant types, mechanisms of operation, and the effect of surfactants on crude oil/brine/rock systems are discussed. Also, other parameters that influence the effectiveness of surfactant EOR such as salinity, temperature, and co-surfactants, are reviewed.

### 2.1 Wettability of a rock surface

Wettability is defined as the tendency of one fluid to spread on or adhere to a solid surface in the presence of other immiscible fluids (Craig, 1971). In a rock/oil/brine system, wettability is the preference the rock has for either the oil or water (Anderson, 1986). The wetting phase, i.e., either oil or water, occupies the small pores and contacts the majority of the rock surface. The wettability of a surface may range from strongly water-wet to strongly oil-wet. Oil recovery from reservoirs is largely dependent on the wetting properties of the oil matrix (Donaldson et al., 1969). Wettability influences the flow pattern of fluids flowing through a reservoir, which ultimately impacts the recovery factor (Zhang et al., 2018).

Several qualitative and quantitative methods exist in the literature for estimating the wettability of a rock surface. These methods include the contact angle method, the

Amott-Harvey method, the USBM method, the use of relative permeability curves, permeability/saturation relationships, reservoir logs, Nuclear Magnetic Resonance (NMR), zeta potential methods, etc. The Amott, USBM, and contact angle methods are the most widely used. The Amott and USBM methods estimate the average wettability of a core by measuring the amount of fluid spontaneously imbibed by the sample. In contrast, the contact angle method estimates the wettability of a single surface based on the angle made by a drop of liquid on the surface.

Recent studies have shown shale reservoir wettability to be typically oil-wet (Alvarez and Schechter, 2017). Typically, rocks are originally water-wet. However, the rocks become oil-wet as a result of desorption of the negatively charged carboxylic groups present in the oil adsorbing onto the rock surface upon contact with the reservoir brine (Standnes and Austad 2000, 2003a, 2003b). Electrostatic interactions cause acidic compounds in oil to be adsorbed on the rock surface, which is positively charged, while basic compounds will be attracted to negatively charged rock surfaces (Feng and Xu, 2015). Hence, carbonates that are positively charged and have weakly basic surfaces would adsorb carboxylic acids in the oil, while sandstones that have negatively charged surfaces will adsorb positively charged basic components in the crude oil. Standnes and Austad (2003), in their study of carbonate surfaces, stated that these carboxylic materials contained in the heavy end fraction of the oil, i.e., resins and asphaltenes, are surface-active molecules that act as anchors for other polar molecules adsorbing onto the surface by hydrophobic and dipole-dipole interactions. These organic materials form an organic layer making the rock surface oil-wet. This wettability shift may occur as oil starts moving

into the rock pores during hydrocarbon generation in the source rock or during secondary migration into a conventional reservoir.

Wettability is an essential property of reservoir rocks because it determines the multiphase flow properties, which govern reservoir performance. Wettability controls the flow, location, and how fluids are distributed in the reservoir. For example, when the formation is preferentially oil-wet, oil recovery from the reservoir is low and much oil is left behind after waterflooding. The high remaining oil saturation in oil-wet formations results from high oil retention in the matrix by capillarity as well as surface trapping (Hirisaki and Zhang, 2004). The matrix retains oil by capillarity leading to the existence of high oil saturation transition zones, which results in high residual oil saturation in these formations. By altering wettability to preferentially water-wet and reducing the IFT to ultra-low values, it is possible to overcome these oil retention mechanisms (Hirisaki and Zhang, 2004).

Waterflooding is more effective if the formation is water-wet, while the impact of waterflooding on oil recovery is poor in oil-wet reservoirs. Waterflooding is more effective in a water-wet reservoir because water occupies the smaller pores first while oil occupies the larger pores leading to a higher relative permeability for oil. Also, capillary forces will cause water to be imbibed into bypassed zones, which reduces oil bypassing in low permeability zones. The opposite is observed in oil-wet, where the relative water permeability is high leading to early water breakthrough. Also, oil bypassing is higher as water is unable to invade the bypassed zones (Sharma and Mohanty 2011). Hence, as a result of the oil-wetting nature, the capillary forces prevent the spontaneous imbibition of

water in the oil-wet reservoirs. This results in low oil recovery through the waterflooding process.

The wettability of the oil-wet rock can be altered by adding surfactants in hydraulic fracturing fluids. Surfactants with proper formulations are known to alter wettability, reduce IFT, and improve recovery in conventional and unconventional reservoirs. The success of surfactant application is reliant on properly tailoring the surfactant chemistry to particular reservoir conditions. Different reservoir characteristics such as mineralogical composition, temperature, formation water composition, crude oil type will influence the effectiveness of different surfactants.

### **2.1.1 Methods of estimating wettability**

Qualitative and quantitative methods exist in the literature for estimating the wettability of a rock surface. The methods include the contact angle method, Amott-Harvey method, the USBM method, the use of relative permeability curves, permeability/saturation relationships, reservoir logs, Nuclear Magnetic Resonance (NMR), zeta potential methods, etc. The first three methods stated are the most widely used.

The Amott and USBM methods measure the average wettability of a core. The Amott method involves the measurement of the amount of fluids spontaneously and forcibly imbibed by a rock sample. The USBM method is similar but considers the work required to do a forced fluid displacement. These methods have been successfully used in the study of wettability in conventional reservoirs. However, in unconventional reservoirs,

these techniques and other wettability measurement methods have limited applications. For instance, the Amott-Harvey index and USBM methods require the acquisition of fluid saturation changes by displacement of brine by crude for the drainage cycle into the matrix. If there is no direct injection to cover the imbibition and drainage cycles, these rocks cannot be utilized for special core analysis in a conventional manner. Hence, in unconventional reservoir rocks, these methods are not applicable because fluids cannot flow through these rocks. The Amott wettability index (I) is expressed as  $I_w - I_o$  where  $I_w$  is the Amott wettability index to water and  $I_o$  is the Amott wettability index to oil.

Nuclear Magnetic Resonance (NMR) method estimates wettability by measuring changes in longitudinal relaxation time. Since the NMR method does not require fluid flow, it can also be used in unconventional reservoir rocks. However, errors may arise because the relationship between the relaxation rate and fractional wettability, as well as sample preparation, may alter the wettability of the sample (Alvarez and Schechter 2017). Zeta-potential measurements are also used to qualitatively investigate the wetting affinity of these rocks. Zeta-potential is based on the dependency of wettability on the double-layer between oil and shale rock surface. Layer thickness and stability are determined by the relative charge of the surface and the fluid interacting with the surface. A stable solution film indicates water-wet systems, while an unstable solution film indicates oil-wet or intermediate-wet. Zeta potential measurements are used to gauge the charge of the aqueous solution. Generally, solutions with zeta potential values higher than +30 mV or lower than -30mV are considered stable, while values between -30mV and +30mV are considered unstable (Alvarez et al., 2017).

Lastly, surface wettability can also be estimated through contact angle measurements.

### **2.1.2 Contact Angle**

Contact angle (CA) is defined as the angle formed by a drop of oil or water on a solid surface immersed in an aqueous phase. This method is used to evaluate wettability in this study. The contact angle arises from an imbalance of forces resulting from the crude oil, brine, and rock interactions. The contact angle is a good indication of wetting preferences and interfacial energies. The contact angle is estimated by captive bubble, sessile drop, tilting plate, vertical rod method, tensiometric method, cylinder method, and capillary rise methods. When contact angle measurements are made, often times the rock sample is submerged in the aqueous phase, a bubble of oil or water is dispersed onto a smooth horizontal surface, and the image of the bubble/drop is captured. The contact angle is estimated from the image of the bubble, and the wettability of the rock surface can be estimated. The flatness and smoothness of the rock surface are important in determining accurate contact angles.

Anderson (1986) established a range of contact angle values for wetting preferences: CA values between  $0^\circ$  to  $75^\circ$  indicate water-wetness;  $75^\circ$  to  $105^\circ$  are intermediate-wet contact angle values, while  $75^\circ$  to  $180^\circ$  indicate oil-wetness. A schematic displaying water- and oil- wetting conditions is displayed in **Figure 2**. Contact angle schematics are shown in For a rock/brine/oil system, the surface energies in the system are related by Young Laplace's equation (**Eq. 2-1**).

$$\cos \theta = \frac{\sigma_{os} - \sigma_{ws}}{\sigma_{ow}} \quad (2-1)$$

Where,  $\sigma_{ow}$  = Interfacial energy between oil and water,  $\sigma_{os}$  = Interfacial energy between the oil and solid,  $\sigma_{ws}$  = Interfacial energy between the water and solid and  $\theta$  = contact angle

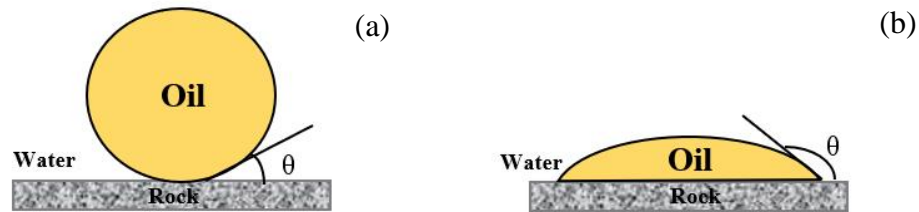


**Figure 2: Schematic of oil drop contact angle indicating (a) water-wet (b) oil-wet wettability conditions.**

## 2.2 Interfacial Tension

The contact angle of a drop on a surface is governed by the amount of interfacial energy gained to form the liquid-solid interface. The interfacial tension (IFT) is a measure of the excess energy present at the interface of two different phases, such as liquid-solid, which arises from the imbalance of forces between molecules at the interface. The shape and angles formed by the drop are a function of the interfacial or surface tension. From **Eq. (2-1)**, higher interfacial energy between the water and the solid surface ( $\sigma_{ws}$ ) than between the oil and the solid surface ( $\sigma_{os}$ ) indicates that the surface is oil-wet. Whereas, when  $\sigma_{os} > \sigma_{ws}$ , the surface is water-wet.

IFT can be either static or dynamic. Static IFT is the IFT of the system independent of time, while the dynamic IFT is the IFT value of a system at a particular surface age or

interface age. The IFT evaluated in this study is Static IFT. IFT (static) measurements are typically made by pendant drop or sessile drop methods, which involve the droplet in an equilibrium shape being deformed by gravity or centripetal force. The pendant drop method is the most widely used in the petroleum industry. The mechanism of this method functions by suspending an oil droplet in an aqueous phase from the tip of a narrow needle where a balance between gravity and interfacial tension is reached. The IFT value is integrated by asymmetrical drop shape analysis using software that fits the drop profile with the Young-Laplace equation using a contour-fitting algorithm.

### **2.3 Spontaneous imbibition**

The wettability of the rock and the IFT of the system both influence the spontaneous imbibition mechanism. Imbibition is the process by which the wetting phase displaces the non-wetting phase; in a water-wet rock, water displaces oil. Spontaneous imbibition takes place by the action of capillary pressure and/or buoyancy when a core sample or matrix block is surrounded by brine. In spontaneous imbibition, the wetting fluid is drawn into a porous medium by capillary action (Morrow and Mason, 2001). By altering rock wettability from oil-wet to water-wet, recovery can be improved by means of spontaneous imbibition. Oil is expelled as water is imbibed into the rock matrix. Factors that affect spontaneous imbibition processes include rock properties such as permeability, porosity; fluid properties such as density, viscosity, IFT, wettability, and initial saturations.



Capillary, gravity, and viscous forces determine imbibition and drainage in porous media (Menoaur and Knapp, 1980). Viscous force is created by pressure difference. Imbibition by gravity forces or buoyancy results from density difference between the oil and aqueous phases- this is observed in experiments when the less dense oil phase moves to the top part of the core sample while the denser aqueous phase is pulled to the bottom where the imbibition process dominates. Imbibition by capillary action results from the exchange process between the oil and aqueous phases caused by adhesive and cohesive forces between oil, water, and rock. In strongly water-wet conditions, the primary driving force of imbibition is usually capillary pressure. However, at low interfacial tension values, gravity drainage or buoyancy becomes the dominant force in the imbibition process (Austad and Milter, 1998; Hirisaki & Zhang, 2004).

Austad & Milter (1997), in their study of the mechanism of the imbibition process on chalk material, observed both gravity and capillary forces active in the imbibition process in water-wet carbonate chalk material. Gravity forces were the dominant force of imbibition and were more active in oil expulsion at low interfacial tension, while capillary forces dominated at high interfacial tension. Recovery rates were faster when imbibition was governed by capillary forces than by gravity. Gupta and Mohanty (2007) achieved a gravity-driven imbibition process in carbonate rocks at lower IFT values. Lowering of IFT has also been shown to decrease imbibition (Cuiec et al. 1990). Schechter et al. (1994), who worked on limestone and sandstone cores, concluded that both gravity and capillary forces could drive spontaneous imbibition. In the imbibition experiments ran by Xie et al. (2005) using dolomite core plugs, capillary forces were the dominant mechanism of

imbibition, and higher IFT was said to be more favorable for recovery. Other studies have also shown capillary forces as the main driving force of the imbibition process (Mattax and KYTE, 1962; Babadagli et al., 1999).

To better understand the balance between gravity and capillary forces in the imbibition process, an inverse bond number,  $N_B^{-1}$  has been defined:

$$N_B^{-1} = C \frac{\sigma \sqrt{\frac{\phi}{k}}}{\Delta \rho g h} \quad (2-2)$$

Where C represents pore geometry,  $\phi$  =porosity, k= permeability, h= characteristic length of the rock,  $\sigma$ = interfacial tension of oil and water,  $\Delta \rho$  = density difference between aqueous and oil phase and g = gravitational constant.

Schechter et al. (1994) defined a range of values for which capillary or gravity forces are dominant: If  $N_B^{-1}$  is less than 1, the gravity force is dominant in the imbibition process,  $N_B^{-1}$  greater than 5 indicates that capillary is the driving force of the imbibition process. Values of  $N_B^{-1}$  between 1 and 5 indicate that the two forces contribute to the imbibition process, which is often more favorable for faster recovery of the non-wetting phase.

Capillary forces are defined by the Young-Laplace equation. The Young-Laplace equation defines capillary pressure in **Eq 2-3**.

$$P_c = \frac{2\sigma \cos\theta}{r} \quad (2-3)$$

Where  $P_c$  is Capillary Pressure between oil and water;  $\sigma$  is interfacial tension between oil and water;  $\theta$  is oil/water contact angle; and r is the radius of the capillary tube.

Low water-wet contact angles have been correlated to higher recoveries (Zhang et al., 2018, Austad and Milner, 1997; Standnes and Austad, 2003). Oil-wet reservoirs have small or negative capillary pressure making water injection ineffective in mobilizing oil. When surface wettability is altered from oil-wet to water-wet, the capillary pressure shifts from negative to positive, which is more favorable for oil recovery (Hirisaki and Zhang, 2004). From **Eq. (2-3)**, it is observed that imbibition can be achieved when there is water-wet behavior and capillary pressure is greater than zero.

In unconventional reservoirs, capillary forces play a big role in imbibition and oil recovery. Hence, it is counterproductive to reduce IFT to ultra-low values as conceived in conventional EOR (Alvarez et al., 2017). High IFT increases capillary pressure, which enhances imbibition and oil recovery. Still, a reduction in IFT has been correlated with an increase in oil recovery. Low IFT will aid oil expulsion from small pores and improve relative permeability. Most suitable will be relatively moderate IFTs as low IFTs improves recovery in small pores and high IFTs increase capillary pressure, which enhances imbibition. Very high IFTs are unfavorable as they may lead to blocking, while ultra-low IFTs are also unfavorable as they will negatively impact capillary forces, and by extension, lower imbibition. Generally, favorable IFT reduction for unconventional reservoirs should be less than that desired in high permeability reservoir flooding applications (Alhashim et al., 2019).

## 2.4 Surfactants and wettability alteration

Surfactant molecules are surface-active agents that are amphiphilic in nature. The molecules consist of a hydrophilic head, which has a higher affinity to the aqueous phase, and a hydrophobic tail with a higher affinity to the oil molecule. The hydrophobic tails consist of hydrocarbon chains; linear, branched or aromatic. The surfactant additives act on the water-rock and oil-rock interfaces. The amphiphilic characteristic of the molecules causes a reduction of the water-oil interfacial tension and has the potential to alter the rock's wettability to preferentially water-wet. The alteration of the rock wettability from originally oil-wet to water-wet changes the capillary pressure. Consequently, spontaneous imbibition is enhanced, and oil is expelled from the pores leading to improved recovery (Gupta & Mohanty, 2007).

### 2.4.1 Types of Surfactants

Based on the electric charges of the headgroups, surfactants are characterized as anionic, cationic, nonionic, and amphoteric. The structures of the different surfactant types are displayed in **Figure 3**. Cationic surfactants have a positive head charge, anionic surfactants have a negative head charge, and nonionic surfactants have no head charge. Surfactants that consist of hydrophilic heads bearing both positive and negative charges are characterized as amphoteric or zwitterionic surfactants. The hydrophobic surfactant tail can be linear or branched, contain different numbers of carbon atoms, fluorocarbon, or siloxane chains, and have variable chain lengths. The number of carbon atoms in the tail may vary from five (5) to thirty (30). While fluorocarbon or siloxane chains are more

effective than linear chains in lowering interfacial tension, fluorocarbon surfactants are unsafe for the environment, and siloxanes may be hydrolytically unstable.

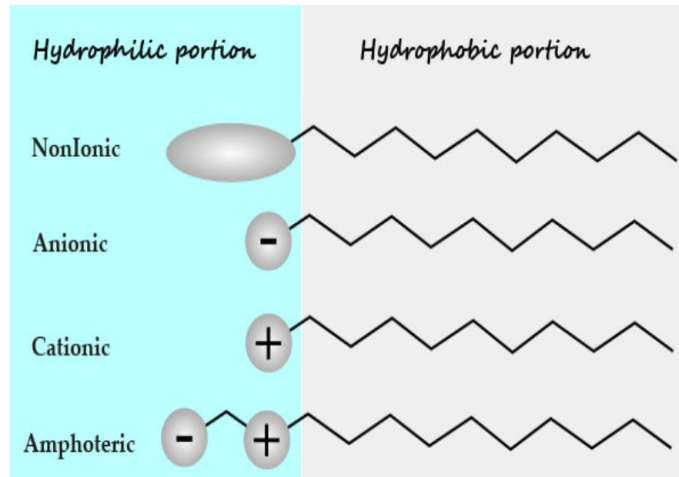


**Figure 3: Amphiphilic structure of different types of Surfactants.**

Anionic surfactants can contain sulfate ( $-\text{SO}_4^-$ ), sulfonate ( $-\text{SO}_3^-$ ), phosphate ( $-\text{PO}_4^-$ ), or carboxylate ( $-\text{COO}^-$ ) headgroups. The sulfate types have an anionic group  $-\text{SO}_3\text{Na}$  group attached to a propylene oxide (PO) or ethylene oxide (EO) group. For sulfonate types,  $-\text{SO}_3\text{Na}$  group is attached directly to a carbon in the alkyl or alkylaryl structure. Sulfonate types are more stable at a higher temperature (140 to 248°F) than the sulfate types. Hocine et al. (2016) showed that oxidation and hydrolysis mechanisms are important in guaranteeing the long-term stability of EOR surfactants. Oxidation is important for maintaining surfactant integrity and performance, while hydrolysis is essential, especially regarding sulfate-based surfactants. Sulfate hydrolysis increases with temperature; hence, sulfonate-based surfactants are preferred for long-term EOR

performances (Hocine et al., 2016). However, sulfate types have a higher tolerance for salinity.

Cationic surfactants contain functional groups such as primary, secondary, or tertiary amines as their head group. For zwitterionic surfactants, cationic parts like in the case of cationic surfactants are also based on primary, secondary, or tertiary amines or quaternary ammonium cations, while anionic parts typically include sulfonates or carboxylates. They are also called amphoteric surfactants and exhibit a high tolerance for temperature and salinity. Nonionic surfactants head groups are commonly composed of ethylene oxide (EO) or ethoxylated alcohols. Typically, surfactants used in EOR processes contain some combination of sulfate, sulfonate, carboxylate, and nonionic surfactants (Pinnawala et al., 2020).

The hydrophobicity of surfactant increases with increased hydrocarbon chain length in the hydrophobic tail. Hydrocarbon chains or structures present in the tail have an impact on chemical interactions. In their study of an anionic surfactant containing a benzene ring, Khalil and Shadoon (2005) observed a lower hydrophobic effect with benzene ring compared to that of the alkyl group as a result of the  $\pi$  system in the aromatic group. The solubility of surfactants and other properties depends on the balance of the hydrophilic and hydrophobic (lipophilic) groups. Hydrophilic-Lipophilic balance (HLB), first proposed by Griffin (1954), is an indicator that quantifies this balance. Several formulas exist to estimate the HLB value. This indicator is even more important for nonionic surfactants, which are unique for their 'no-charge bearing nature. The cloud point is another important indicator to understand the characteristics of nonionic surfactants.

For surfactant use to be effective, the surfactant must be stable at conditions within the target reservoir. Surfactant performance is influenced by water salinity, pH, and temperature. In the case of anionic surfactants, for instance, sulfonates are typically more thermally stable than sulfates. One approach in improving stability and solubility is by use of branched hydrocarbon constituents (Szlendak et al., 2013, Kiani et al., 2019). The high branching factor allows for an increase in carbon number while maintaining a short effective chain length. Generally, anionic, cationic, zwitterionic, and nonionic surfactants have been shown to be effective to varying degrees in altering the wettability of carbonate-rich surfaces. Anionic surfactants are usually less effective compared to cationic and nonionic surfactants due to adsorption issues in carbonates. These surfactants are able to produce low IFTs but have reduced potential in wettability alteration of the carbonate-rich rocks. Although cationic surfactants are more expensive and require use at higher concentrations, they are effective in altering wettability in these rocks (Seethepalli et al., 2004).

#### **2.4.2 Nonionic Surfactants and Cloud point Limitation**

An important property of nonionic surfactants is the cloud point. At temperatures above the cloud point, there is an increase in the turbidity or cloudiness of nonionic surfactant systems. Cloudiness results from phase separation; the water molecules formally bonded to the polyoxyethylene group separate as temperature rises (Nakama, 2017). The decreased hydration of oxyethylene chains beyond the cloud point temperature causes the surfactant solution to turn cloudy (Das et al., 2018). Nonionic surfactants

experience a reduction in solubility as the temperature is increased. The cloud point value is, therefore, a reference for the solubility of the surfactant. Above the cloud point, the surfactant can no longer dissolve in water.

The cloud point temperature has been shown to increase with an increase in the number of ethoxy units (Gupta and Mohanty 2007). Also, cloud point decreases with increasing alkyl carbon chain length (Huibers et al.,1997). The cloud point can also be influenced by the presence of anions or cations in the aqueous solution. High salinity conditions may have an effect on the nonionic surfactants; however, the physiochemical properties of nonionic surfactants are not as affected by electrolytes compared to the ionic surfactants. It is important to check the aqueous stability of nonionic surfactants to determine their tolerance for temperature and salinity. This is typically monitored over time by checking the clarity of aqueous solution, haziness, phase separation, and chemical precipitation.

Empirical relationships between cloud point and the ethylene oxide number have been developed. Gu and Sjoblom (1992) derived an equation (**Eq. 2-4**) for the relationship between the cloud point (CP) and the logarithm of the ethylene oxide (EO number) for alkyl ethoxylates and alkyl phenyl ethoxylates; as well as the relationship between the cloud point and alkyl carbon number (C#) for linear alkyl ethoxylates, where A and B are empirical constants depending on the surfactant class.

$$CP = A \log (EO\#) - 5.5C\# - B \quad (2-4)$$



Huibers et al. (1994) further developed a general empirical relationship for estimating the cloud point of pure nonionic surfactants of the alkyl ethoxylate class using the logarithm of the ethylene oxide count as well as three topological descriptors that account for hydrophobic domain derivation. Schott (2003) described the relationship (**Eq. 2-5**) between the cloud points (CP) of water-soluble poly ethoxy nonionic surfactants and the average number of ethoxy units (P) where a, b and P<sup>o</sup> are constants.

$$\frac{P - P^o}{CP} = a + b(P - P^o) \quad (2-5)$$

While the absence of charged head groups makes nonionic surfactants suitable for multiple applications, their applicability is limited by the cloud point. The turbidity/cloudiness above the cloud point of these systems impairs contact angle and IFT measurements which limits the investigation of these surfactants for EOR applications. Typically, the cloud point of the nonionic surfactant must be above the reservoir temperature for EOR applications. However, there is a limited number of nonionic surfactants with very high cloud points up to 300 °F. The cloud points of typical nonionic surfactants will need to be improved to enable their application at high-temperature conditions. This study is focused on the application of ionic/charged surfactants for high-temperature reservoir conditions.

### **2.4.3 Mechanism of Surfactant Operation**

Different mechanisms have been proposed for the role of the surfactant in altering rock matrix wettability. Depending on the crude oil composition, rock mineralogy,

surfactant charge, and ionic composition of the brine, surfactants can alter wettability by means of ion-pair formation (Standnes and Austad, 2000, Standnes and Austad, 2003a), surfactant adsorption (Standnes and Austad, 2000; Standnes and Austad, 2003a), and micellar solubilization of adsorbed organic components (Kumar et al., 2008). The mechanisms of wettability alteration in shale rocks remain to be established. However, similar mechanisms expected in carbonate-rich conventional rocks are observed in carbonate-rich shale rocks.

Electrostatic interactions occur as a result of electric charges of the surfactant head group and the mineral surface. When there are dissimilar charges, electrostatic attraction occurs, while electrostatic repulsion occurs with similar/like charges. For example, there will be an electrostatic attraction between a positively charged calcite mineral and the negatively charged carboxylate acids present in the oil, which results in the negatively charged carboxylates coating the surface of the calcite mineral, making the surface negatively charged. The electrostatic attraction will occur between this negatively charged system and a cationic surfactant, improving the adsorption of the surfactant. On the flip side, electrostatic repulsions will occur between the negatively charged system and an anionic surfactant.

Feng and Xu (2005) established a better understanding of the interactions among crude oil, rock mineralogy, and surfactant molecules. Oil samples from Wolf Camp and Eagle Ford of varying total basic numbers (TBN) and total acid numbers (TAN) were used in the study, along with Berea sandstone and Indica limestone rocks. Electrostatic attraction and ion-pair formation between oppositely charged shale oil and surfactants,

taking into consideration mineralogy, was found to be a major factor resulting in wettability alteration and oil recovery. It was observed that for carbonates and oil samples with higher TAN, a cationic surfactant showed a higher potential to sweep oil than an anionic surfactant. For sandstone with shale oil having higher TBN, an anionic surfactant showed higher potential to sweep oil than a cationic surfactant.

An oil-film stability experiment conducted by Das et al. (2018) to observe the behavior of wettability alteration on carbonates in the presence of surfactant solutions showed that in the presence of surfactants, the oil layer retreated across the surface with a gradual decrease in the oil coverage with time. Based on the oil-film experiments and oil detachment experiments carried out, Das et al. proposed a conceptual model involving 'coating' and 'sweeping' mechanisms to explain wettability alteration in the presence of surfactants. In the model, the hydrophobic part of the surfactants adsorbs on hydrophobic surfaces, with the head group pointing into the solution. A temporary hydrophilic surface is generated as a result of surfactant coating, which promotes favorable interactions with the water molecules near the surface. Near the three-phase contact line, the dangling hydrophilic components reduce the water-calcite surface energy. Water aided by surfactant molecules displaces ("sweeps") the oil away, exposing the solid surface underneath.

Hammond and Unsal (2009, 2011) performed numerical modeling studies on the coating and cleaning mechanisms and observed that the amount of surfactant adsorbed is important for the coating mechanism as imbibition will not occur until a finite amount of surfactant is adsorbed to alter the wettability of the surface. However, the concentration

threshold is not important for the cleaning mechanism as ion-pair formation will occur at any concentration of surfactants in the solution.

Hydrophobic interactions occur in the absence of electrostatic interactions. Hydrophobic interactions occur between the hydrophobic tail surfactant and the hydrocarbon chain of polar components of the oil. Electrostatic interaction is the more prominent chemical interaction in surfactant performance. Other chemical mechanisms include hydrogen bonding and chain-chain interactions.

Surfactant adsorption occurs as a result of the electrostatic attraction between the charged surface of the solid and the charged head group of the surfactant molecule. The surfactant adsorption in a reservoir depends on various factors such as surface charge of the reservoir, type of surfactant, temperature, pH, and salinity of formation water (Saxena et al., 2019). Adsorption of surfactants may be favorable or unfavorable, depending on the purpose of surfactant application. Adsorption of surfactant at rock-aqueous phase interface is beneficial for modification of rock surface properties such as for wettability alteration. However, the loss of surfactant molecules due to adsorption is unfavorable, where the presence of surfactant molecules in the aqueous phase is crucial for its effective application, such as in surfactant flooding. In this case, the effectiveness of surfactants for oil recovery is decreased due to the reduction of surfactant concentration in the aqueous phase, where it is required to lower oil-water IFT.

Somasundaran and Zhang (2006) evaluated the effect of surfactant adsorption on minerals. The authors stipulated that the effect of surfactants on wettability alteration depends on the amount of surfactant adsorbed as well as the mechanism of adsorption.

Mechanisms for adsorption include electrostatic attraction/repulsion, ion exchange, chemisorption, chain-chain interactions, hydrogen bonding, and hydrophobic bonding. The mechanism of adsorption will depend on the nature of the surfactants, minerals and solution conditions, and the mineralogy of the reservoir rock.

#### **2.4.4 Surfactant Concentration**

The concentration of surfactant influences its effectiveness in EOR applications. Surfactant systems have an increased potential to alter wettability at higher concentrations, reduce the IFT and improve oil recovery. The efficiency of surfactants depends on properties such as the CMC value. The critical micellar concentration is defined as the concentration of surfactants above which micelles are spontaneously formed (Sheng 2011). When surfactants are introduced, there is a reduction in the interface energy and the removal of the hydrophobic groups of the surfactants from contact with water. As the surfactant concentration increases in the system, surfactant molecules start to aggregate into micelles. The formation of micelles further decreases the system free energy by decreasing the contact between the hydrophobic groups of the surfactant and water until the surfactant concentration reaches critical micellar concentration, CMC. Above the CMC, a further increase in surfactant concentration increases the number of micelles but hardly reduces the surface tension energy. Krafft temperature is the critical micellar temperature above which surfactants can form micelles.

## 2.5 Surfactant Assisted Spontaneous Imbibition (SASI)

Surfactant Assisted Spontaneous Imbibition (SASI) is a method of improving oil recovery in an oil well by the addition of surfactant molecules. Surfactant molecules alter the wettability and increase the capillary pressure. This causes the imbibition of the aqueous phase and the expulsion of oil from the rock. Different types of surfactants have been examined for wettability alteration and improving oil recovery in calcite-rich conventional and unconventional reservoirs. Contact angle ( $\theta$ ) and IFT ( $\sigma$ ) are two important parameters that influence capillarity. Relatively high IFT and low contact angle (water-wet) are favorable for capillary forces. However, one disadvantage in using surfactants in wettability alteration is that the IFT is reduced. Hence, the extent of oil recovery using surfactants will depend on the extent to which wettability is altered can counterbalance the reduction in IFT. In the surfactant evaluation study by Nguyen et al. (2014) on carbonate-rich shale cores, wettability alteration was observed to be more dominant than IFT alteration in increasing oil recovery rate from oil-wet reservoirs.

On calcite-rich or carbonate surfaces, the mechanisms of anionic and cationic surfactants vary considerably. Standnes & Austad (2000b) suggested the mechanism of operation of cationic surfactants improving oil recovery on chalk carbonate surface as shown in **Figure 4**. In the aqueous zone where surfactant micelles and monomers are in equilibrium, electrostatic forces will cause interaction between the cationic monomers and the adsorbed negatively charged materials from the crude oil resulting in an ion-pair formation. The oil molecules are then desorbed from the rock surface, making the surface

oil-wet. Hence, water penetrates into the pore system, and oil is expelled through connected pores.

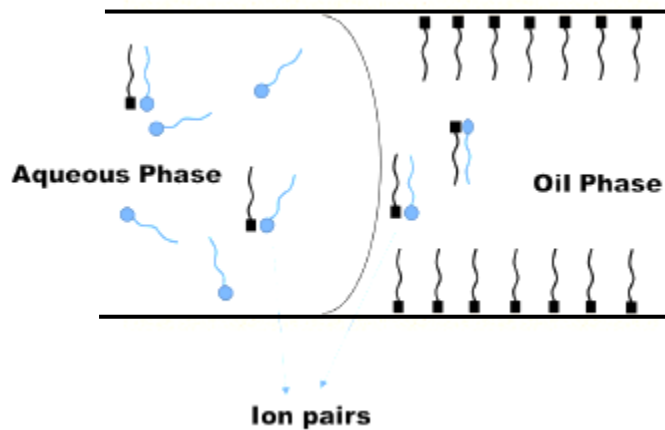


**Figure 4: Schematic for the suggested mechanism for the wettability alteration caused by ion-pair formation (adapted from Standnes and Austad, 2000b)**

Standnes and Austad (2000b) examined the effect of several surfactants, mainly cationic and anionic types, on aged calcite crystals. The cationic surfactants tested produced the lowest contact angles, hence showed great potential in improving the water wetness of the rock sample. In the imbibition tests, a cationic surfactant (dodecyl trimethylammonium bromide, C12TAB) resulted in oil being displaced from the core immediately, whereas brine only produced a negligible amount of oil after 35 days. The cationic surfactants were more effective than anionic surfactants in expelling oil from the oil-wet chalk material. Cationic surfactants of the type  $R-N^+(CH_3)_3$  desorbed organic carboxylates from the chalk surface, and 70% of OOIP was recovered within 30 days by spontaneous imbibition process of the aqueous surfactant solution.

Imbibition experiments were performed on nearly oil-wet chalk in the presence of cationic surfactant C<sub>12</sub>TAB in a study by Austad and Milner (1997). Oil recovery by brine alone was very low; in contrast, 1.0 wt.% cationic surfactant solution resulted in immediate oil production with total oil recovery up to 65 % OOIP. The cationic surfactants increased the water-wetness of the chalk, and imbibition was by a counter-current flow mechanism. In one study (Sharma and Mohanty, 2011), no wettability alteration was observed on aged calcite plates in the presence of cationic surfactants. However, in this case, the contact angles were estimated qualitatively.

Generally, anionic surfactants showed less effectiveness in altering wettability and recovering oil in carbonate-rich surfaces compared to cationic surfactants. For the imbibition operation of anionic surfactants of the sulfonate type, Standnes and Austad (2000) suggested a mechanism where the hydrophobic part of the EO-surfactant adsorbs onto the hydrophobic surface of the chalk. Interactions between the water-soluble head-group of the surfactant, the EO-groups, and the anionic sulfonate group form a small water zone between the organic coated surface and the oil, which increases the water-wetness of the rock. Weak capillary forces are created during the imbibition process. Surfactants with the highest ethoxylation degree were the most efficient. An increase in wettability alteration with an increase in EO numbers was also observed by Gupta and Mohanty (2008).

Adibhatla and Mohanty (2008) examined anionic surfactants to observe their effect on oil recovery in fractured carbonates. Increasing pH and decreasing salinity reduced the adsorption of anionic surfactants on calcite. For the study, surfactants were prepared at



their optimal salinity  $\text{Na}_2\text{CO}_3$  concentration. Results showed that the sodium carbonate/anionic surfactant system altered the wettability of the oil-wet carbonate to moderately water-wet. Spontaneous Imbibition measurements made on aged cores resulted in up to 42% OOIP recovery in 50 days of imbibition and approximately 60% in 200 days for the surfactant system tested.

In some studies, anionic surfactants have been shown to perform better than cationic and nonionic surfactants in carbonate-rich rocks. Nguyen et al. (2014) evaluated the application of anionic, cationic, and amphoteric surfactants in spontaneous imbibition tests on saturated core plugs from carbonate-rich Eagle Ford play. Anionic surfactants recovered 48% OOIP and cationic surfactants 23% to 38% OOIP. Nguyen et al. (2014) highlighted that the recovery mechanism was driven by both buoyancy and countercurrent capillary imbibition. Alvarez et al. (2014) also investigated the potential of nonionic and anionic surfactants to alter wettability and improve oil recovery in liquid-rich unconventional rocks. The core chips were originally intermediate-wet, and the presence of anionic surfactants led to more water-wet behavior in the chips compared to nonionic surfactants.

The effect of different surfactant types in improving oil recovery by SASI has also been evaluated on rocks from the unconventional plays with the typical values of low porosities and permeabilities. The presence of surfactants improved oil recovery significantly in these reservoirs. Alvarez et al. (2017) studied the effect of surfactants on carbonate-rich core plugs from the liquid-rich part of the Wolfcamp, and Eagle Ford plays. Cationic, anionic, and a blend of anionic surfactants were evaluated. The contact angles

measured were as low as  $38^\circ$  for cationic surfactants compared to the original oil-wet CA values ( $121^\circ$  and  $127^\circ$ ) measured for Wolfcamp and Eagle Ford, respectively. The cationic surfactants showed the highest wettability alteration among surfactants tested as a result of the electrostatic interactions discussed. The cationic surfactants produced more oil than the other surfactants, with 47.3% OOIP in Wolfcamp samples and 9.0% OOIP in Eagle Ford samples.

Wang et al. (2012) surveyed wettability in Bakken Shale using two anionic surfactants, one amphoteric surfactant, and one nonionic surfactant. Cores were obtained from the middle member of the Bakken shale with porosity and permeability in the range of 1% to 16% and 0 mD to 20 mD, respectively. The cores were determined to be originally oil-wet or intermediate-wet. The surfactant formulations altered the wettability of the Bakken cores towards water-wet, and up to 6.8 to 10.2% OOIP incremental recovery following brine flooding was displaced by surfactant use. Surfactant imbibition tests resulted in improved recovery from 15.7 to 25.4% OOIP. The results showed that the surfactants were effective in improving oil recovery in shale formations.

The Bakken core samples evaluated by Morsy and Sheng (2013) had permeability and porosity values of 0.05md and 5.8%, respectively. Ten surfactants were evaluated in this study, and contact angle measurements were performed by drop shape analysis. Measurement showed that the Bakken oil surface was originally intermediate-wet, indicating equal affinity to both oil and water. In the presence of surfactant, the contact angle was reduced to  $20^\circ$  (from  $80^\circ$ ), indicating an increase in water-wetness. Spontaneous imbibition experiments showed a high recovery factor (up to 30%) with surfactants than

brine alone. The presence of surfactant was observed to be effective in improving recovery.

Alvarez & Schechter (2017) examined the combined effect of wettability alteration and reduction in IFT by surfactant additives in improving oil recovery in unconventional reservoirs in the Permian Basin. Nonionic, anionic, nonionic-cationic, and nonionic-anionic systems were evaluated. Contact angle results showed that all the surfactant systems altered the wettability of the original oil- and intermediate-wet cores to water-wet. The anionic surfactants showed the best results in lowering contact angles (as low as  $38^\circ$ ) compared to the other surfactants. Surfactants were able to reduce IFT to values from 21.8mN/m to as low as 0.4mN/m (for anionic surfactants). Anionic surfactants were the most efficient in lowering the IFT. It was also observed that IFT decreased as the surfactant concentration increased. The surfactants were able to increase oil recovery from shale cores (up to 33.9% OOIP) compared to the fracturing water alone.

The presence of surfactants has been shown to improve oil recovery by SASI from both conventional and unconventional cores. On calcite-rich surfaces, both anionic and cationic can lead to wettability alteration and, consequently, improved oil recovery from cores. However, anionic surfactants have limited use because of adsorption issues on carbonate-rich surfaces. While cationic surfactants may yield more favorable results, they are more expensive and require use at higher concentrations (Seethepalli et al., 2004). Anionic surfactants typically result in the most reduction in IFT (Alvarez et al., 2017). In the study by Seethepalli et al. (2004), the anionic surfactants lowered IFT to very low

values of approximately  $10^{-2}$  mN/m. However, the cationic surfactant did not generate such low IFT values even at a concentration of 1wt%.

## **2.6 Parameters for Surfactant EOR**

### **2.6.1 Salinity**

Brine composition or chemistry can alter the wettability of the rock surface. The presence of divalent ions, specifically sulfate, calcium, and magnesium ions, can change the surface charges on calcite-rich rocks and alter the wettability of surface to water-wet. Sulfate is a strong potential determining ion towards  $\text{CaCO}_3$  and is able to impart a negative zeta-potential to carbonate surface (Zhang and Austad 2005). Strand et al. (2006) showed that the addition of sulfate and other potential determining ions altered the wettability of originally oil-wet chalk surfaces to preferentially water-wet at high temperature ( $>194^\circ\text{F}$ ). Brine formulations with varying  $\text{Ca}^{2+}$  and  $\text{SO}_4^{2-}$  concentrations resulted in increased imbibition rate and oil recovery with temperature. Higher oil recovery was observed as the concentration of sulfate increased due to stronger adsorption of  $\text{Ca}^{2+}$  and  $\text{SO}_4^{2-}$  onto the chalk surface. The adsorption of  $\text{Ca}^{2+}$  and  $\text{SO}_4^{2-}$  onto the initially positively charged chalk surface facilitated the desorption of negatively charged carboxylic materials by changing the surface charge of the chalk.

Gupta and Mohanty (2008) also observed that divalent ions could alter the wettability of carbonates at high temperatures ( $>194^\circ\text{F}$ ). However, in this case, sulfate and calcium ions played a more significant role in altering wettability than magnesium ions. Sulfate and calcium ions were effective in altering wettability to water-wet conditions

when used individually and in combination. Higher sulfate concentration and moderate magnesium and calcium ions concentrations led to the highest degree of wettability alteration. A similar compositional system was suggested by AlShaikh and Mahadevan (2016) in their study of the impact of brine composition on calcite wettability. A combination of higher concentrations of sulfate anions with lower cation concentration and reduced salinity was found to lead to more water-wet conditions.

Shubham et al. (2012) also established the impact of these ions in altering wettability. In this study,  $Mg^{2+}$  ions were ineffective in altering wettability compared to  $Ca^{2+}$  ions. Also,  $SO_4^{2-}$  ions alone did not reduce the contact angle. Alotaibi et al. (2010) also identified the impact of sulfate ions in altering wettability. Different concentrations of sulfate ions were tested. Adsorption of the sulfate ions onto the carbonate surface decreased the positive surface charges. It was determined that an optimum sulfate concentration for effective wettability alteration.

The presence of carbonate and bicarbonate ions also impacts the wettability of the rock surface. Carbonate and bicarbonate ions are potential determining ions (Hirisaki & Zhang, 2004; Gupta & Mohanty, 2007). Hirisaki & Zhang (2004), in their experimental studies on carbonate rocks, identified that excess bicarbonate or carbonate ions made the surface negatively charged. The ions are able to impart a negative zeta-potential to a calcite/brine interface, which promotes water wetness. Gupta and Mohanty (2008) used  $Na_2CO_3$  to keep brine pH above the point zero charges of calcite. This changed the surface charge of the calcite from positive to negative.

Lastly, lower salinities have been determined to be more favorable towards water-wet conditions (Mohanty and Chandrasekhar, 2013; AlShaikh and Mahadevan, 2016). In contrast, higher salinity brines can be unfavorable for wettability alteration and, in some cases, increase oil-wetness (Shubham et al., 2012). Alameri et al. (2014), in their study of low salinity water flooding, examined the impact of different concentrations of diluted seawater in carbonate cores. Lower salinity seawater was the most effective in wettability alteration. In the study, the mechanism of wettability alteration involved the interaction of  $\text{Na}^+$ ,  $\text{Cl}^-$ ,  $\text{Ca}^{2+}$ ,  $\text{Mg}^{2+}$ ,  $\text{SO}_4^{2-}$  ions, and crude oil carboxylate ions ( $\text{R-COO}^-$ ) with the rock in the electrical double layer (EDL) near the surface of the carbonate pores. With one of the lower salinity brines tested, up to 8% incremental oil recovery was observed.

The presence of ions in the solution influences the electrostatic and hydrophobic interactions of the charged surfactant molecules. As discussed, these salt ions interact with the rock surface and will determine the degree of surfactant adsorption and, by extension, the surfactant effectiveness. Surfactant, in combination with brine high in potential determining ions, could lead to improved oil recovery. Also, the combination of surfactants and low salinity brine systems can further improve oil recovery due to the synergistic effect on wettability alteration (Teklu et al., 2018). The presence of salt ions in the solution also impacts the solubility of the surfactant molecules.

## 2.6.2 Temperature

Temperature has a significant impact on surfactant behavior. For surfactant systems to be effective, they must be stable at reservoir temperature. Thermal instability and aqueous instability have been identified as limitations of surfactant applicability at high temperatures (Sharma and Mohanty, 2013; Belhaj et al., 2020). Also, an increase in temperature may cause reduction in the adsorption of the surfactant molecule due to an increase in the kinetic energy of the molecules (Somasundaran and Fuerstenau, 1972; Ziegler and Handy, 1981).

Standnes and Austad (2000) observed that the imbibition rates of surfactants increased upon increasing temperature from 104°F to 158°F. While a 1.0 wt.% cationic surfactant concentration produced less than 30% of the oil at 104°F after 14 days, 60% was produced after the same time at 158°F. The rate of spontaneous imbibition of the aqueous surfactant solution at 158°F was almost double the rate of imbibition at 104°F. Gupta & Mohanty (2010) performed wettability measurements and spontaneous imbibition experiments with dilute concentrations of anionic and nonionic surfactants at varying temperatures (77°F to 194°F). Results showed that the degree of water wetness increased with temperature. An increase in temperature resulted in a reduction in oil viscosity and contact angle, which enhanced the oil recovery rate.

Belhaj et al. 2020 evaluated surfactant partitioning behavior with temperature at temperatures up to 176°F to 223°F. The partition coefficient,  $K_p$ , of the surfactant is defined as the ratio between the concentration of the surfactant in the oil phase and the aqueous phase. The behavior of surfactant partitioning varied with the increase of

temperature.  $K_p$  values were higher at 223°F compared to 176°F. It has been suggested that at low temperatures, low partitioning coefficient values are expected as a result of decreased solubility, which results in lower mobility of the surfactant molecules. However, at higher temperatures, more adsorption sites become available at the interface due to the increase of the interface surface area caused by the expansion of the solvents (Rosen and Kunjappu, 2012).

In most studies, surfactant effectiveness was observed to increase with increasing temperatures. However, these measurements were evaluated below 220°F. Studies for surfactant application – wettability alteration and IFT studies, solubility and stability studies, partitioning studies - in ULRs have not been evaluated at high temperatures. Above the boiling point of water, which is the base of the aqueous phase, a different behavior than previously suggested will be observed.

### **2.6.3 Co-surfactants**

Co-surfactants may refer to chemical compounds used in combination with surfactants to enhance their effectiveness (e.g., short-chain alcohols) or the combination of two or more different surfactants, i.e., surfactant blends for the same purpose. In this work, co-surfactants are used to describe surfactant mixtures or blends.

Surfactant blends show synergistic results with mixtures of anionic-cationic, anionic-anionic, zwitterionic-cationic, zwitterionic-anionic surfactant systems able to induce favorable wetting properties in rock samples. Single surfactant systems have



stability issues and reduced efficiency at high-temperature conditions. However, the combination of different surfactant types results in an improvement in surfactant behavior. Surfactant mixtures exhibit unique properties, improved interfacial characteristics and have also shown effectiveness in improving oil recovery.

Mixtures of two different surfactant types may lead to a synergy that produces a new compound with completely different characteristics. The new co-surfactant system produced may have improved properties making it less sensitive to temperature and improving the interfacial performance (Kurnia et al., 2020). Rosen (1989) surmised that the synergism between two surfactants in a mixture is a result of the mutual electrostatic attraction of their charged hydrophilic head groups or through Van der Waals attraction of their hydrophobic groups. Synergism can occur with a mixture of two surfactants that show equal surface or interfacial tension at their critical micelle concentration (CMC), such as with the use of oppositely charged surfactants with equal tail length.

Mixtures of anionic and cationic surfactants impart ultralow IFT and higher surface activity compared to single surfactant systems as a result of increased electrostatic interactions between the oppositely charged head groups as well as the intermolecular attraction between the hydrophobic hydrocarbon chains (Li et al., 2016). Kumari et al. (2019) observed synergism between mixed systems of anionic surfactant (sodium dodecyl sulfate) and cationic surfactant (cetyltrimethylammonium bromide) which resulted in a higher oil recovery compared to the single surfactant systems. The surface activity and effectiveness of the mixed surfactant systems varied based on the combination molar ratios. In some combination, the mixed systems resulted in a cumulative oil recovery of

up to 90% OOIP. Li et al. (2016, 2020), in their study on low permeability sandstone reservoirs, observed recovery of more than 16% OOIP upon application of novel mixtures of anionic-cationic surfactants in surfactant polymer flood. The mixture was effective in lowering the contact angle and the IFT of the system evaluated.

Mixtures with zwitterionic surfactants have also been investigated. Rosen (1990) showed that zwitterionic surfactants are able to interact favorably with other ionic surfactants. Zwitterionic surfactants capable of accepting or donating protons exhibit favorable interactions with both cationic and anionic surfactants. Generally, interactions between the zwitterionic and other ionic surfactants are largely dependent on the zwitterionic net charge. Singh and Miller (2021) performed contact angle experiments with synergistic surfactant blends of zwitterionic and anionic surfactants and observed that they were effective in altering the wettability of Eagle Ford and Wolfcamp rock samples favorably to water-wet contact angles and, in some cases, outperformed the individual surfactant system. Mixtures of anionic and zwitterionic surfactants have also been shown to result in reduced IFTs (Zhong et al., 2018).

Zeng et al. (2018) investigated the application of single surfactants, as well as surfactant blends for shale EOR at high temperatures. Contact angle results showed that most of the stable single surfactant systems and blends were effective in altering the wettability of the shale plates from oil-wet to preferentially water-wet in high and low salinity brines. The final contact angle measured was as low as  $18.1^\circ$  for one of the blends. In some cases, the blends resulted in lower CA values in the higher salinity brine. Oil recovery by single surfactant systems ranged from 1.3% to 23.6%, while oil recovery by

surfactant blends ranged from 17.8% to 21.4%. Generally, surfactant blends showed higher oil recovery compared to single surfactants.

In conclusion, surfactant application has been investigated in both conventional and unconventional reservoirs, with different mechanisms of operations proposed. Altering the rock wettability to preferentially water-wet has been determined to be the key to improving oil recovery by this method. The use of single surfactant systems, as well as surfactant blends, has also been investigated. The majority of these studies and applications have been conducted at low-temperature conditions (below 220°F), which opens up further areas of investigation for high-temperature applications.

### 3 METHODOLOGY

A workflow process was designed in order to carry out a successful surfactant selection study for high-temperature unconventional reservoirs. The workflow is presented in **Figure 5**. For the wettability alteration and IFT studies, a crude oil/brine/rock system representative of the reservoir was first established. The aging of cleaned rock chips sample, pre-processing of the crude-oil sample, and preparation of stable brine and surfactant solutions are essential to establish the crude oil/brine/rock system for the surfactant selection study.

The surfactants are tested in the crude oil/brine/rock system to assess their effectiveness in wettability alteration and their effect on the interfacial tension. Wettability was evaluated by measuring the contact angle produced by the crude oil/brine/rock system. Eight (8) single surfactant systems and three (3) surfactant blends (mixtures of cationic and zwitterionic surfactants) at five (5) combination ratios are investigated.

To observe wettability over a wide range of temperature conditions, contact angles were measured at both low-pressure temperature (LPT) and high-pressure high-temperature (HPHT conditions). LPT studies were first used in identifying surfactants able to induce favorable water-wet CA conditions and moderate IFTs. Surfactants, which showed promising results at LPT conditions, were then further evaluated by HPHT studies.

Based on HPHT studies, surfactants that were effective in producing water-wet systems and moderate IFTs at high-temperature conditions were selected for spontaneous

imbibition experiments. HPHT SASI experiments were carried out with the goal of observing the effect of the surfactant systems on the overall oil recovery in the reservoir core samples. It is expected that these surfactant systems, which produce water-wet CAs and moderate IFTs, are able to improve oil recovery from the rock core samples.

A combination of contact angle, IFT, surfactant stability, and imbibition results provides a solid framework for the selection of surfactant systems for field applications in high-temperature unconventional reservoirs with the end goal of improving/enhancing oil recovery.

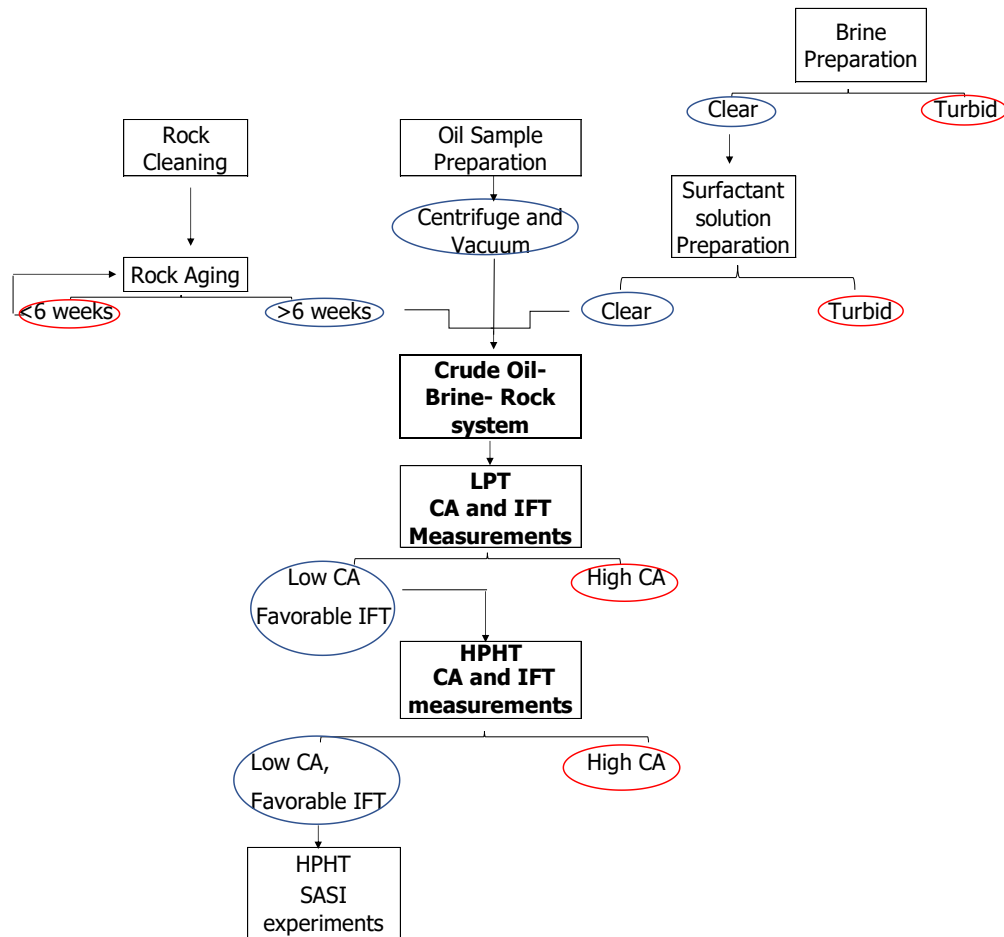


**Figure 5: Workflow chart for ionic surfactant studies.**

### **3.1 Rock and oil properties**

#### **3.1.1 Rock Sample**

Sidewall cores retrieved at different depths from an Eagle Ford well were used in all experiments for the surfactant selection study. The cores were received preserved in wax. The core samples were prepared by carefully removing the wax casing and retrieving the core sample enclosed within. The core samples were cut into 1cm by 1cm square chips for the contact angle studies. 1" diameter cores of lengths 2" to 3" were used in the spontaneous imbibition experiments.

X-Ray Diffraction analysis was performed on the retrieved core samples to examine the rock mineralogical composition. The rock sample was found to contain several minerals; Calcite, Quartz, Illite, Chlorite, Albite, Microline, Pyrite, Gypsum, and Dolomite, as shown in **Figure 6**. Calcite was found to be the most dominant mineral in the rock accounting for 61.9% of the mineralogical composition. Quartz and clay minerals also make up a significant portion of the rock minerals. Of the clay minerals present, Illite content is the most significant, accounting for 11.3% of the rock's mineral composition, while other clays are present in smaller percentages. The rock sample may be considered carbonate or carbonate-rich since the calcite content is about seven (7) times more than the Quartz (sandstone) content. Other rock properties are presented in **Table 1**.

Rock mineralogy influences rock wettability and is an important parameter in establishing the dynamics of wettability alteration. As established in the earlier section, carbonate-rich rocks typically have positive surface charges. As a result, electrostatic interactions between the rock surface and acidic compounds in the oil cause the surface to

become oil-wet (Standnes and Austad, 2003). The reverse will be the case for quartz-rich rock, which typically has negatively charged surfaces and a higher affinity for the basic components of the crude oil.

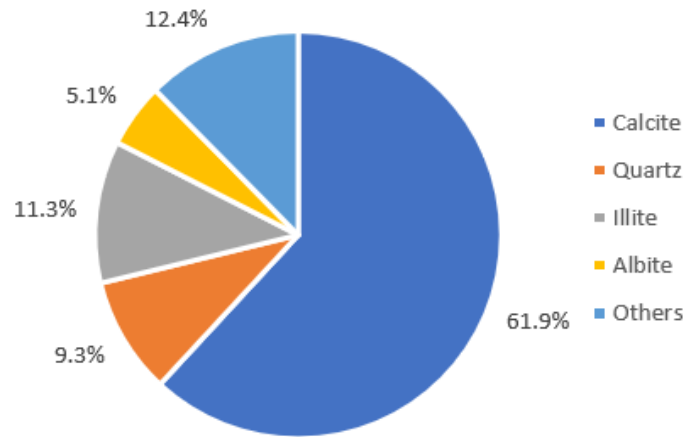


**Figure 6: Mineral composition of Eagle Ford rock sample (Sample depth: 14,049ft to 14,050ft).**

Rock Properties	Values
Porosity (%)	12.5
Permeability ( $\mu$ D)	0.11
Density (g/cc)	2.3
TOC (wt.%)	6.13

**Table 1: Eagle Ford sample rock properties.**

### 3.1.2 Rock cleaning and aging

In order to conduct a robust and detailed surfactant selection study, contact angle measurements were made on the square rock chips under a variety of conditions: preserved, cleaned, and aged states. For the preserved chips' case, contact angle

measurements were made on freshly cut chips immediately after the core preserved wax casing was removed. Chips were cleaned by following the procedure described in **Table 2**.

Chips were then aged in the crude oil at reservoir temperature for different time durations in order to determine an optimal aging time. Once optimal aging time was established, cores or chips were subsequently aged for that time duration. Rock samples adsorb oil during aging and become oil-wet, restoring the reservoir wetting conditions. For each sample case, 8-10 measurements were made to ensure consistency, accuracy, and repeatability.

<b>Step</b>	<b>Cleaning/aging procedure for rock chips</b>	<b>Time duration</b>	<b>Purpose</b>
1	Toluene soak	Two days	To remove hydrocarbons, including asphaltenes.
2	Methanol soak	One day	To remove salt contaminants and brine
3	Vacuum Oven	One day	To remove gas and cleaning chemicals.
4	Aged in crude oil at high temperature	Six weeks (optimal aging time)	To restore original reservoir wetting conditions

**Table 2: Rock cleaning and aging procedure for rock chips in contact angle study.**

For the spontaneous imbibition study, cores are cleaned using the Dean-Stark method. The cores are boiled in toluene in the Dean-Stark apparatus (**Figure 7**) for two weeks. The procedure is repeated for methanol for one week, after which the cores are



then dried in the oven for one week. To re-saturate the cores and restore the original oil in place (OOIP), the cores were aged in crude oil at reservoir temperature for 6 to 8 weeks.

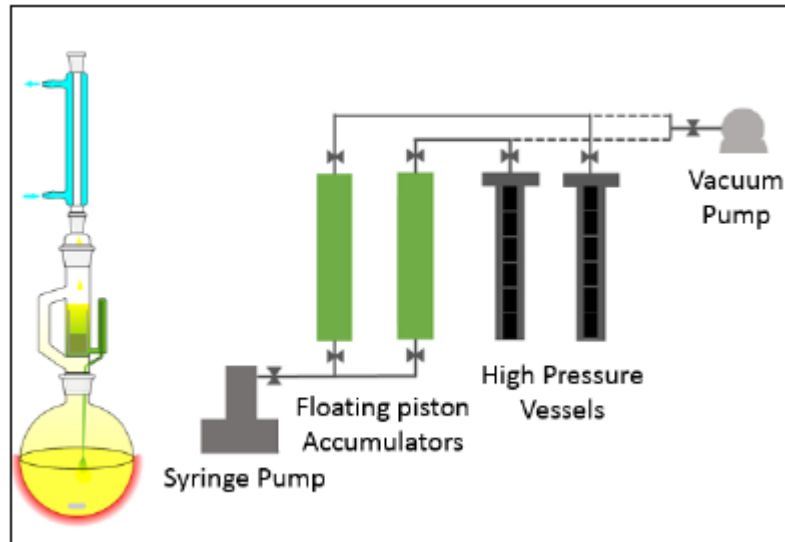


**Figure 7: Schematic of the Dean-Stark apparatus for core plug cleaning (left) and the pressurized saturation vessels and pumps (right).**

### 3.1.3 Oil Sample Properties

The crude oil used in the study is the corresponding oil from the Eagle Ford formation. Saturates, Asphaltenes, Resins, and Aromatics (SARA) analysis was performed on the oil sample. SARA analysis identifies the amount of polarity or non-polarity of the components of the oil sample. The extent of the polarity of the different fractions is shown in **Figure 8**. The SARA measurements showed that the oil sample comprises 88% saturates, 8% aromatics, 4% resins, and 0% asphaltenes. This indicates that the oil sample contains more non-polar fractions.

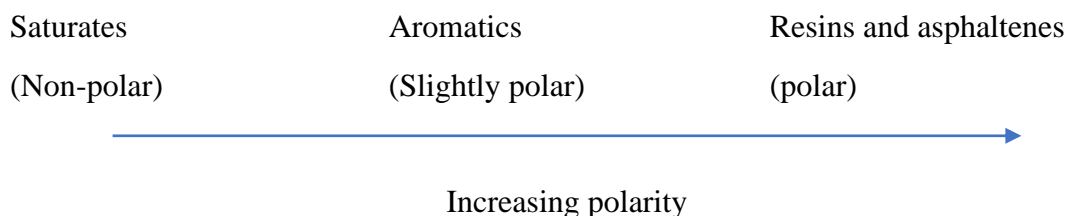


**Table 3: Polarity of crude oil fractions.**

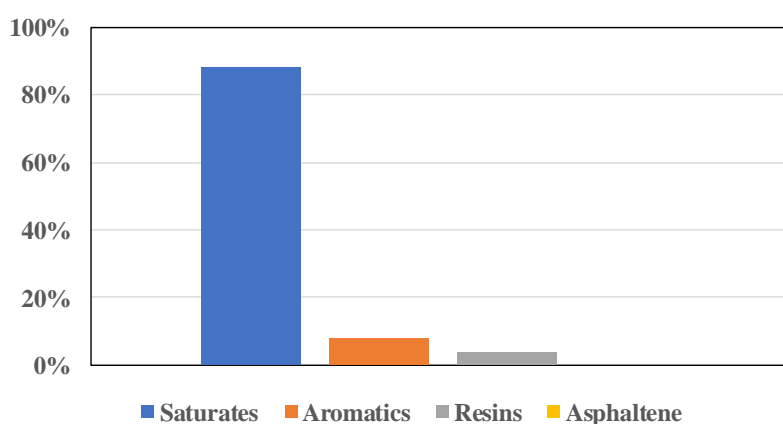


**Figure 8: SARA composition of crude oil sample.**

To characterize the oil sample, density was measured as a function of temperature. The Anton-Paar DMA 4100M shown in **Figure 9** was used for the oil density measurements at atmospheric pressure. The equipment measures density at different temperatures up to the temperature at which the sample begins to vaporize. Since oil density is a linear function of temperature, density values at higher temperatures can be extrapolated. For the vacuumed oil used in the study, at ambient temperature and 170°F, the density of the Eagle Ford oil was 0.7787g/cc and 0.7390g/cc, respectively. The oil density is an important parameter in determining the interfacial tension of the oil and

water. API gravity of the oil was determined to be 50.15. Based on density and API gravity measurements, the oil sample was identified as light oil. The total acid number (TAN) was also determined to be 0.02 mgKOH/g oil.

**Table 4** highlights the properties of the oil sample.



**Figure 9: Anton-Paar DMA 4100M for measuring density.**

Properties	Values
TAN (mgKOH/g oil)	0.02
Density at 70°F (g/cc)	0.7787
Density at 170°F (g/cc)	0.7390
API (°)	50.15

**Table 4: Properties of Eagle Ford oil sample.**

### 3.1.4 Oil Sample Preprocessing

The oil sample was centrifuged to remove solid particles, water, and other impurities, which may cause inaccuracies in results and affect the repeatability of measurements. The crude oil sample was also vacuumed to remove gas components which may impair the contact angle measurements.

## 3.2 Fluid system properties

### 3.2.1 Surfactant Properties

Three ionic surfactant types were evaluated in this study - cationic surfactants, which have a positive head charge; anionic surfactants, which have a negative head charge; and zwitterionic surfactants, which have both positive and negative charges in their head group. Surfactant blends (co-surfactant systems) at different combination ratios were also evaluated. The surfactants were tested at different concentrations. Surfactant concentration is measured in gallons per thousand gallons (gpt). In the laboratory, surfactants were prepared in terms of wt.% (1 gpt is the equivalent of 0.1 wt.%). The required surfactant concentration is prepared with deionized water (DI Water) or brine. The required amount of surfactant is mixed with the required amount of solution; the mixture is then agitated for about 10-15 minutes till it is uniform and homogenous.

The surfactants evaluated are listed in **Table 5**. The molecular structures of the surfactants are shown in **Figure 10**. The cationic surfactants evaluated (C-1, C-2, C-3, C-4, C-5, C-6, and C-7) have tail lengths within C10 – C18 range with either Trimethyl Ammonium Chloride (TAC) or Dimethyl Ammonium Chloride (DAC) in their head

groups. Anionic surfactants evaluated (A-1, A-2, A-3, A-4, and A-5) have tail lengths in the range C20 – C24 with different lengths of Propylene Oxide Sulfates (POS) lengths (7 – 13) in their head groups or an Internal Olefin Sulfonate (IOS) head group. The zwitterionic surfactant evaluated (Z-1) is the Cocoamidopropyl betaine (CPAB) type and contains a long hydrocarbon chain. A nonionic surfactant type, N-1, was evaluated in the surfactant time stability study.

SURFACTANT	CHARGE	HEAD	TAIL	TAG
C18TAC	C	TAC	C18	C-1
C12TAC	C	TAC	C12	C-2
C12TAC-37	C	TAC	C12	C-3
C16TAC-25	C	TAC	C16	C-4
2C10DAC	C	DAC	2 x C10	C-5
C16TAC-50	C	TAC	C16	C-6
S-13A	A	7PO + AS	C12 – C13	A-1
S-13C	A	11PO + AS	C12 – C13	A-2
S-13D	A	13PO + AS	C12 – C13	A-3
S-2	A	IOS	C15 – C18	A-4
S-3B	A	IOS	C20 – C24	A-5
CG-50	Z	B	C12 *	Z-1
TD-12	N	12 EO	C13	N-1
C12 *	C12 Cocoamidopropyl			
B	Betaine			
TAC	Trimethyl Ammonium Chloride			
DAC	Dimethyl Ammonium Chloride			
IOS	Internal Olefin Sulfonate			
EO	Ethoxylate			

**Table 5: List of ionic surfactants evaluated (C = Cationic, A = Anionic, Z = Zwitterionic, N = Nonionic).**

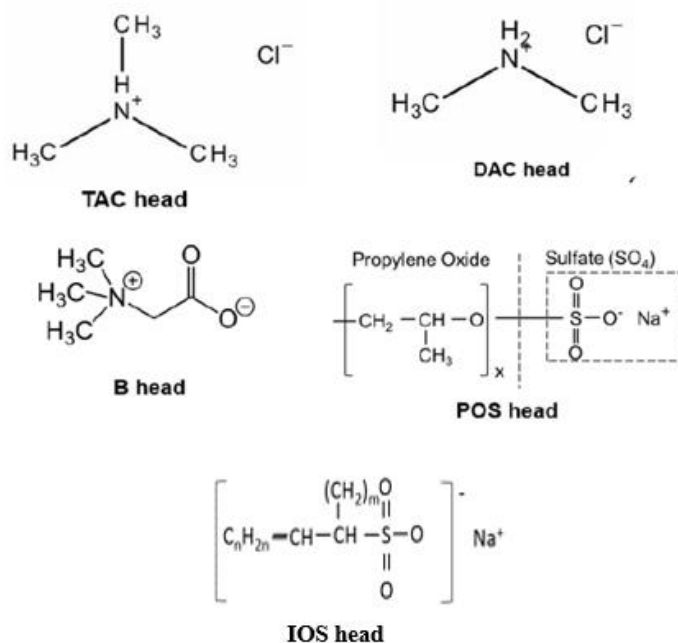


**Figure 10: Molecular structure of surfactant head groups.**

### 3.2.2 Brine Properties

Different brine systems were evaluated in the surfactant selection, surfactant stability, and salinity studies. The brine sample is prepared in the laboratory by adding the required mass of salt to the required volume of DI water based on a recipe and agitating the mixture for about 1-3 hours. Two brine samples were prepared based on the recipe acquired for the produced water and make-up water. The make-up water, tagged 'A', is a low TDS brine of 0.2%. The produced water from the formation tagged 'B' contained total dissolved solids (TDS) of approximately 2.50%.

Other brine samples evaluated were formulated using NaCl salt alone to attain different levels of salinity. A range of salinities from 1% - 24% were evaluated across various sections of the study. Details on the ionic composition of brines are shown in

**Table 6.** The brines were used in the formulation of various surfactant solution systems.

DI water alone was also used in the formulation of some surfactant systems.

Brine Tag	A	B	1D	2D	1E	2E	1C	2C	3C
TDS	0.2%	2.5%	1.0%	2.0%	2.5%	4.0%	6.0%	12.0%	24.0%
<b>Ions</b>									
Na +	497.32	8937.30	3333.3	6666.7	8,333.3	13333.3	20000	40000	80000
Cl -	813.60	14474.56	6666.7	13333.3	16666.7	26666.7	40000	80000	160000
Mg 2+	8.98	21.03	0	0	0	0	0	0	0
K +	24.47	268.93	0	0	0	0	0	0	0
Ba 2+	0.06	11.24	0	0	0	0	0	0	0
Li 2+	0.18	0	0	0	0	0	0	0	0
Sr 2+	1.01	201.04	0	0	0	0	0	0	0
Ca 2+	95.72	259.93	0	0	0	0	0	0	0
HCO <sub>3</sub> -	0	292.58	0	0	0	0	0	0	0
CO <sub>3</sub> 2-	2.21	0	0	0	0	0	0	0	0
Br -	2.16	104.27	0	0	0	0	0	0	0
F -	0.43	0	0	0	0	0	0	0	0
SO <sub>4</sub> 2-	229.48	39.21	0	0	0	0	0	0	0

**Table 6: Composition of synthetic brines.**

### 3.2.3 Aqueous phase stability

In this study, aqueous phase stability is defined as the complete equilibration of the salt ions and or surfactant molecules in the aqueous phase (water or brine) such that no turbidity or salt precipitation is observed. Typically, CA or IFT measurements are made using a visual cell on both LPT and HPHT apparatus. Images of the oil drop are recorded using a camera, and the data is then analyzed via a computer program. In order to be able to generate the images, light must pass through the visual cell. If the solution is cloudy or unclear, the equipment camera is unable to generate usable images of the oil drop during the experiment. Depending on how turbid the surfactant system is, the images recorded can vary from dark grey to completely dark pictures. In any case, the computer program

is unable to analyze the images and cannot generate contact angle or IFT results. This is one reason why unstable surfactant systems cannot be used in experimental studies.

### **3.2.3.1 Brine Stability**

Brine samples become turbid as a result of the limited solubility of the comprising salts; the presence of a significant amount of carbonate or bicarbonate ions; and or precipitation from interactions between divalent cations and divalent anions or bicarbonate anions in the solution. Turbid brine systems are unusable in contact angle and IFT measurements. When the brine system is not completely turbid, but a significant amount of undissolved salts and precipitates are present, lack of solution homogeneity will lead to inaccuracies in contact angle and IFT measurements. The representative brine sample prepared based on the produced water composition for the formation being studied was turbid, as shown in **Figure 11**. Hence, the salt composition was reformulated to ensure brine sample clarity while still accounting for all the required ions.



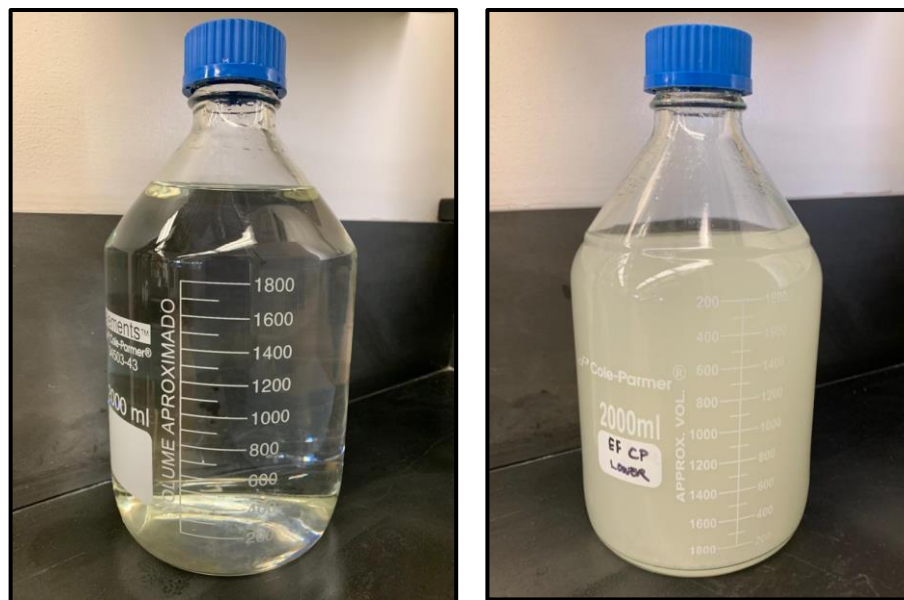


**Figure 11: Images of (I) clear and (II) turbid brine samples.**

### **3.2.3.2 Ionic surfactant Stability**

Stability is a very important property in the application of ionic surfactants. It is dependent on the brine composition, salinity, and temperature of the system. Ionic surfactants have charged structures, which makes them sensitive to the salt composition within the aqueous phase. When a surfactant is stable in an aqueous brine phase, a perfectly clear solution is observed. However, in the case of an unstable solution, the solution is unclear or turbid, and emulsions may be clearly visible.

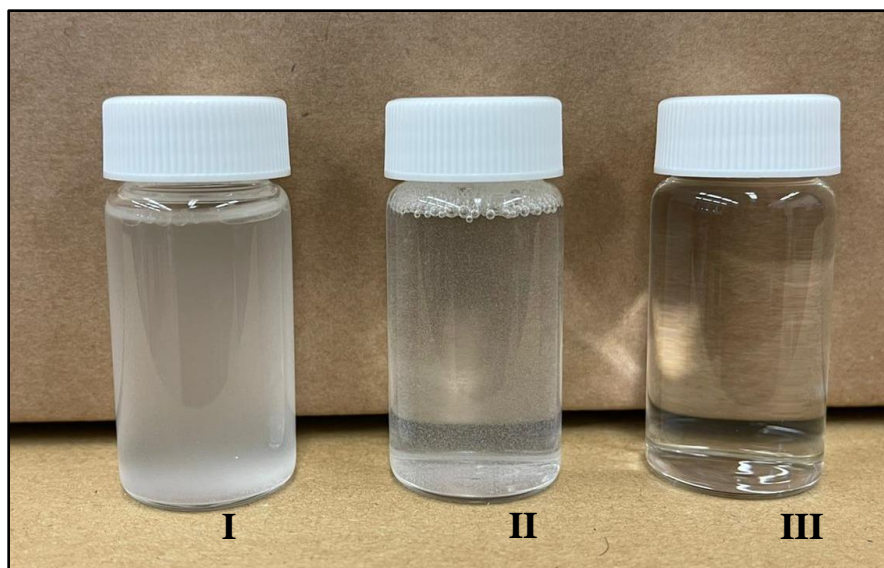


**Figure 12: Images of unstable (I and II) and stable (III) surfactant solutions.**

**Figure 12** displays images for stable and unstable surfactant solutions. Vial I shows a turbid solution indicating that the surfactant solution is unstable. Vial II shows a less turbid solution than vial I; however, the surfactant is still unstable in the mixture. Vial C shows a perfectly clear solution indicating that the surfactant is well equilibrated in the brine, and there are no precipitates or emulsions formed.

One of the determining factors of surfactant stability is the surfactant type. The different surfactant types evaluated showed different degrees of stability. While cationic surfactants typically formed stable solutions in brine, most anionic surfactant solutions were unstable. This stability difference between the anionic and cationic surfactants was most visible in the preparation of surfactant blends. Anionic surfactants in combination with cationic or zwitterionic surfactants resulted in unstable solutions. Surfactant solutions A-1, A-2, A-3, A-4 and A-5 at low concentrations 0.02 wt.% - 0.1 wt.% resulted in turbid unstable solutions in combinations with either C-1, C-2, C-4, or Z-1 at 0.1 wt.%

concentration. On the other hand, cationic surfactants resulted in stable solutions in combination with Z-1.

Brine salinity and composition are other determining factors. Typically, in the absence of salt ions in the solution, such as the case with DI water, ionic surfactants are stable. However, the presence of salt ions impacts the stability of surfactants in the aqueous phase to varying degrees. Anionic surfactants showed greater stability limitations compared to other ionic surfactants. Surfactants A-4 and A-5, which are internal olefin sulfonate types (head group) with long hydrophobic tails, C<sub>15</sub> – C<sub>18</sub> and C<sub>20</sub> – C<sub>24</sub>, respectively, resulted in turbid solutions at concentration 0.2wt.% in brine A. However, surfactant solutions A-1, A-2, and A-3 of the propoxyl sulfate types with shorter hydrophobic C<sub>12</sub> – C<sub>13</sub> were stable and clear at the same concentration in brine A. This is indicative that anionic surfactant tail length plays a role in the stability of the surfactant system. Similarly, 0.2wt.% of A-4 and A-5 resulted in turbid (unstable) solution in brine 1E. The same concentration of A-1 and A-2 produced clear solutions in the brine 1E. However, surfactant A-3, which has a larger head group but the same tail length as surfactants A-1 and A-2, was unstable in this case. These details are displayed in **Figure 13**. The trend of results indicated that as the salinity of the aqueous phase increased, the stability of the surfactants with longer hydrophobic tails and larger head groups decreased.

Temperature was also shown to have a significant effect on surfactant stability. Surfactant solutions may be stable during preparation at room temperature and become turbid upon heating and temperature increase.

	DI	A	1E
A-1	✓	✓	✓
A-2	✓	✓	✓
A-3	✓	✓	✗
A-4	✓	✗	✗
A-5	✓	✗	✗

**Figure 13: Aqueous phase stability of anionic surfactants (A-1, A-2, A-3, A-4, and A-5) at 72°F at concentration 0.2 wt.% in DI, brine A, and brine 1E. (Green color represents stable mixture. Red color represents an unstable mixture).**

### 3.2.4 Surfactant and rock damage

Some surfactants were observed to cause damage to rock samples. This behavior was observed specifically with cationic surfactants at slightly elevated temperatures. For example, surfactant C-5 showed severe rock damage, as shown in **Figure 14**. The molecular structure of the surfactant is made of a double C<sub>10</sub> tail with dimethyl ammonium chloride in its head. Any concentration of C-5 surfactant solution in EFM brine was observed to cause damage to the calcite-rich shale rock chip. The damage is characterized by the dissolution of the rock structure. The solid rock lattice was observed to fracture and break down in the surfactant solution. The damage to the rock chip was also observed to be proportional to the concentration of the surfactant solution: the damage was observed to increase as the C-5 solution concentration increased.

To investigate the observed behavior, the pH of the surfactant was evaluated. An acidic pH may explain rock damage resulting from chemical reactions with the calcite-rich rock. **Figure 15** displays results of the pH study for the surfactant C-5 and other surfactant systems, C-1, A-1, and Z-1, at a concentration of 0.2 wt.% in DI and brine A aqueous phases. The results showed that while the surfactant C-5 solution was slightly

acidic, it was less acidic than the C-1 surfactant, which resulted in minimal rock damage. Different concentrations of surfactant C-5 solutions had the same pH value. Hence, the acidity of the surfactant solution did not explain the dissolution of the calcite-rich rock.

It was observed that salinity had an impact on the surfactant behavior in relation to rock damage. Higher salinity systems resulted in less rock damage compared to lower salinity systems. However, the main reason for the rock damage in the presence of surfactant molecules remains to be established.

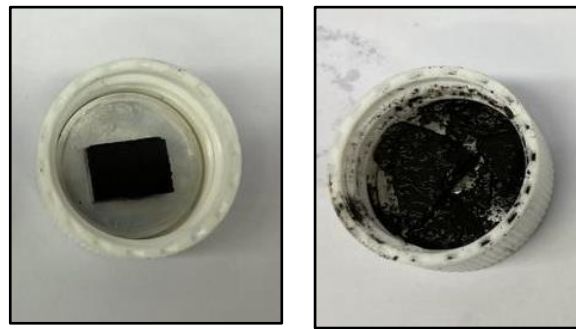


**Figure 14: Rock chips retrieved from C-5 solution at a) 72°F b) 200°F.**

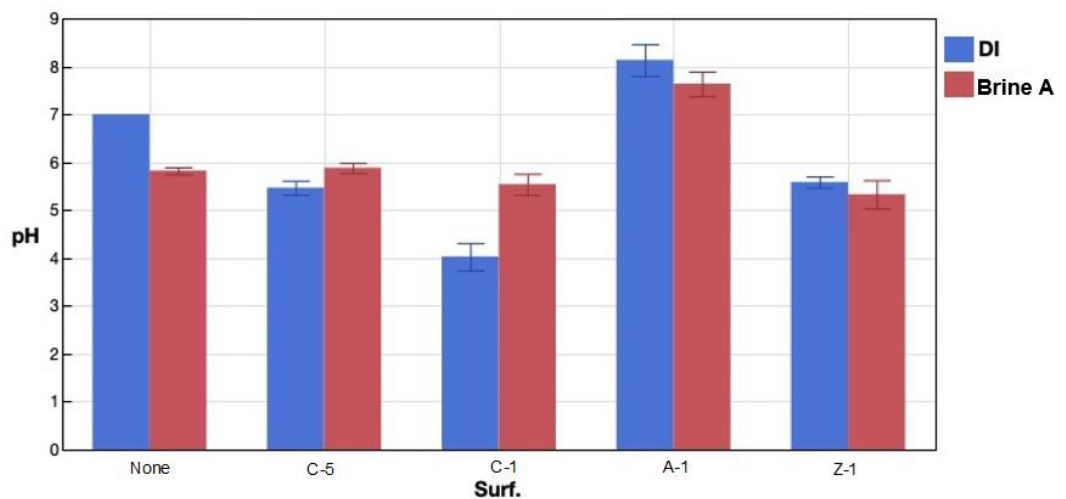


**Figure 15: pH of ionic surfactants at 0.2 wt.% concentration.**

### 3.3 Contact angle and IFT measurements

Two types of CA and IFT measurements are carried out:

1. High Temperature – Atmospheric Pressure measurements (tagged LPT) performed at 170°F.
2. High Temperature – High-Pressure studies (tagged HPHT) performed over a wide range of temperature and pressure conditions up to 325°F.

#### 3.3.1 LPT CA and IFT Measurements

**Figure 16** displays the different experimental set-ups for contact angle and IFT measurements, while **Figure 17** shows CA and IFT images extracted during measurements. LPT CA measurements are performed by utilizing the captive bubble method on the Dataphysics Optical Contact Angle goniometer (OCA15 Pro). Contact angle measurements were made by the captive bubble method. The experiment is set up by placing the square rock chip (1cm x 1cm) on a special stage submerged in the aqueous phase. The rock-aqueous phase system occupies a glass container. Typically, the aqueous phase is filled to  $\frac{3}{4}$  the height of the glass cell (about 60 ml volume). The glass cell is then set on the equipment's stage. The temperature of the equipment's stage and, by extension, the aqueous phase can be regulated on the apparatus or by using the system's software. The apparatus syringe is filled with the oil sample. A J-shaped needle is used to dispense 0.15-0.20  $\mu\text{L}$  of oil, which is then brought up to the bottom of the rock surface. The oil adheres as a drop to the surface of the rock sample at an angle. A built-in high-speed

camera is used to capture the image of the oil drop on the rock surface. The contact angle of the oil bubble on the surface was estimated using the equipment's computer program. The estimated contact angles were then converted by applying **Eq 3-1** so that conventional interpretation systems may be applied. To ensure repeatability and accuracy of measurements, 8-10 trials were taken, and an

$$\theta_w = 180 - \theta_o \quad (3-1)$$

Where,  $\theta_o$  is the contact angle in degrees with respect to the oil phase as estimated by the apparatus and  $\theta_w$  is the required contact angle in degrees estimated with respect to the aqueous phase. The contact angles reported throughout this document will be that of the water phase.

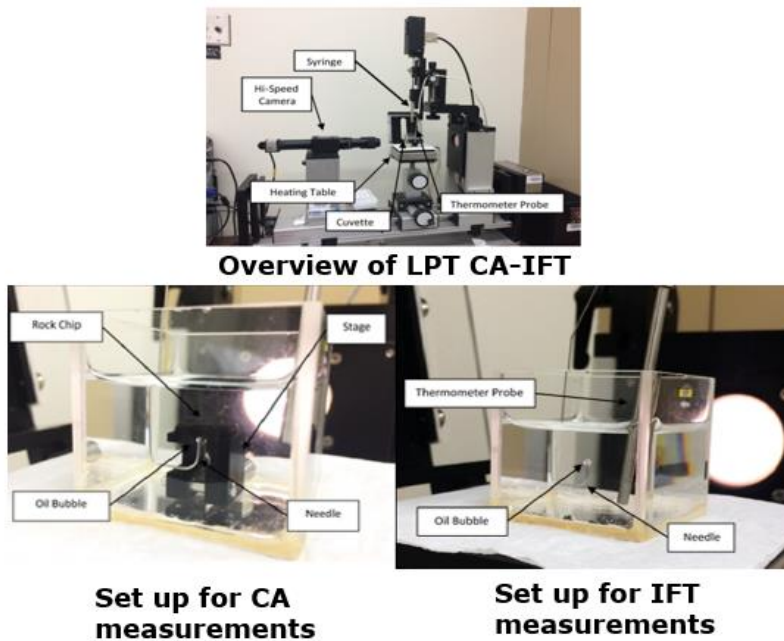


**Figure 16: Dataphysics OCA Pro Apparatus for LPT CA and IFT measurements.**

For LPT interfacial tension (IFT) measurements, the pendant drop method was utilized. For this experimental set-up, oil is dispensed upward through the J-shaped needle submerged in the aqueous phase. This orientation of the drop is important because of the density difference between the oil and aqueous phases. The oil is dispensed continuously till it lifts off the needle. A built-in high-speed camera records the entire experiment. The video recording is reviewed and analyzed on the computer program, where the densities of the drop phase (oil) and the aqueous phase (brine or surfactant mixture) are inputted. The IFT at the exact point when the oil drop is just about to leave the needle is then noted as the IFT value for the oil-aqueous phase system.

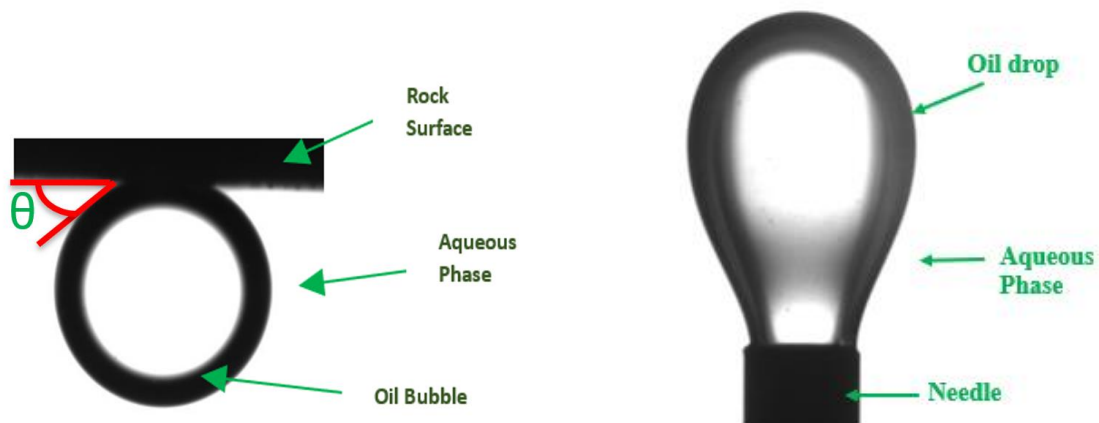


**Figure 17: Images recovered from 1) CA and 2) IFT measurements.**

### **3.3.2 HPHT CA and IFT measurements**

HPHT measurements are performed using the Biolin Theta HPHT apparatus displayed in **Figure 18**. The apparatus has a maximum pressure limit of 410 Bar (5946 psi) and a maximum temperature limit of 392 °F (200 °C). It consists of a high-pressure



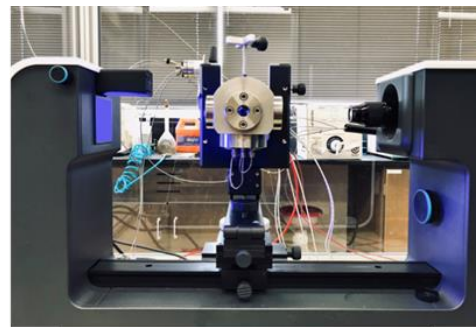
steel chamber where the crude oil/rock/brine system is housed. The aqueous phase is introduced into the chamber using a syringe. The rock chip is placed on a stage housed within the chamber. The crude oil sample is dispensed on the bottom-facing rock sample through a needle connected to an external oil line. Once the crude oil/brine/rock system is set up, the cell chamber is sealed.

Pressure is built up in the chamber using a pump that regulates the piston's movement in the high-pressure steel chamber. Another pump is used in dispensing the crude oil sample on the rock surface. The goal of pressurizing the system is to prevent vaporization of the aqueous phase at temperatures above its boiling point. Hence, temperature and pressure are increased in tandem during the CA and IFT measurements. Typically, measurements are performed within the temperature range of 70°F (room temperature) up to 355°F. During measurements, pressure can be increased from 500 psi to 3000 psi.

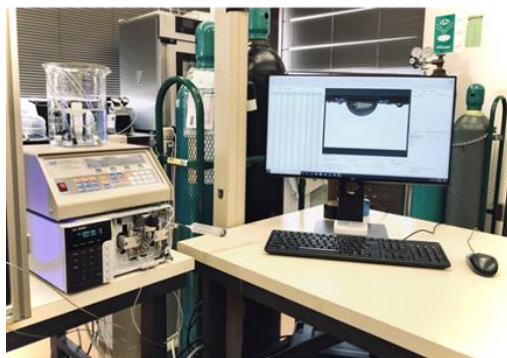
The HPHT CA measurements are performed using the captive bubble method as well. Typically, an oil drop is dispensed on the rock surface at low pressure and temperature conditions. The temperature and pressure of the system are then increased up to the required conditions. Hence, the behavior of a singular drop is monitored for the entire length of the experiment. The apparatus's camera is used in recording the entire experimental process. The contact angle of the oil drop on the surface is then estimated from the video file using the equipment's computer program. Similar to the LPT measurements, the pendant drop method was also applied for the HPHT IFT measurements.



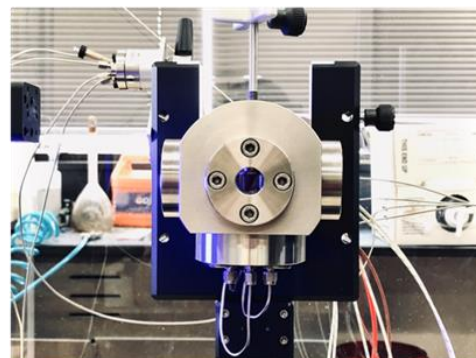
**Overview of HPHT CA-IFT**



**Cell and Camera System**



**Pump and Software Controller**



**HPHT Cell**

**Figure 18: Biolin Theta apparatus for HPHT CA and IFT measurements.**

### **3.4 Spontaneous Imbibition Experiments**

Surfactant-Assisted Spontaneous Imbibition (SASI) experiments are a crucial step for surfactant selection study for field applications. SASI experiments quantify the amount of oil recovery expressed by the recovery factor (RF) of the surfactant systems on the saturated rock core samples. The HPHT SASI experiments require a custom setup because typical glass Amott cells are unable to withstand the required temperature and pressure conditions for this study. The modified set-up for HPHT SASI is presented in **Figure 19**. The set-up consists of a core holder shown in **Figure 20**, which contains the fluid phase

and the core sample. The accumulators control the flow of fluid during the experiments, while Pump 1 is used to regulate the pressure of the system. Pump 2 controls the pressure at the back pressure regulator (BPR) and allows for fluid flow when there is a pressure differential. The Temperature and Pressure of the SASI system are observed on a computer that uses a program to chart changes in temperature and pressure values. During oil production, the oil sample is collected in a graduated cylinder, which measures the volume of oil produced.

The HPHT spontaneous imbibition experiments were performed on cores that had been cleaned and aged following the procedure earlier described. **Table 7** provides details on the dimensions of the core plugs evaluated in the SASI studies. The core plugs were placed horizontally at the bottom of the HPHT cell, which contains about 500ml of surfactant solution. A total of seven (7) fluid systems were evaluated in this study. The SASI experiments were performed for a time period of 8 days (192 hours). Due to set-up constraints and measurement conditions (high temperature and high pressure), the amount of oil expelled from the rock could not be monitored over an incremental time frame. The total amount of oil expelled from the rock was determined at the 144h and 192h time mark.

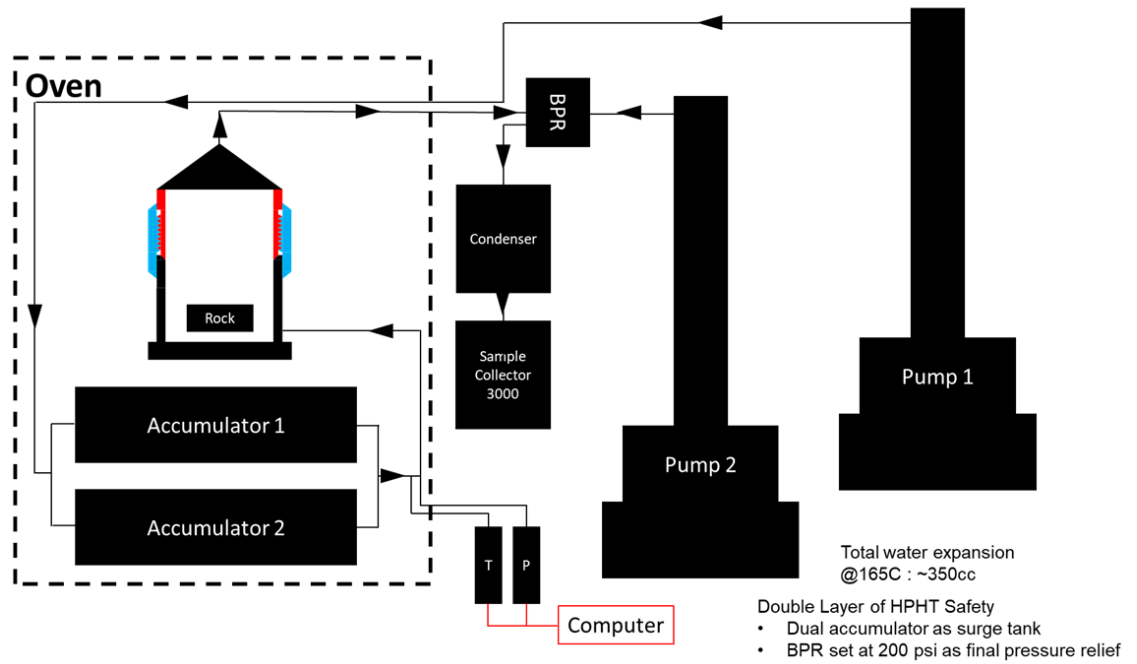


**Figure 19: Set-up for HPHT SASI experiments.**



**Figure 20: HPHT core holder cell for spontaneous imbibition experiments.**

Core Sample	Diameter (in)	Length (in)	Bulk Volume (cc)	Mass	Rock Density (g/cc)
				After Cleaning (g)	
<b>Q0</b>	0.985	1.970	24.547	56.004	2.310
<b>Q1</b>	0.946	2.049	23.527	60.115	2.555
<b>Q2</b>	1.024	2.167	29.205	63.505	2.223
<b>Q3</b>	0.985	1.891	23.565	54.595	2.349
<b>Q4</b>	0.985	2.049	25.529	59.170	2.367
<b>Q5</b>	0.985	2.916	25.275	62.994	2.367
<b>Q6</b>	1.024	2.049	27.612	60.334	2.214

**Table 7: Dimensions and data of core samples**

Computed Tomography (CT) scan, which is a non-destructive imaging technique, was used to observe the fluid saturation distribution within the core sample after oil was produced during spontaneous imbibition experiments. The Toshiba Aquilion TSX-101A CT scanner (shown in **Figure 21**) was used. The CT scan emits x-rays that pass through the rock sample and are then reabsorbed. These signatures are processed by a computer program and are converted to a CT number variable by a complex algorithm. This CT number is a function of density. High CT number is correlated to high-density value and vice versa. Hence, since the aqueous phase density is higher than the oil density, a high CT number indicates the presence of the aqueous phase, while a lower CT number indicates oil saturation. Images gathered from the CT scan were processed using ImageJ software. Color-coded slices were generated based on density contrast.

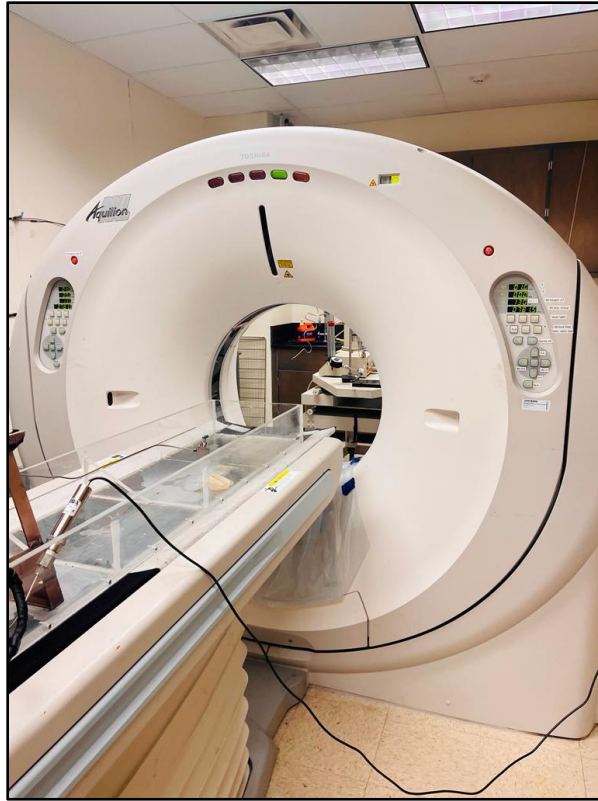


**Figure 21: Toshiba Aquilion TSX-101A CT-scan equipment.**

#### 4 TIME STABILITY OF SURFACTANT SYSTEMS

The stability of ionic surfactants in the crude oil/brine/rock system presents an important issue. Typically, differences exist between the behavior of ionic and nonionic surfactants due to different molecular structures. While nonionic surfactants are less sensitive to salt ions present in the aqueous phase, the behavior of ionic surfactants is dictated by the brine composition and salinity. The presence of salt ions in the aqueous phase has been observed to cause a change in the surfactant behavior over time.

Initially, a surfactant may be effective in imparting some contact angle value. However, over time, interactions between the surfactant and the salt ions in the aqueous phase may cause the surfactant to become less effective. Surfactants become less effective over time as a result of increased solubility in the aqueous phase. Depending on the degree of salinity and the minerals present, surfactant molecules may re-dissolve into the brine phase as time proceeds. This indicates the surfactant's preferential interaction with ions in the brine phase rather than at the oil/brine/rock interface. Technically, this is explained as an increase in surfactant partitioning towards the brine phase.

To establish the surfactant time dependency phenomenon, the change in the contact angle of a singular drop of oil on a rock surface surrounded by an aqueous phase was monitored over time. The measurements were performed at a temperature of 72°F and ambient pressure conditions. The change in contact angle ( $\Delta CA$ ) is defined as the difference between the final and initial contact angle of the system. High CA values show that the surface is oil-wet, and a positive  $\Delta CA$  value indicates a reduction in the

surfactants' ability to alter the rock surface wettability. Small  $\Delta CA$  values over the time period evaluated indicate good time stability. At the same time, large  $\Delta CA$  values, where the difference between the initial and final CA values is significant, indicate poor time stability.

The change in contact angle was observed to be a function of surfactant head charge, surfactant concentration, and brine salinity. Surfactants with different head group charges exhibited different time stability behaviors. The surfactant concentration had a significant effect on the time stability of the system, dictating varied behavior based on the salinity of the aqueous phase. There is a very interesting interplay between the surfactant concentration and the brine salinity. A good understanding of the balance between both factors (surfactant concentration and brine salinity) will help in the creation of stable and effective surfactant systems.

#### **4.1 Time stability of ionic and nonionic surfactant systems**

Time stability was first established as a more significant issue for ionic surfactants. Ionic surfactants (C-1 and A-1) and nonionic surfactant (N-1) were investigated at the same concentration of 0.2wt% in brine A at a temperature of 72°F and ambient pressure conditions.

**Figure 22** displays results for contact angle values of a singular oil drop measured over time for up to 120 minutes. Results for cationic surfactant (C-1 highlighted in red color), anionic surfactant (A-1 highlighted in green color), and nonionic surfactant (N-1 highlighted in blue color) systems in brine A are presented. The baseline for each case is



established based on the initial CA value. This is shown so that the level of deviation from the ideal case is easily observed. The base case (highlighted in brown color) is also presented, i.e., CA value in brine A with no surfactants present for comparison. A time-lapse of CA images for the investigated systems are displayed in **Figure 23**.

As observed in **Figure 22**, the oil drops in ionic surfactant systems (C-1 and A-1) were observed to spread and become more oil-wet over the 2-hour time frame evaluated. However, very minimal spreading was observed for nonionic surfactant mixtures. Initially, the three surfactant types tested were effective in altering the contact angle of the aged chips from oil-wet ( $133.9^\circ$ ). C-1 initially altered the wettability to intermediate-wet at  $70.7^\circ$ ; A-1 initially altered wettability to water-wet at  $53.5^\circ$ . N-1 showed the highest wettability alteration tendency by lowering the contact angle to  $35.1^\circ$ . Within the first five minutes, notable change was observed in the contact angle for the C-1 and A-1 aqueous phases, while the contact angle in N-1 remained fairly constant.

By the 25 minutes mark, the CA value of the C-1 system had increased by 21.5%. The CA value in the A-1 system had increased by 76.6%. On the other hand, only a 3.7% change in the CA value was observed for the N-1 system. At 45 minutes, the change in CA for the C-1 system is up to 27.9% increasing from  $70.7^\circ$  to  $95.9^\circ$ . The CA value continued to increase and did not stabilize. For the surfactant A-1 system, at 45 minutes, the CA value had changed by 87%, increasing from  $53.4^\circ$  to  $99.8^\circ$ . At this point in the A-1 system, the CA value appears to become relatively stable.

Within the two-hour time frame, the contact angle of the drop in the ionic surfactant aqueous phases was observed to increase. There was an increase in oil-drop

spreading, indicating some reversibility of the wettability alteration, which is hypothesized to be caused by the increased solubility of the surfactant molecules in the aqueous phase. By the end of 120 minutes, the contact angle for C-1 had increased up to 100.55°, a 42.3% increase from its initial value. Surfactant A-1 had a final CA value of 100.8°, which is 89% higher than the initial CA value. System N-1 had a final CA value of 37.5°, which is a 6.8% change from the initial CA value.

It is important to note that for surfactant system A-1, the change in CA was most significant in the first 45 minutes, after which it becomes fairly stable. This indicates that the interactions between the A-1 surfactant and the salt ions in the aqueous phase become equilibrated. The CA value for the C-1 system did not stabilize at any point in time but continued to increase steadily. The change in contact angle in N-1 remained relatively constant, with very minimal change in the contact angle.

By the end of the study (at 120 minutes), the  $\Delta$ CA values were 47.5, 29.9, and 2.4 for surfactant systems A-1, C-1, and N-1, respectively. This confirmed that the time stability was a more significant issue for ionic surfactants compared to nonionic surfactants. The ionic surfactants have head charges, making them more sensitive to the ions in the aqueous phase. **Figure 23** presents images and contact angles that show the change in CA for singular oil drops as observed in the C-1, A-1, and N-1 systems over 120 minutes.

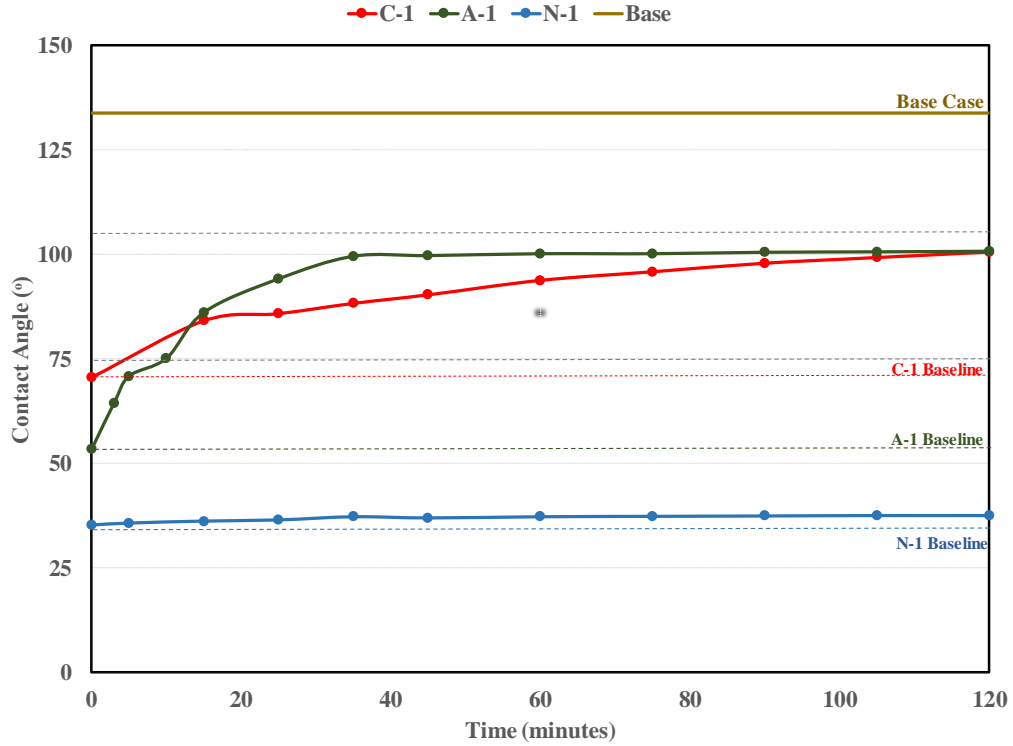


Figure 22: Time stability behavior of ionic and nonionic surfactants. CA versus time results for the base case and surfactants C-1, A-1, and N-1.

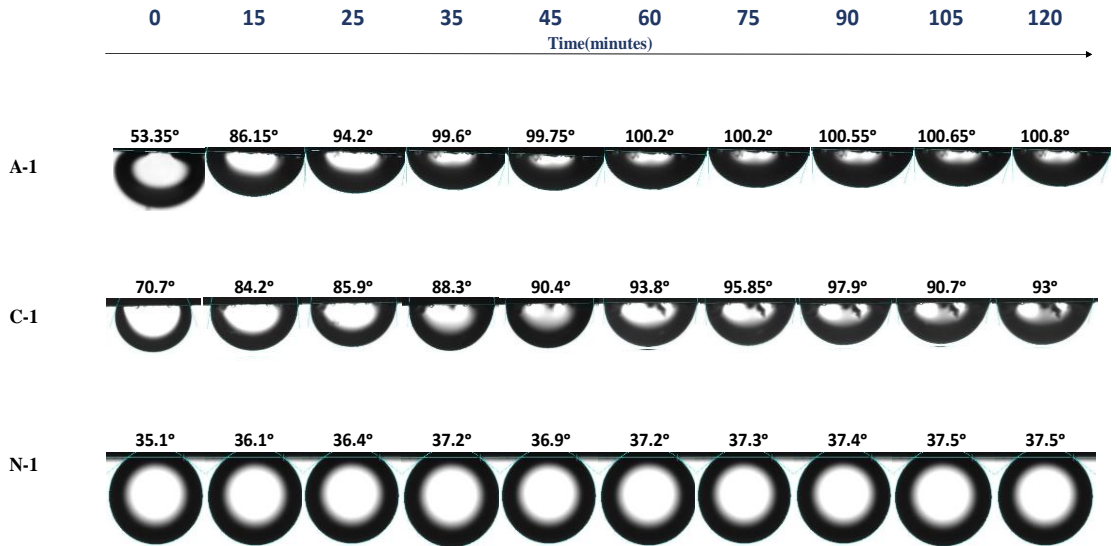


Figure 23: Timelapse of CA images showing time stability behavior in ionic and nonionic surfactants.

## 4.2 Effect of salinity on time stability

**Figure 24** presents the effect of cationic surfactant concentration and brine salinity on the time stability phenomenon. The results for  $\Delta CA_m$ , which is the difference between two consecutive contact angles measured at consecutive time steps, are plotted against time. Cationic surfactant C-1 is investigated in this study at different concentrations—results for C-1 concentrations of 0.02 wt.%, 0.1 wt.%, and 0.2 wt.% are highlighted as colors blue, red, and green, respectively. The plot is grouped into five sections based on salinity. Results are presented for salinities of 0% (tagged 'DI'), 0.2 % (brine A), 6% (brine 1C), 12% (brine 2C), and 24% (brine 3C). Data is displayed for each salinity and concentration pair for a time period of 120 minutes.

As observed in **Figure 24**, at a low cationic surfactant concentration of 0.02 wt.%, a trend of reduced stability is observed over time as brine salinity is increased. Within the first 15 minutes, the  $\Delta CA$  value in DI where salt ions are absent was 14.05, which is more than five times smaller than the  $\Delta CA$  observed in the higher salinity brine 3C, up to 63.8 within the same time frame. By the 25 minute mark,  $\Delta CA$  was observed to increase for all salinity cases with values 19.6, 35.5, 37.6, 39.9, and 70.9 in DI, brine A, brines 1C, 2C and 3C, respectively. Generally, the  $\Delta CA$  was observed to increase as the salinity of the aqueous phase increased. By the end of 120 minutes, the  $\Delta CA$  values observed are as follows: DI - 20.4, Brine A – 37.3, Brine 1C – 41.6, Brine 2C – 40.5. The change from the initial to final CA was more significant in higher salinity brine 3C, where the  $\Delta CA$  value was 75.4. It appeared that low surfactant concentrations resulted in more stable systems at lower salinity.

When the surfactant concentration is increased to 0.1 wt.%, a correlation between surfactant concentration and brine salinity is also observed. For the range of salinity explored, results for concentration 0.1 wt.% presents a parabolic trend, which is intermediate of the upward trend for concentration 0.02 wt.% and the downward trend for concentration 0.2 wt.%. Within the first 15 minutes, the  $\Delta CA$  were 21 in DI, 29 in brine 1C, 16.1 in brine 2C, and 13.5 in brine 3C. By the 25 minute mark, the  $\Delta CA$  values were 21.6, 30.5, 16.6, and 19.8, respectively. These values are generally lower than those measured for the 0.02 wt.% concentration case. By the end of 120 minutes, in brine 1C, the  $\Delta CA$  is 33.1, while in brines 2C and 3C,  $\Delta CA$  values are 18.9 and 23.2, respectively. In comparison to concentration 0.02 wt.%, at a higher concentration of 0.1 wt.%, the  $\Delta CA$  values were reduced by up to 70% in the high salinity brines 2C and 3C. In DI, the  $\Delta CA$  value is 24.8. This is higher than the  $\Delta CA$  values in brines 2C and 3C.

For the case of surfactant concentration of 0.2 wt.%, the  $\Delta CA$  was observed to be more significant at lower salinity. Within the first 15 minutes, the measured  $\Delta CA$  in DI was 43.6, which was significantly larger than the  $\Delta CA$  value measured in the higher salinity brines: 13.5 in brine A, 1.9 in brine 1C, 3.1 in brine 2C, and 0.1 in brine 3C. By the 25 minutes mark, the  $\Delta CA$  remained fairly constant at 43.1 in DI, 15.2 in brine A, 2 in brine 1C, 3.5 in brine 2C, and -0.7 in brine 3C. Generally, a reversal from the initial trend of reduced surfactant stability with increasing salinity at low surfactant concentration is observed at a surfactant concentration of 0.2 wt.%.

At a concentration of 0.2 wt.% in DI, by the end of 120 minutes, the surfactant system is the most unstable compared to lower concentrations evaluated with a significant

$\Delta CA$  value of 46.8. However, as the brine salinity increases, the stability of the solution increases compared to the other systems. In brine A, the  $\Delta CA$  value is reduced to 29.9. In brines 1C and 2C,  $\Delta CA$  values are further reduced to 3.1 and 4.5, respectively. The most interesting result is observed with the higher salinity brine 3C, where the system is not only stable as there is minimal  $\Delta CA$  over time, but there also appears to be an increase in water-wetness of the system. In brine 3C, the system had a  $\Delta CA$  value of -1.4.

The general trend observed is that in order to create stable surfactant systems, surfactant concentration must be directly correlated with salinity. For cationic surfactants, low surfactant concentrations create stable systems in low salinity brine. This conclusion is based on concentration 0.02 wt.% producing the lowest  $\Delta CA$  in lower salinity brines compared to other surfactant concentrations evaluated. Whereas higher surfactant concentrations create more stable systems in higher salinity brines. This conclusion is based on concentration 0.2 wt.% resulting in the lowest  $\Delta CA$  in higher salinity brines compared to other concentrations evaluated.

An explanation for the improved time stability of lower surfactant concentrations at lower brine stability is that for the cationic surfactants, the presence of fewer salt ions in the solution enables the surfactant to stay at the brine/oil/rock interface as opposed to partitioning preferentially into the brine phase. The low surfactant concentration wraps around the oil drop with the hydrophilic tail in the aqueous phase and the hydrophobic head in the oil phase. This enables the surfactant system to remain effective in maintaining the initial CA value observed over time, hence better time stability.

However, an increase in the salt ions present increases chemical interactions between the surfactant molecules and the salt ions in the brine. The interaction is more significant when the surfactant concentration is low. At low concentrations, salt ions in the solution interact with and overpower the surfactant molecule making it ineffective. This is observed in the case of surfactant concentration 0.02 wt.% in brine 3C, where the most significant  $\Delta CA$  value for the study was produced.

At higher surfactant concentrations, a similar explanation can be made. For the low salinity cases, the absence of salt ions and the presence of more surfactant molecules causes more of the surfactant to go into the brine phase as opposed to staying at the interface. There is an increase in solubility of the surfactant in the brine phase when there are fewer salt ions present in the solution. The aqueous phase is able to dissolve more surfactant molecules since there are no other ions/ fewer ions present in the solution. This increased solubility of the surfactant molecule in the brine phase reduces the number of surfactant molecules present at the interface. Based on this, reduced time stability will be observed in higher concentration surfactant systems at low salinity

This also explains the behavior of the high surfactant concentration system when there is an increased amount of salt ions in the aqueous phase. The presence of a high amount of salt ions in the solution reduces the degree of solubility of the surfactant system. Since the salt ions are already dissolved in the aqueous phase, the solution is well equilibrated. As a result, fewer surfactant molecules are able to dissolve into the solution. This reduced solubility ensures that the surfactant molecules remain at the crude oil/brine/rock interface. This ensures that the surfactant system remains effective for a

long time resulting in improved time stability. This is observed in the case of surfactant 0.2 wt.% in high salinity brine 3C, where not only does there improved time stability, the surfactant system is also observed to become more effective over time.

This understanding of the interplay between surfactant concentrations and salinity will enable the design of the best and most stable surfactant systems for EOR application.

This knowledge is applied in the surfactant HPHT studies performed in this work.

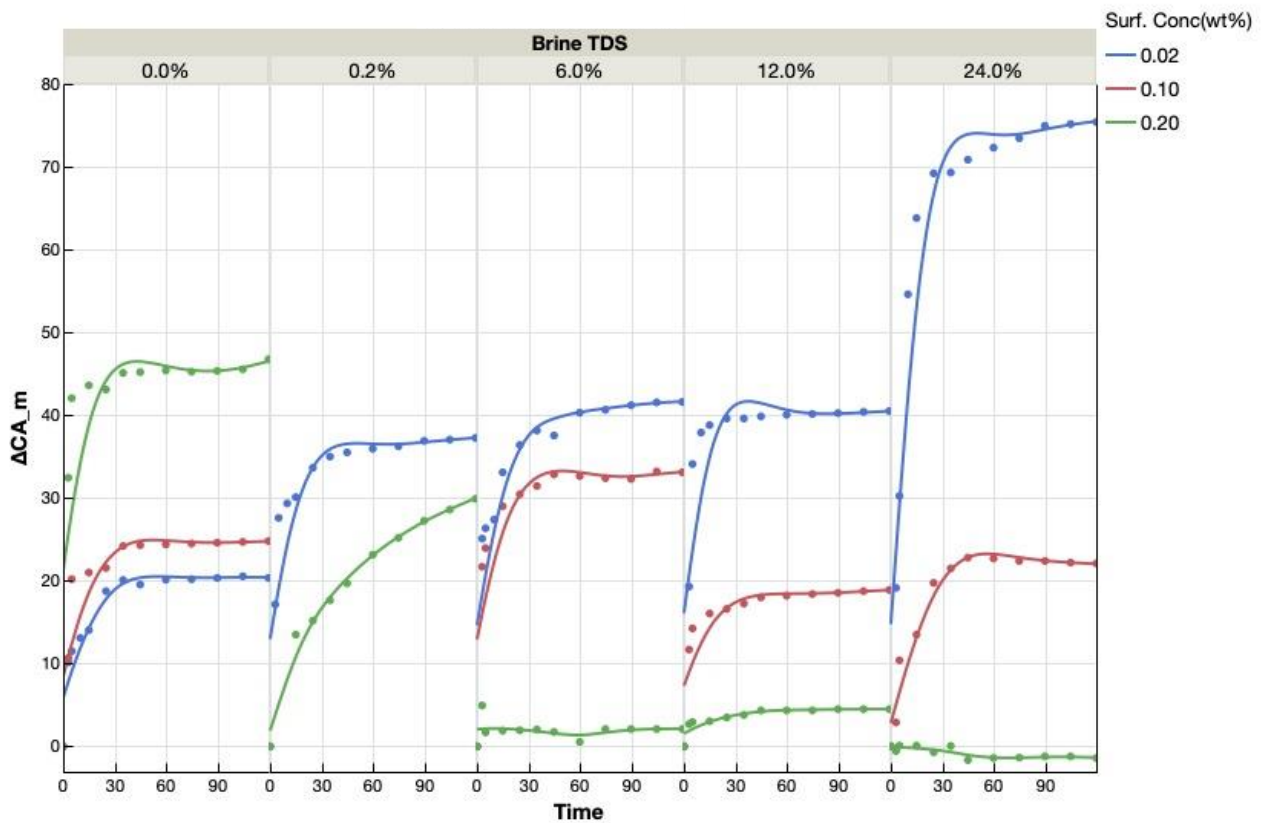


**Figure 24:  $\Delta CA_m$  ( y-axis) versus time (x-axis) for C-1 at different surfactant concentrations (0.02 wt.% - Blue color, 0.1 wt.%- Red color, and 0.2 wt.% - Green color) in varying salinity aqueous phases (Brine TDS on x-axis) (0% - DI, 0.2% - brine A, 6% -brine 1C, 12% - brine 2C, 12% - brine 3C).**



### 4.3 Effect of ionic surfactant head group charge

**Figure 25** presents results for time stability analysis of anionic surfactant A-1. The results for  $\Delta CA_m$ , which is the difference between two consecutive contact angles measured at consecutive time steps, are plotted against time. Surfactant concentrations of 0.02 wt.% (highlighted in blue color), 0.1 wt.% (highlighted in red color), and 0.2 wt.% (highlighted in green color) are evaluated. Results are shown at salinities of 0% (DI) and 0.2% (brine A) for a time frame of 120 minutes.

**Figure 26** compares results for surfactants C-1 (represented with blue color) and A-1 (represented with red color). The results for  $\Delta CA_m$ , which is the difference between two consecutive contact angles measured at consecutive time steps, is plotted against time. The plot is grouped by surfactant concentration (0.02 wt.%, 0.1 wt.%, and 0.2 wt.%) on the y-axis and salinity on the x-axis (0% 'DI'; 0.2% 'brine A'; 6% 'brine 1C'; 12% 'brine 2C'; and 24% 'brine 3C'). Results are shown for a time frame of 120 minutes for each combination.

In the DI system, different surfactant concentrations produced different degrees of time stability. Within the first 15 minutes, the  $\Delta CA$  for concentration 0.02 wt.% was 26.7, while  $\Delta CA$  were 33.3 and 3.2 in 0.1 wt.% and 0.2 wt.%, respectively. By the 25 minutes mark,  $\Delta CA$  for concentration 0.02 wt.% increased to 43.4, while  $\Delta CA$  for 0.1 wt.% and 0.2 wt.% remained constant. By the end of 120 minutes,  $\Delta CA$  values for concentrations 0.1 wt. % and 0.2 wt.% remained fairly constant while  $\Delta CA$  in 0.02 wt.% had continued to increase up to 123.6.

The behavior of anionic surfactants in DI systems showed a different trend than that observed in cationic systems. In DI, there was an increase in time stability for anionic surfactant as the concentration increased as observed from a reduction in  $\Delta CA$  values ( $\Delta CA = 123.6, 33.3, 4.7$  for surfactant concentrations of 0.02 wt.%, 0.1 wt.%, and 0.2 wt.% respectively). However, for cationic surfactant, there was a reduction in time stability as observed from the increase in  $\Delta CA$  values with concentration ( $\Delta CA = 20.4, 24.8, 46.8$  for surfactant concentrations of 0.02 wt.%, 0.1 wt.% , and 0.2 wt.% respectively).

Also, for the anionic system, in brine A, at the end of 120 minutes, the  $\Delta CA$  value was reduced to 47.5, as compared to 123.6 in DI. As observed in **Figure 26**, for anionic surfactant systems, higher surfactant concentrations appeared to be more stable at lower brine salinity. This could be indicative of a trend of low concentration anionic surfactant systems increased time stability with increasing brine salinity. Whereas cationic surfactant showed a trend of reduced time stability at low concentrations as the brine salinity increased.

However, definite conclusions cannot be made for the correlation between anionic surfactant concentration and salinity. Any such conclusions will warrant more extensive studies, which are limited in this case because anionic surfactants created turbid unusable solutions in higher salinity brines.

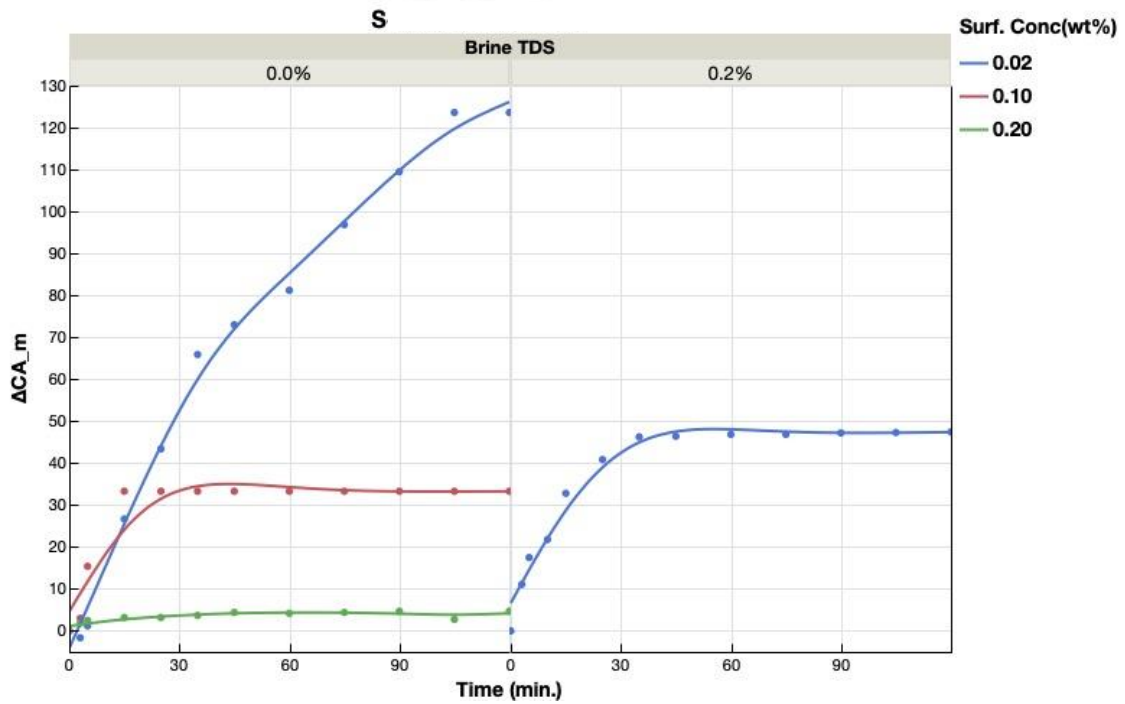
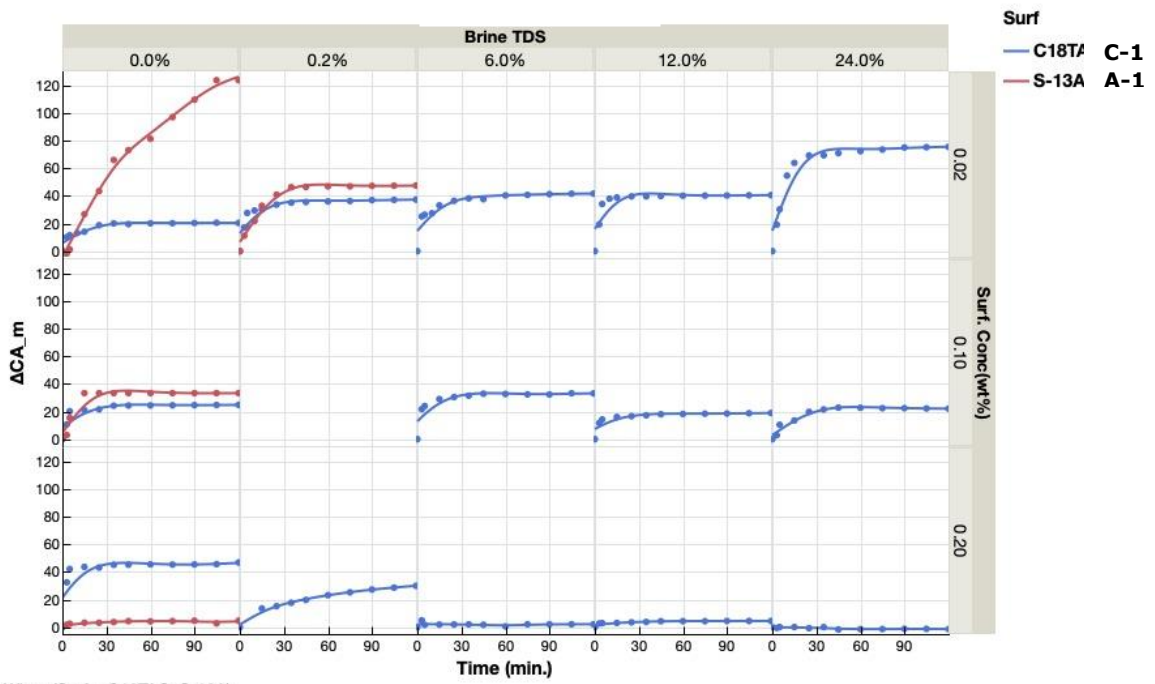


Figure 25:  $\Delta CA_m$  ( y-axis) versus time (x-axis) for A-1 at different surfactant concentrations (0.02 wt.% - Blue color, 0.1 wt.%- Red color, and 0.2 wt.% - Green color) in varying salinity aqueous phases (Brine TDS on x-axis) (0% - DI, 0.2% - brine A).



**Figure 26:  $\Delta CA_m$  ( y-axis) versus time (x-axis) for C-1 (blue color) and A-1 (red color) at different surfactant concentrations (y-axis - 0.02 wt.%, 0.1 wt.%, and 0.2 wt.%) in varying salinity aqueous phases (Brine TDS on x-axis) (0% - DI, 0.2% - brine A, 6% -brine 1C, 12% - brine 2C, 12% - brine 3C).**

## **5 WETTABILITY ALTERATION AND IFT REDUCTION BY SURFACTANT**

In this section, the effect of surfactant additives in altering wettability and the impact on interfacial tension are investigated through contact angle (CA) and interfacial tension (IFT) measurements. These measurements are an essential step that precludes the SASI experiments. It is essential to identify surfactant systems that are effective in producing low water-wet CA values and favorable IFTs at the required high-temperature conditions. These surfactant systems are then further investigated by SASI experiments. Two phases of CA and IFT measurements are conducted in the study – LPT and HPHT measurements which are described in the methodology section. The LPT measurements are conducted at a temperature of 72°F or 170°F, while HPHT measurements are conducted for a wide range of temperatures up to 325°F. The primary brine evaluated in this section is brine A except otherwise stated. The results are presented and analyzed subsequently.

### **5.1 Contact angle results**

#### **5.1.1 Effect of preservation on rock wettability**

Core samples from different depths were received from the Eagle Ford reservoir in a preserved state. Square 1cm by 1cm chips were cut from the cores retrieved. The formation depths evaluated are presented in **Table 8**. The tags ‘Set 1’, ‘Set 2’, ‘Set 3’, and ‘Set 4’ are designated for easy identification of chips cut from the core samples.

Initial CA measurements were made before any oil/water saturation to determine the wettability of the chips. Oil-wet CA values are an indication that the original rock wettability was preserved. In contrast, water-wet CA values indicate that the original rock wettability was not preserved. In any case, chips will be subjected to an aging process in order to restore original rock wettability before the surfactant selection process is commenced.

Tag	Depth (ft.)
Set 1	14049.00 – 14050.00
Set 2	14049.20 - 14049.90
Set 3	14206.65 - 14207.50
Set 4	14026.20 - 14026.70

**Table 8: Depths of core samples retrieved from Eagle Ford formation used in contact angle study.**

CA values were measured for the different sets of chips at LPT conditions in varying aqueous salinity conditions (DI, brine A, and brine B), as shown in **Figure 27**. Across the formation depths, contact angles measured in DI at 72°F were water-wet with CA values in the range of 18.3° to 32.8°. Similarly, contact angle values measured in brine A and brine B were water-wet with values in the range of 25.5° to 35.1° and 20.6° to 36.2°, respectively. CA values at 170°F also indicate water-wetness - CAs measured in DI were in the range of 19.4° to 26.0°, while CA values in brine A and brine B were in the range of 13.5° to 20.6° and 14.3° to 24.1° respectively. Generally, the CA values measured at the

higher temperature of 170°F were slightly lower than contact angle values measured at 72°F.

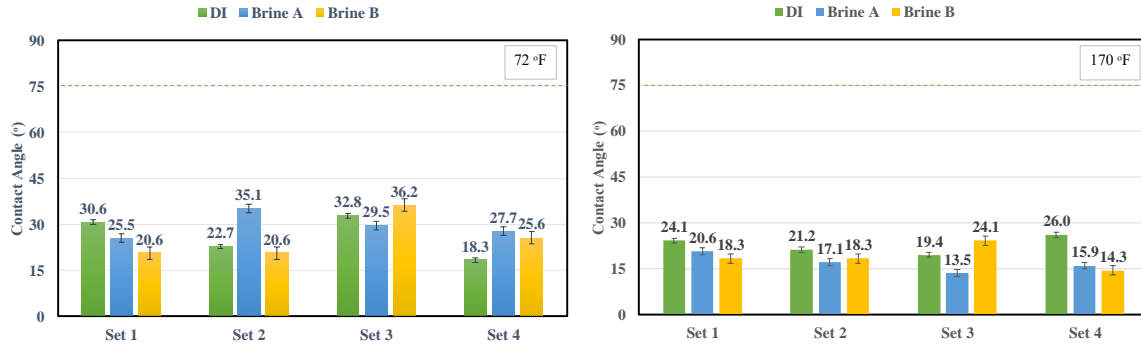


**Figure 27: CA of preserved chips measured at 72°F (left) and 170°F (right) indicate water-wetness.**

Based on the contact angles of the preserved rock chips, it can be inferred that the wettability of the core samples was not preserved. The contact angles of the preserved chips were water-wet across all the temperature and salinity conditions evaluated. Hence, there was a need to restore the reservoir wetting conditions in order to carry out an accurate surfactant selection study. The reservoir wetting conditions were restored through an aging process.

### 5.1.2 Aging of rock chip samples

In order to induce reservoir wetting conditions in the water-wet preserved chips, the chips were aged in formation oil at a high temperature. Before undergoing the aging process, the chips were first cleaned following the cleaning procedure described in the methodology section. Rock chip cleaning ensures that any hydrocarbons, salt contaminants, or brine are removed from the samples. Following the cleaning procedure, the chips were submerged in crude oil and heated in an oven at reservoir temperature.

**Figure 28** presents the changing CA values during the aging process of the rock chip sets. The results are displayed for CA measured in DI (highlighted in black color) and brine B (highlighted in red color) at temperatures of 72°F and 170°F. The aging process is evaluated for a period of eight (8) weeks for each case. During the aging process, wettability was altered from water-wet to intermediate wet to oil-wet for all chips studied. As discussed in the literature review section, chips become oil-wet as a result of the adsorption of the polar compounds in the crude oil by the rock samples. As adsorption proceeded, the hydrophobicity of the rock surface increased, thereby altering wettability to the oil-wet region. For all the rock chips evaluated, the final contact angles were in the range of 124° to 157°, indicating that the chips attained oil-wet properties.

It has been established that the optimal aging time of shale rock samples is about six (6) weeks. Optimal aging time is indicated by little to no variation in the measured contact angle over a period of time. As observed in **Figure 28**, the wettability of sets 1, 2, 3, and 4 rock chips was stable at the 6-week mark. Generally, contact angle measurements for weeks 7 and 8 show little to no deviation from week 6. Hence, the optimum aging time is confirmed to be at the 6-week time frame.



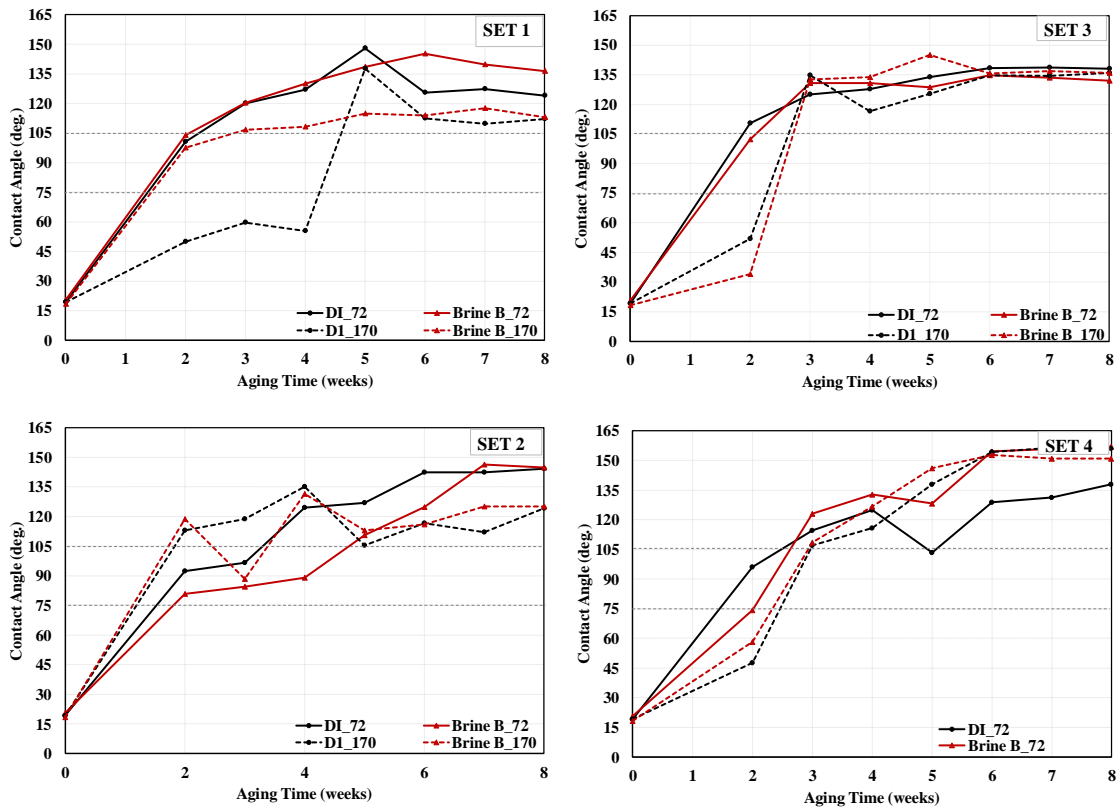


**Figure 28: Changing CA values over an aging time of 8 weeks for different sets of rock chips measured in DI and brine B at temperatures of 72°F and 170°F.**

The final CA after aging was also evaluated at HPHT conditions. CA of set 1 rock chips was evaluated in brine A aqueous phase. The average contact angle measured was  $151^\circ (\pm 1.6^\circ)$ , indicating chips were oil-wet. The measured contact angle remained fairly constant over the temperature range evaluated.

At similar temperature and pressure conditions, some variation was observed in contact angles measured using the Biolin equipment and the Dataphysics equipment. This variation is attributed to measurement artifacts as well as different mechanisms of

operations of the equipment. However, the overall picture remains the same: oil-wet chips were determined to be oil-wet by both equipment and vice-versa.

### ***5.1.2.1 Alternative approaches to the aging process***

#### **5.1.2.1.1 Brine Pre-soak method**

A different approach to the aging procedure was also evaluated. For this method, the chips were first pre-soaked in the produced water (brine B) for two (2) weeks before aging in oil. Initial measurements on the brine-soaked chips showed expected water-wet conditions. After two weeks, the pre-soaked chips were then submerged in oil to commence the aging process. The contact angles were measured intermittently.

Comparing the aging results of pre-soaked chips and non-pres soaked chips at different time intervals showed that pre-soaked chips attained oil-wet properties earlier (at two weeks) compared to non-pres soaked chips. Also, measured CA value stabilizes early for pre-soaked chips (at four (4) weeks), while variation in CA is observed in non-pres soaked chips for up to 5 weeks. Final CA angles were in the same range for the brine pre-soaked and non-pres soaked chips.

#### **5.1.2.1.2 Use of standard deviation as an indicator for aging**

Another indicator of optimum aging is the standard deviation of measured contact angle over the aging period. In the earlier weeks of aging, generally, the standard deviation in contact angle measurements was observed to be high. The deviation was observed within contact angles of different oil drops along the same rock surface and between

different rock chips in the same set. One reason for this is that chips may not be uniformly aged across their surface area over short aging periods.

As the aging process proceeded, the standard deviation in contact angle measurements decreased. This is an indicator that chips have become more uniformly aged, and the wettability is stable. **Figure 29** shows changes in standard deviation for set 1 rock chips over the aging period. Standard deviation was as high as ten (10) after the first two weeks of aging. By 6 to 8 weeks, the standard deviation was in the range of 0 – 4, which is an indication that stable wettability has been attained.

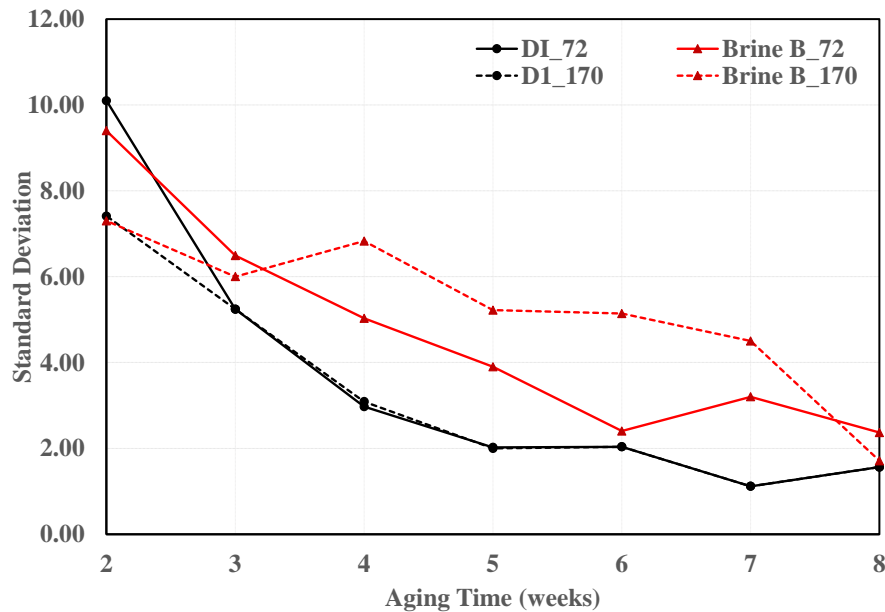


**Figure 29: Standard deviation of measured contact angle values for set 1 rock chips during the aging process in DI and brine B at temperatures of 72°F and 170°F.**

### 5.1.3 Surfactant selection study

Following a successful aging process, the surfactant selection process was commenced. The main goal of the surfactant selection process is to identify surfactants

that are effective in altering the wettability of the aged chips from oil-wet to preferentially water-wet conditions and is effective in maintaining a moderate IFT. The surfactant selection study was conducted in two phases: LPT and HPHT measurements. The results are presented in subsequent sections.

#### **5.1.4 LPT CA Results**

##### **5.1.4.1 Single Surfactant Systems**

Single systems of cationic (C-1, C-2, C-3, C-4, and C-5), anionic (A-1, A-2, A-3), and zwitterionic (Z-1) surfactants were evaluated at LPT conditions to observe their effectiveness in altering rock wettability from oil-wet to water-wet conditions. **Figure 30** shows the CA results measured at LPT conditions (170°F) on chips from various depths using different surfactants at varying concentrations. The concentrations evaluated were 0.02 wt.%, 0.04 wt.%, 0.1 wt.%, and 0.2 wt.%.

In brine A, the final CA after aging was determined to be 133.9°. For set 1 rock chips, as shown in **Figure 30**, cationic surfactants were ineffective in altering wettability favorably at low concentrations. Whereas, some anionic surfactants (A-1 and A-2) did show favorable wettability alteration tendencies even at a low surfactant concentration of 0.02 wt.%. Surfactants C-2, C-3, and Z-1 were ineffective in altering the wettability from oil-wet to favorable water-wet conditions even at high concentrations of 0.2 wt.%. These surfactants resulted in higher CA than the initial conditions. Surfactant C-1 altered rock wettability from oil-wet to intermediate-wet conditions. In this case, a reduction in CA was observed as the concentration of the surfactant was increased with a final CA of 98°

at a concentration of 0.2 wt.%. Surfactants C-4, C-5, A-1, A-2, and A-3 altered wettability to the water-wet window. While C-4, C-5, and A-3 resulted in higher CA as compared to the initial conditions at low concentrations (0.02 wt.% and 0.04 wt.%), as surfactant concentration increased, lower CA values were observed. Even at very low concentrations, Surfactants A-1 and A-2 showed effectiveness in altering wettability from initial oil-wet conditions. Lowest CA at 0.2 wt.% was observed with surfactants C-4 and A-1 with CA values 39.4° and 40.2°, respectively.

For Set 3 rock chips, the cationic surfactants were also less effective in altering wettability favorably at low concentrations. At the same time, some anionic surfactants did show favorable wettability alteration tendencies even at low concentrations. Also, surfactants C-2, C-3, and Z-1 were ineffective in altering the wettability from oil-wet to water-wet conditions even at high concentrations of 0.2 wt.%. These surfactants resulted in higher CA than the initial conditions. At a concentration of 0.2 wt.%, surfactants C-1 and A-2 altered the wettability of set 3 chips from oil-wet to intermediate wet conditions, whereas surfactants C-4, C-5, A-1, and A-3 altered wettability to the water-wet window. While C-4, C-5, and A-3 resulted in higher CA as compared to the initial conditions at low concentrations (0.02 wt.% and 0.04 wt.%), as surfactant concentration increased, lower CA values were observed. Lowest CA at 0.2 wt.% was observed with surfactants C-4 with a CA value of 37.7°.

Generally, results were consistent for both sets of chips with surfactants C-4, C-5, A-1, A-2, and A-3 resulting in the most wettability alteration and the lowest CA values. There was some variation in the CA values for the different chip sets under similar

conditions, which is a result of variation in the rock mineralogical components across the formation depth.

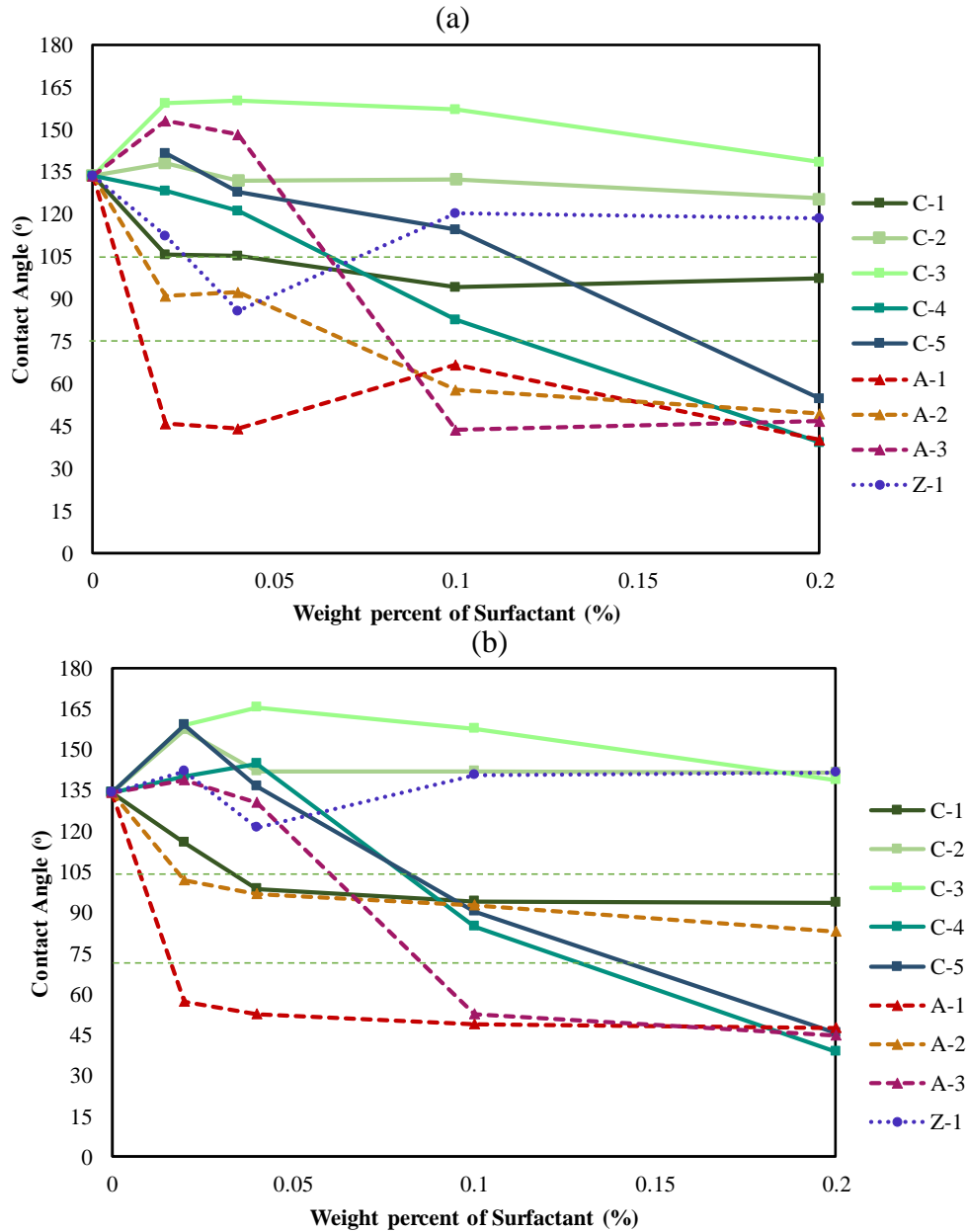


**Figure 30: Wettability alteration by ionic surfactants for rock chip sets (a) 1 and (b) 3.**

**Note: A-1, A-2, A-3, C-4, and C-5 altered wettability from initial oil-wet conditions (CA = 133.9°) to favorable water-wet conditions at concentration 0.2 wt.%.**

#### 5.1.4.2 Co-Surfactant Systems

In order to expand the number of surfactant systems analyzed and to manipulate surfactant properties to ensure surfactant effectiveness at high-temperature conditions, cationic-cationic, cationic-anionic, and cationic-zwitterionic surfactant blends were evaluated. Cationic-cationic blend did not show any significant improvement in system properties upon initial analysis. Anionic blends with cationic or zwitterionic surfactants created turbid unstable surfactant systems. However, cationic-zwitterionic blends showed promising results.

The cationic-zwitterionic co-surfactant systems were evaluated in brine A at a temperature of 170°F. Their wettability alteration properties were assessed at 0.2 wt.% total surfactant concentration. To present an overarching concept, wettability results for single surfactant systems at 0.2 wt.% concentration are compared with results of different blend combinations that add up to 0.2 wt.%. **Table 9** shows the different blend combinations evaluated.

Blend Number	Ratio	Cationic Concentration Surf. A (wt.%)	Zwitterionic Concentration Surf. B (wt.%)	Total Surf. Concentration (wt.%)
1	1:0	0.20	0	0.2
2	3:1	0.15	0.05	0.2
3	3:2	0.12	0.08	0.2
4	1:1	0.1	0.1	0.2
5	1:3	0.05	0.15	0.2
6	2:3	0.8	0.12	0.2
7	0:1	0	0.2	0.2

**Table 9: Formulation of cationic-zwitterionic surfactant blends.**

**Figure 31** displays the results for C-2 and Z-1 blends. Initial CA values for the single surfactant systems were oil-wet (C-2 = 125.7°, Z-1 = 118.8°). The different blend

combinations showed different results. Favorable synergism was observed with blends 3:2, 1:1, 1:3, and 2:3. While 3:2 and 2:3 showed intermediate results with CA values of 82° and 89.9°, respectively, blend 1:1 had a higher intermediate-wet CA value of 102.6°. Blend 1:3 showed produced very water-wet results with a CA value as low as 37.8°. However, no favorable synergism was observed for blend 3:1.

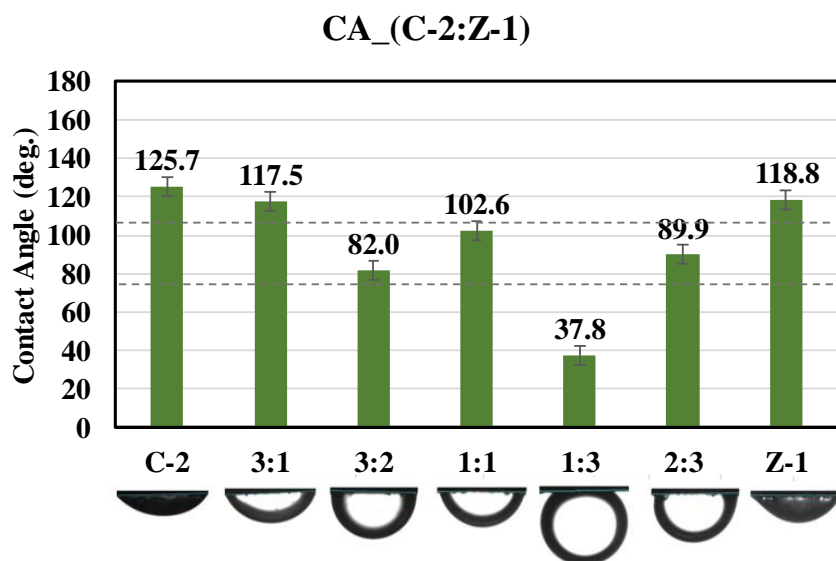


**Figure 31: Contact angles of surfactants C-2 and Z-1 blends in brine A at 170°F. Corresponding CA images are displayed below each bar.**

**Figure 32** displays the results for C-6 and Z-1 blends. Initial CA value for C-6 in this case was also oil-wet (C-6 = 116.4°, Z-1 = 118.8°). In this case, some favorable synergism was observed with blends 1:3 and 2:3. For both blends, intermediate-wet results were observed (CA = 96.3°, 102.6°). Blends 3:1, 3:2, and 1:1 produced very little to no synergism – in one case (blend 3:1), the CA value was more oil-wet than those observed with the single surfactant systems.



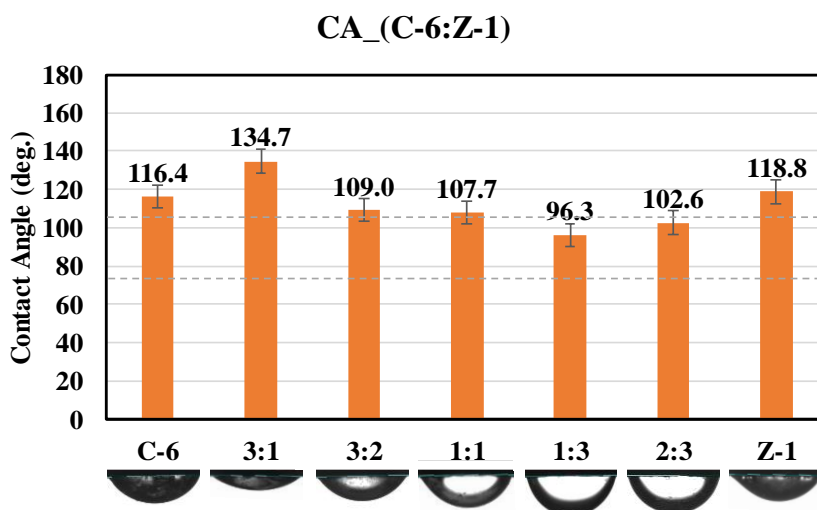


**Figure 32: Contact angles of surfactants C-6 and Z-1 blends in brine A at 170°F. Corresponding CA images are displayed below each bar.**

**Figure 33** displays the results for C-1 and Z-1 blends. Initial CA value for C-1 surfactant system is intermediate-wet (CA = 97.6°). No favorable synergism was observed for the different surfactant blends in this case. All the blends produced oil-wet results with CA values higher than the initial CA value for single system C-1.

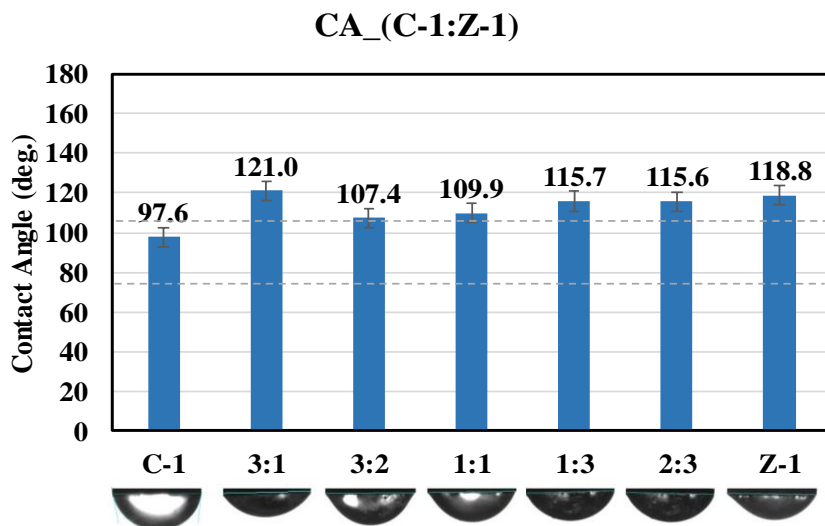


**Figure 33: Contact angles of surfactants C-1 and Z-1 blends in brine A at 170°F. Corresponding CA images are displayed below each bar.**

Blends of different surfactants with the same tail length show more favorable synergism. Rosen (1989) suggested that better synergism is observed between surfactants with equal tail lengths. Surfactant C-2, which showed the most favorable synergism in combination with Z-1, has the same hydrocarbon tail length as Z-1 (both have C<sub>12</sub> tails). When the tail lengths of the co-surfactants are more different, less favorable synergism is observed. This is further confirmed by the results of surfactants C-2 and C-6. Surfactants C-2, C-6, and C-1 have hydrocarbon tail-lengths C<sub>12</sub>, C<sub>16</sub>, and C<sub>18</sub>, respectively. While surfactant C-2 showed very favorable synergism in some blends, the longer tail-length surfactant C-1 did not show synergism in any of the blends evaluated. In comparison, surfactant C-6 of intermediate tail length showed relatively intermediate results of the C-2 and C-1 co-surfactant systems.

Also, the longer the surfactant chain length, the higher the effectiveness in altering the wettability favorably as a single system. Surfactant C-2 (C<sub>12</sub>) system resulted in a CA value of 125.7°; C-6 (C<sub>16</sub>) system resulted in a CA value of 116.4°; while C-1(C<sub>18</sub>) system resulted in a CA value of 97.6°. Single surfactants with long hydrophobic tails were more effective in altering wettability more favorably. However, these systems are more stable and showed less synergism in combination with other surfactants. Hence, the surfactant that produced the lowest CA value as a single system showed less favorable (more oil-wet) when combined with the co-surfactant. Surfactant C-2, which was the least effective in altering wettability as a singular system, showed the best results in combination.

#### **5.1.4.3 Effect of concentration on co-surfactant systems**

Different combination ratios of C-2:Z-1 have been previously evaluated at a total concentration of 0.2 wt.%, as shown in **Figure 31**. It was determined that blends 3:2 and 2:3 showed favorable synergism and resulted in intermediate wet CA values (82° and 89.9° respectively). Also, blend 1:3 resulted in a low water-wet CA value of 37.8°. Since favorable synergisms were observed with these blends, different concentrations of the systems were further evaluated to observe results.

**Figure 34** displays the result for combination ratios 1:3, 3:2, and 2:3 at different total concentrations in brine A at 170°F. Blends 3:2 and 2:3 show a trend of reduction in CA values as the total concentration of the system is increased. At a concentration of 0.2 wt.%, both blends produce intermediate-wet CA values. At 0.4 wt.% and 0.6 wt.%, further reduction in CA values was observed. At a total concentration of 0.8 wt.%, there was a

slight increase in CA value compared to the generally observed trend. When concentration is increased to 1.0 wt.%, very low water-wet CA values are observed: blend 2:3 had a CA value of 34.3° while blend 3:2 produced a CA value of 30.4°.

A more interesting trend of surfactant effectiveness with increasing concentration is observed with blend 1:3. At the low total concentration of 0.2 wt.%, a low water-wet CA value was produced. However, at a concentration of 0.6 wt.%, CA was observed to increase. Above 0.6 wt.% CA was observed to decrease to a low water-wet value. For this blend, the interactions of the co-surfactant molecules in the system were observed to vary significantly with concentration. Designing surfactant blends is a precise process as the volume of each of the co-surfactants will play a role in their synergism and interactions.

Several systems at different combination ratios at different concentrations were identified for further evaluation at high-temperature conditions. However, the focus was placed on promising systems with lower total surfactant concentrations. Higher surfactant concentrations will significantly increase the cost of the EOR program.

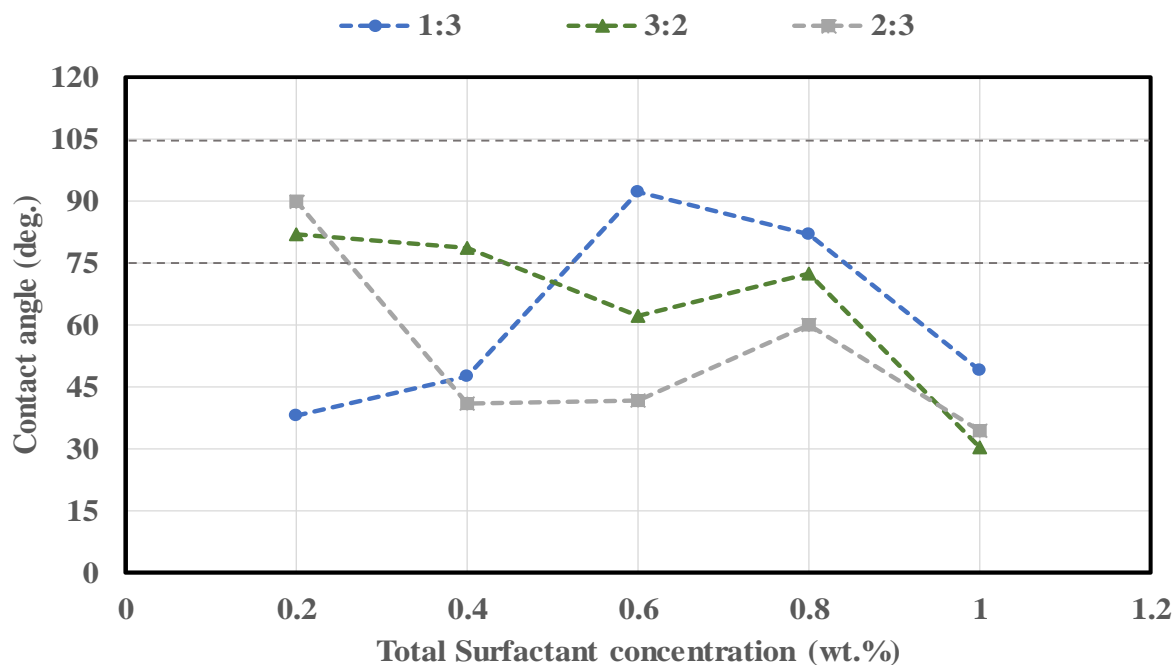


**Figure 34: Co-surfactant system C-2:Z-1 at combination ratios 1:3, 3:2, and 2:3 evaluated at varying total surfactant concentrations.**

#### 5.1.4.4 Effect of salinity on single and co-surfactant systems

Salinity is an important parameter in the wettability alteration of a crude oil/brine/rock system. The degree of salinity, as well as interactions between charged salt ions and the charged head of the surfactant molecules, impacts the effectiveness of the surfactant system. The effect of salinity was investigated on different ionic surfactant systems. Single surfactant systems C-1, A-1, and Z-1; and cosurfactant systems C-2:Z-1 (1:3) were evaluated at a concentration of 0.2 wt.% in different salinity aqueous phases. A range of salinity from 0% TDS (DI water) to 4% TDS was investigated. Results are presented in **Figure 35**.

The initial wettability of the rock without any surfactant was oil-wet ( $CA = 133.9^\circ$ ). When no salt ions are present, i.e., in a DI water system, surfactants C-1 and A-1 resulted in a slight reduction in CA ( $99.8^\circ$  and  $92.7^\circ$  respectively) while Z-1 increased the CA considerably ( $141.7^\circ$ ). When the salinity was increased to 1%, C-1, A-1, and Z-1 systems produced significantly lower CA values ( $44.3^\circ$ ,  $40.2^\circ$ , and  $32.4^\circ$ , respectively). Further increase in salinity up to 4% resulted in even lower CA values:  $33.4^\circ$  for C-1 and  $25.4^\circ$  for Z-1. System A-1 could not be evaluated at 4% as a result of surfactant instability at high salinity, which led to aqueous phase turbidity.

Blend C-2:Z:1 at combination 1:3 also showed a reduction in CA value as system salinity was increased. However, CA values did not vary considerably with salinity. When no salt ions are present, the surfactant system was able to induce very water-wet conditions with a CA value as low as  $39.3^\circ$ . As salinity increased to 1% TDS, CA was reduced to  $38.9^\circ$ . Further, an increase in salinity up to 4% TDS produced a low CA value of  $31.2^\circ$ .

Generally, it was observed that as the salinity of the system increased, the contact angle of the system was reduced. Hence, higher salinity surfactant systems resulted in increased water-wetness at the LPT conditions.

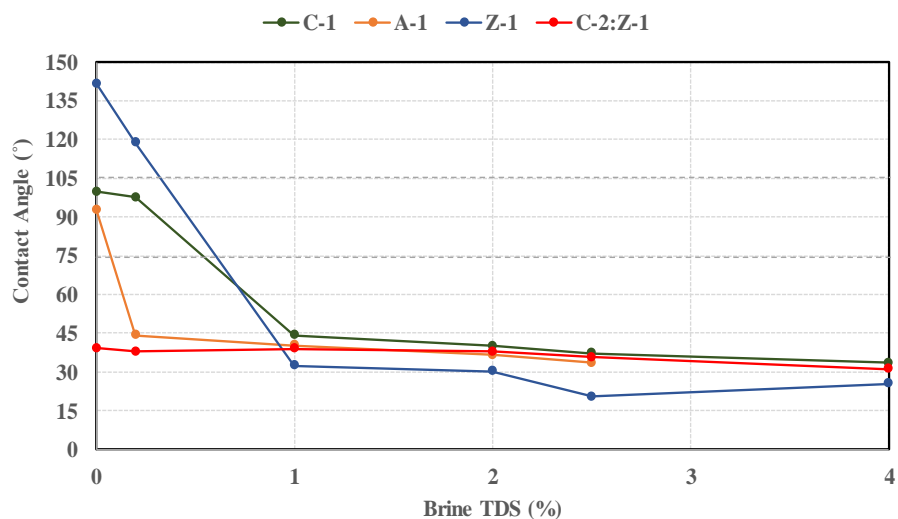


**Figure 35: Surfactants C-1, A-1, Z-1, and C-2:Z-1(1:3) at concentration 0.2 wt.% evaluated at varying salinity conditions.**

#### 5.1.4.5 Summary of observations from LPT CA Results

LPT results showed that some single ionic surfactants were effective in altering wettability from initial oil-wet conditions to favorable water-wet conditions. As observed in **Figure 30**, surfactants C-4, C-5, A-1, A-2, and A-3 altered wettability favorably at a surfactant concentration of 0.2 wt.%. Other surfactants evaluated produced intermediate-to oil-wet results with CA values higher than the initial base CA in some cases. At a total concentration of 0.2 wt.%, co-surfactant systems, which were a blend of cationic surfactant C-2 and zwitterionic surfactant Z-1, also showed favorable wettability alteration at certain combination ratios. Other cationic surfactants evaluated (C-6 and C-1) did not show favorable synergism. Synergistic mixture of C-2:Z-1 resulted in CA values as low as 37.8°.

Evaluating the effect of concentration on the synergistic blends showed that interactions of the co-surfactant molecules varied with the concentration of the surfactant systems. In some cases, improved synergism was observed at higher concentrations, while some other blends showed a reduction in synergism as the system concentration was increased. The impact of salinity on the single and co-surfactant systems showed a more definite trend. The presence of single systems C-1, A-1, Z-1, and co-surfactant system C-2:Z-1 resulted in lower CA values as the salinity of the aqueous phase was increased.

#### **5.1.5 HPHT CA Results**

A new term is used in this section – the Ionic Surfactant Temperature Limit (ITL). The ITL is defined as the temperature beyond which a surfactant system becomes ineffective in producing a favorable water-wet system as a result of the increased solubility of surfactant molecules in the aqueous phase.

For the HPHT study, the base case for a crude oil/brine/rock system without surfactants was first established. The system was observed to be oil-wet in brine A with an average contact angle of 152°. Surfactants that successfully altered wettability to water-wet at LPT conditions were further evaluated at the HPHT conditions.

The potential of single ionic surfactant systems (C-1, C-5, A-1, and A-3) and co-surfactant systems (C-2:Z-1) in altering the wettability to favorable water-wet conditions at high-temperature conditions was investigated. The effect of surfactant concentration, surfactant molecular structure, and aqueous phase salinity on the effectiveness of the surfactant systems was also evaluated.



### ***5.1.5.1 Single surfactant systems***

#### **5.1.5.1.1 Cationic surfactants**

Cationic surfactants C-1 and C-5 were investigated at high-temperature conditions at a concentration of 0.2 wt.% in brine A. Results are presented in **Figure 36**. Surfactant C-5 produced a water-wet system at initial conditions of low temperature (CA = 48.62° at 72°F). Above ITL of 85°F, the system transitioned into intermediate wetting conditions, and a steady increase in CA value was observed up to 150°F. The CA increase continues into the oil-wet zone until the drop is observed to be completely flat, indicating very oil-wet conditions. CA images for system C-5 at 0.2 wt.% for varying temperature and pressure conditions are presented in **Figure 37**.

Surfactant C-1 produced a water-wet system at initial conditions. A slight increase in water-wetness was observed in the system, with an average CA value of  $34.8^\circ \pm 6.5^\circ$  up to ITL of 250°F. The system then transitioned into intermediate wetting conditions up to 313°F. At temperatures higher than 313°F, the system was observed to have become oil-wet. Corresponding CA images at various temperature and pressure conditions are shown in **Figure 38**.

It appears that although the cationic surfactants were effective in producing water-wet results at low temperatures, as heating proceeded and the temperature of the system was increased, the surfactant effectiveness was reduced. This is observed in the transition from water-wet to intermediate-wet to oil-wet CA values as the temperature was increased. Different surfactant systems have different ITLs and become ineffective above

the ITLs. This was determined to be a result of the increased solubility of the surfactant with temperature. As the temperature is increased, an increased number of surfactant molecules dissolve into the aqueous phase. Hence, fewer surfactant molecules are present at the crude oil/brine/rock interface to alter wettability favorably. Solubility is an important issue in the behavior and effectiveness of ionic surfactants.

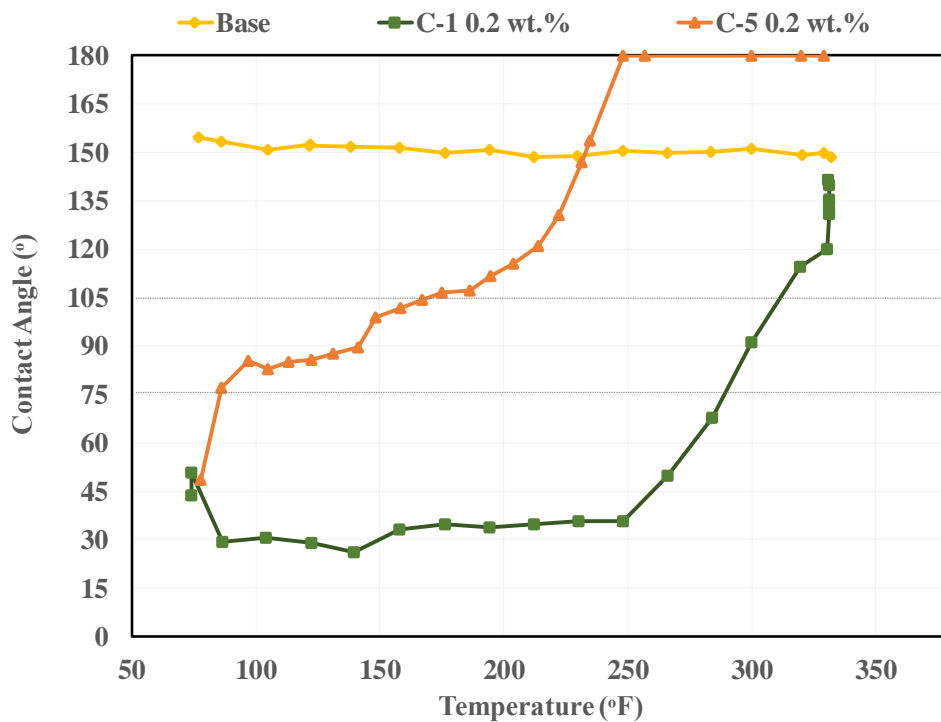


**Figure 36: Contact angle results for surfactants C-1 and C-5 at 0.2 wt.% concentration in brine A at high-temperature conditions.**

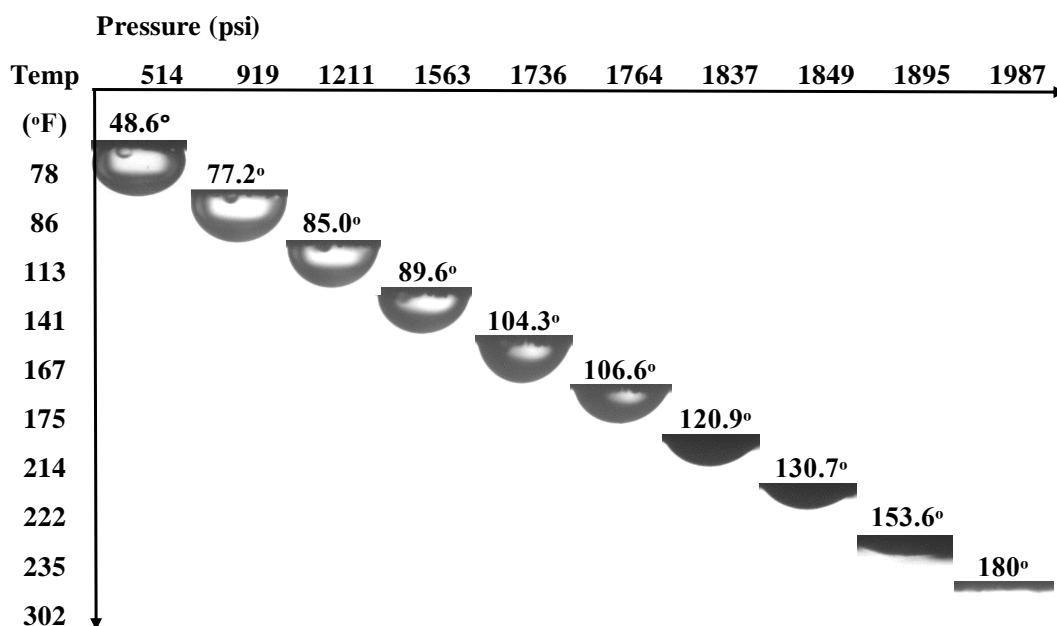


**Figure 37: Contact angle images and values for surfactant C-5 at 0.2 wt.% concentration in brine A at high-temperature conditions. CA observed to be water-wet up to ITL of 85°F.**

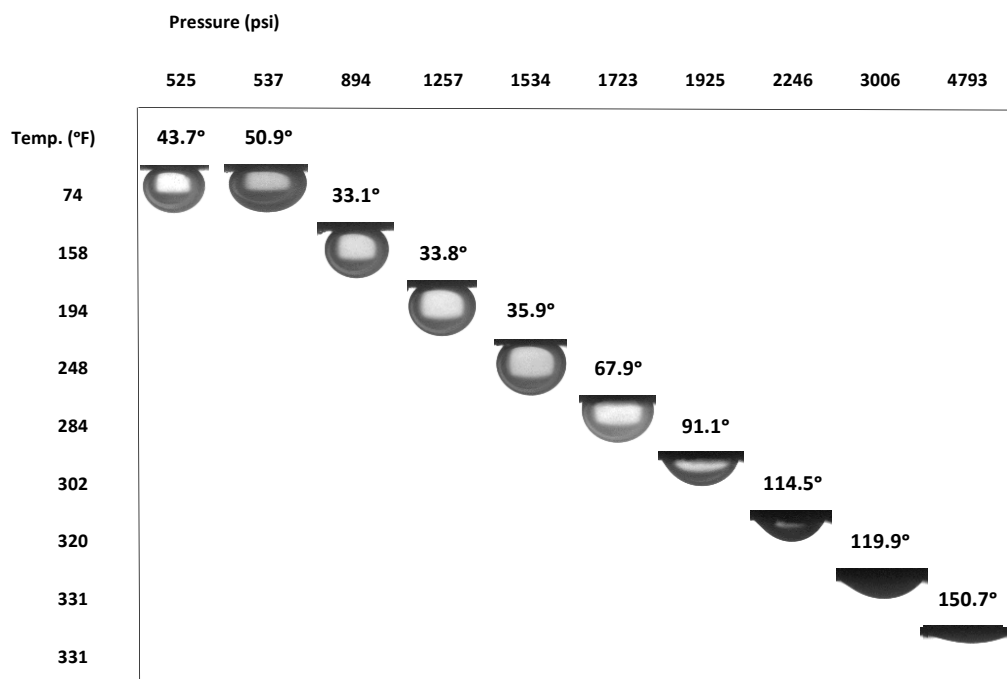


**Figure 38: Contact angle images and values for surfactant C-5 at 0.2 wt.% concentration in brine A at high-temperature conditions. CA observed to be water-wet up to ITL of 250°F.**

#### 5.1.5.1.2 Anionic surfactants

Based on favorable results observed at LPT conditions, surfactants A-1 and A-3 were evaluated at HPHT conditions. The results are displayed in **Figure 39**. Surfactants A-1 and A-3 are sulfate types that have high sensitivity to temperature. The anionic surfactants were successful in altering wettability and produced favorable water-wet systems with low CA values (44.5° for A-1 and 31.6° for A-3) initially at low temperatures.

A similar trend was observed for both surfactants. While the anionic surfactants produced low CA values initially, the oil drop spread from water-wet to oil-wet within the first 13 minutes as heating commenced. This indicates that the anionic surfactant systems have low ITL values making them ineffective for applications in high-temperature

reservoirs. The stability of ionic surfactants in this crude/oil-brine/rock system presents an issue. The time stability issue (discussed in the time stability section) has been shown to be of greater significance with anionic surfactants, where the change in CA is substantial over a period of time. This limited further evaluation and analysis of anionic surfactants.

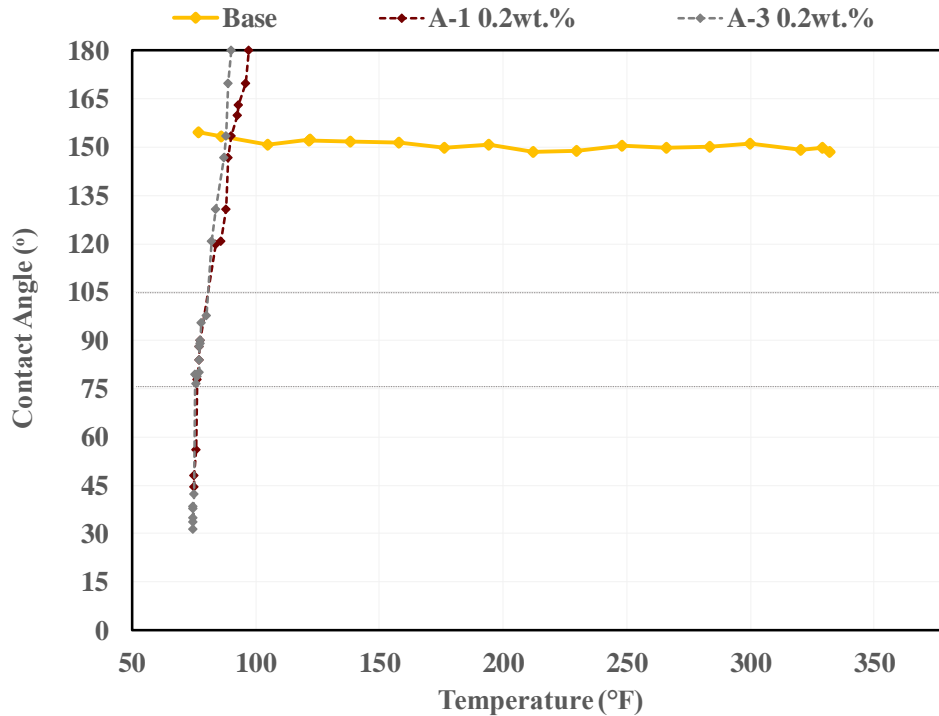


**Figure 39: Contact angle results for surfactants A-1 and A-3 at concentrations 0.2wt% in brine A. CA values are initially water-wet (44.5° for A-1 and 31.6° for A-3). The system becomes oil-wet within the first 13 minutes.**

#### 5.1.5.1.3 Effect of surfactant molecular structure on solubility

Different ionic surfactants have different solubility limits. As observed in **Figure 36** and **Figure 39**, cationic surfactants have higher solubility limits compared to the anionic surfactants evaluated. While cationic surfactants produced water-wet systems up

to ITLs of 250°F, anionic surfactant systems had become fully dissolved in the aqueous phase at a low temperature of 100°F. Hence, cationic surfactants are determined to be more suitable for high-temperature applications.

Varying solubility limits were also observed with the cationic surfactants tested. As shown in **Figure 36**, at 0.2 wt.%, surfactant C-1 produced a more water-wet system than surfactant C-5. Moreover, it produced lower CA values compared to C-1 at the temperatures evaluated. C-1 produced a water-wet system for a wider range of temperature (ITL = 250°F) compared to C-5 (ITL = 85 °F). This behavior is a result of different molecular structures. While C-5 has two-branched tail groups attached to its head group, C-1 contains a linear hydrocarbon tail group. On the hydrophilic side, C-5 is divalent, while C-1 is monovalent. Hence, the solubility of the larger C-5 molecule with temperature is increased compared to the smaller C-1 molecule. C-5 system dissolves in the aqueous phase as opposed to remaining at the crude oil/brine/rock interface at higher temperatures. This explains why an improved behavior was observed with the unbranched monovalent surfactant C-1 compared to surfactant C-5.

#### **5.1.5.2 Co – Surfactant systems**

As discussed previously, the advantage of using co-surfactants is to improve the properties of the surfactant systems. One of such improvements may be a reduction in the sensitivity of the surfactant systems to temperature. Co-surfactant systems were created to produce surfactant systems able to maintain water-wet systems for a wider range of temperatures than single surfactants.

As shown in **Figure 31**, blends of cationic surfactant C-2 and zwitterionic surfactant Z-1 at 0.2 wt.% showed favorable results at certain combinations. Blend 3:1 showed oil-wet properties at LPT conditions, while blend 1:3 showed water-wet properties at LPT conditions. Both blends were evaluated at HPHT conditions to observe behavior at higher temperatures. The results are presented in **Figure 40**.

Consistent with LPT studies, blend 3:1 produced oil-wet CA values, whereas blend 1:3 showed water-wet properties. Blend 1:3 was able to produce and maintain a water-wet CA system (average CA=  $53.6^\circ \pm 7^\circ$ ) up to ITL of 300°F. Above 300°F, CA value increased steadily: remained intermediate-wet up to 313°F before transitioning into the oil-wet phase. Corresponding CA images at various temperature and pressure conditions are shown in **Figure 41**.

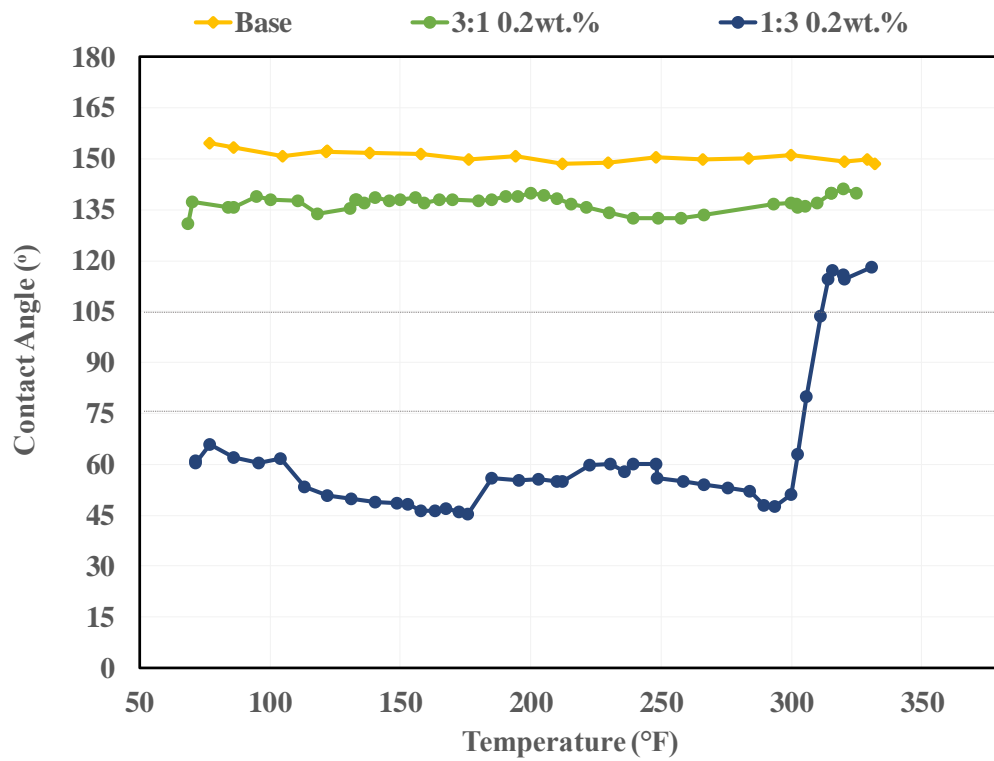


**Figure 40: Contact angle results for co-surfactants C-2:Z-1 at combinations 3:1 and 1:3 at a total concentration of 0.2 wt.% in brine A at high-temperature conditions.**



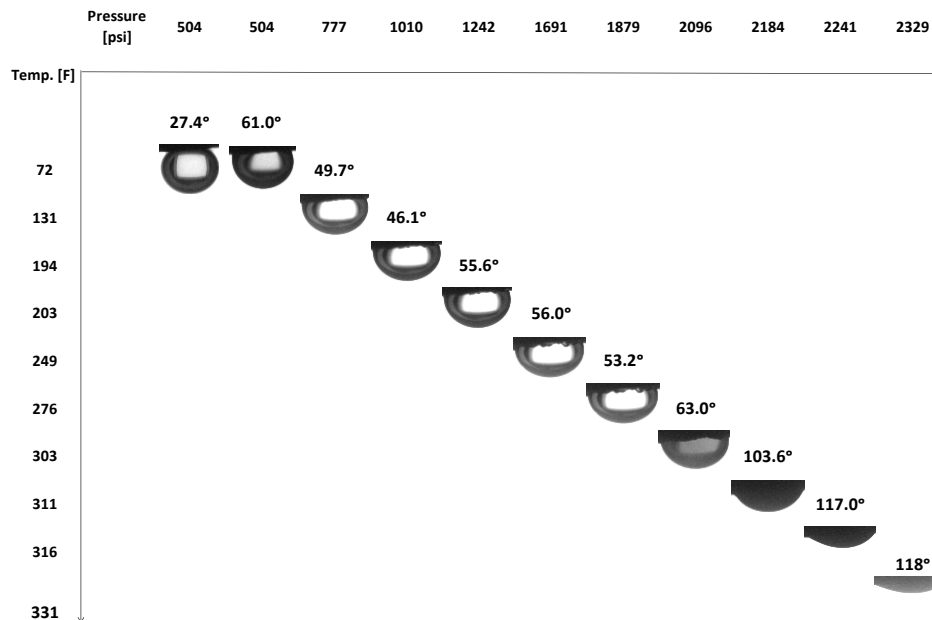


**Figure 41: Contact angle images and values for co-surfactants C-2:Z-1 at combinations 3:1 and 1:3 at a total concentration of 0.2 wt.% in brine A at high-temperature conditions.**

**CA observed to be water-wet up to 300°F.**

### 5.1.5.3 Effect of surfactant concentration on single and co-surfactant systems

#### 5.1.5.3.1 Single surfactant systems

Cationic surfactant C-5 was evaluated at high-temperature conditions at concentrations of 0.2 wt.%, 0.4wt.%, and 0.6 wt.%. The results are displayed in **Figure 42**. While a concentration of 0.2 wt.% produced a water-wet system up to ITL of 85°F, higher ITL values were observed for the higher concentration systems. Compared to the concentration of 0.2 wt.%, 0.4 wt.% system produced a lower initial CA (37° at 72°F). The system is observed to be more water-wet compared to the lower concentration system at

higher temperature conditions and remains water-wet up to 265°F with average CA values of  $39.5^\circ \pm 6.1^\circ$ . Above 265°F, CA value increases steadily up to very oil-wet conditions.

The lowest initial CA value was observed at 0.6 wt.% (CA =  $22.94^\circ$  at 72°F) compared to the lower concentrations of 0.4 wt.% and 0.2 wt.% (CA =  $37^\circ$ ,  $48.6^\circ$  respectively). While C-5 at 0.4 wt.% increased the efficiency of the surfactant up to a higher temperature range compared to 0.2 wt.%, this trend was not consistent upon increasing the concentration to 0.6 wt.%. Surfactant C-5 at 0.6 wt.% had a smaller temperature range where the system was water-wet (average CA values of  $45.4^\circ \pm 9.8^\circ$  up to 215°F). For 0.6 wt.%, above 215°F, CA values were observed to also increase steadily to the oil-wet phase.

Results showed that higher concentrations could provide a more effective surfactant system in establishing water-wet conditions at higher temperature ranges. However, an optimum surfactant concentration for best results may exist.

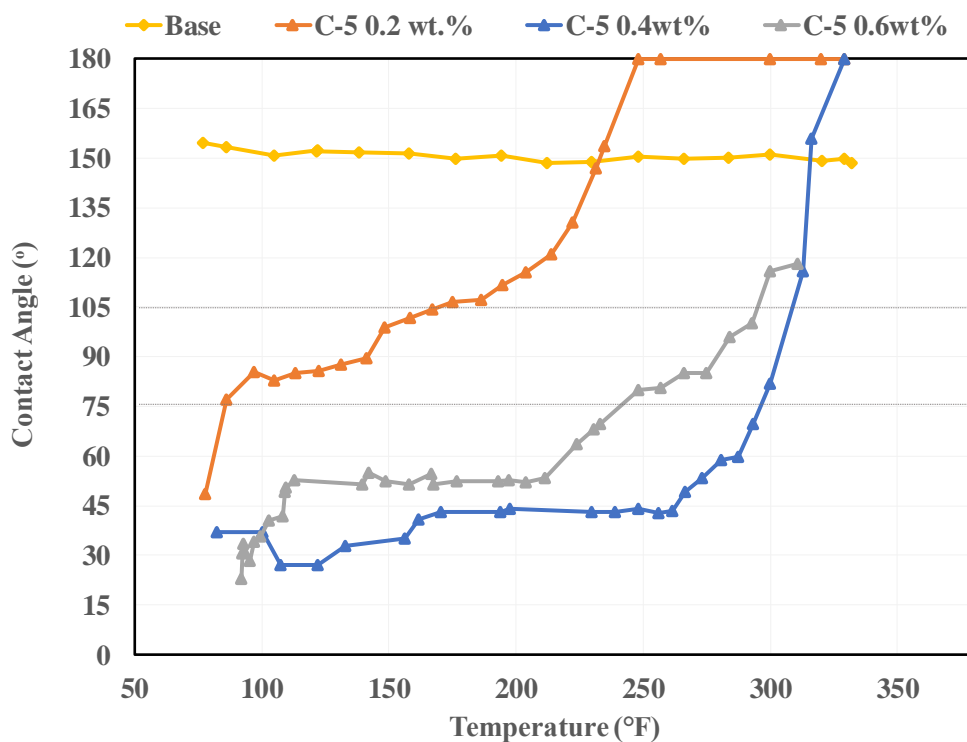


**Figure 42: Contact angle results for surfactants C-1 at concentrations 0.2 wt.%, 0.4 wt.%, and 0.6 wt.% evaluated at high-temperature conditions. Higher surfactant concentrations are more suitable for high-temperature applications.**

#### 5.1.5.3.2 Co-surfactant systems

As shown in **Figure 34**, some higher concentrations of blends 1:3, 2:3, and 3:2 produced low CA values at LPT conditions. This was further investigated at HPHT conditions. Results for blends C-1:Z-2 (1:3) are compared at concentrations 0.2 wt.% and 0.4 wt.% in **Figure 43**. The results for the blend of C-1:Z-1 (2:3) at 0.4 wt.% are also presented.

For the case of blend 1:3 at a total concentration of 0.4 wt.%, an initially water-wet system was produced. This system remains water-wet for a wider temperature range (ITL = 355°F) compared to the lower concentration 0.2 wt.% (ITL = 300°F). This higher

concentration surfactant system also produced lower water-wet CA values (average CA=  $28.9^{\circ} \pm 7^{\circ}$ ) for the temperature range evaluated up to the ITL. A significant increase in CA value is observed above 355 °F. Corresponding CA images at various temperature and pressure conditions are shown in **Figure 44**.

Results for blend 2:3 at a total concentration of 0.4 wt.% also show a decrease in temperature sensitivity compared to the blend evaluated at 0.2 wt.%. In this case, a water-wet system was also achieved with average CA values of  $30.5^{\circ} \pm 5.2^{\circ}$  for the temperature range evaluated up to ITL of 333°F. Above 333°F, a gradual increase is observed in the CA values indicating that beyond that temperature, the system becomes less effective. Corresponding CA images at various temperature and pressure conditions are shown in **Figure 45**.

HPHT results showed that increasing the surfactant concentration also increased the effectiveness of the surfactant system in producing favorable water-wet systems at higher temperature conditions. Higher concentration systems had higher ITLs indicating improved effectiveness at high-temperature conditions.

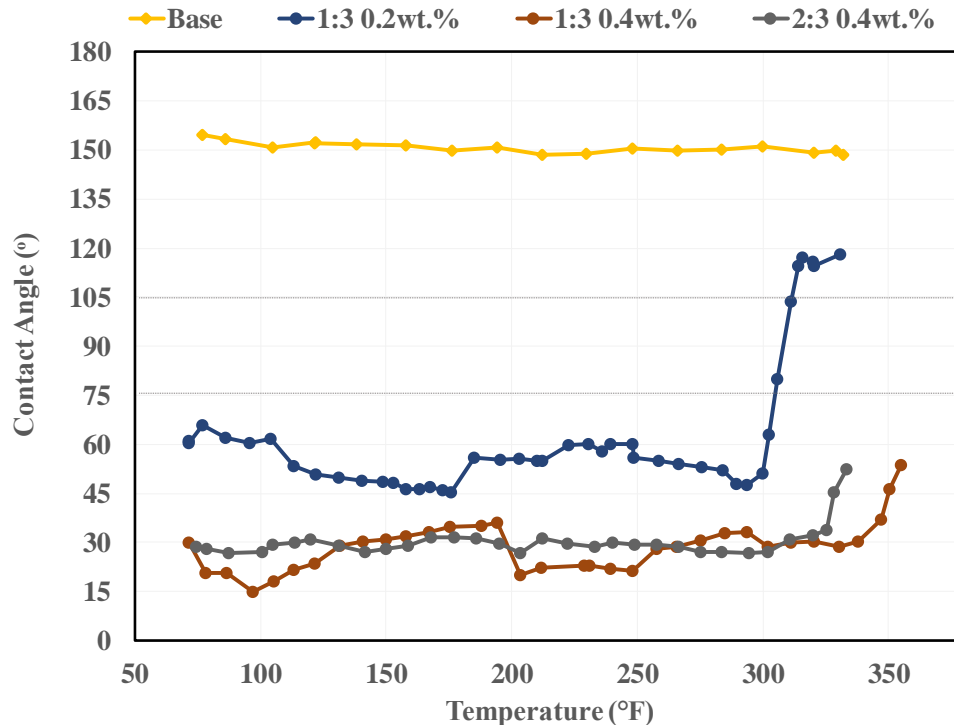


**Figure 43: Contact angle results for co-surfactants C-2:Z-1 at combination 1:3 at total concentration of 0.2 wt.% and 0.4 wt.% and combination 2:3 at total concentration of 0.4 wt.% evaluated at high-temperature conditions.**

#### 5.1.5.3.3 Understanding the surfactant concentration effect

A trend has been established in the behavior of single and co-surfactant systems where higher ITL values/ improved surfactant effectiveness are typically observed at higher surfactant concentrations. The solubility problem of ionic surfactants has been previously discussed, where there is a reduction in surfactant effectiveness at higher temperatures as a result of the increased solubility of the surfactant molecules. The dissolution of the surfactant molecules in the aqueous phase leaves a reduced number of surfactants at the crude oil/brine/rock interface.

However, at higher concentrations, an increased number of surfactant molecules are present in the system. A higher surfactant concentration increases the saturation of the aqueous phase, which reduces the solubility of the surfactant molecules. When the saturation of the aqueous phase is increased, fewer surfactant molecules are able to re-dissolve into solution, thereby ensuring that a higher number of surfactant molecules are present at the crude oil/brine/rock interface to alter wettability. Hence, higher ITL values and improved surfactant performance is observed with higher surfactant concentration systems at high-temperature conditions.

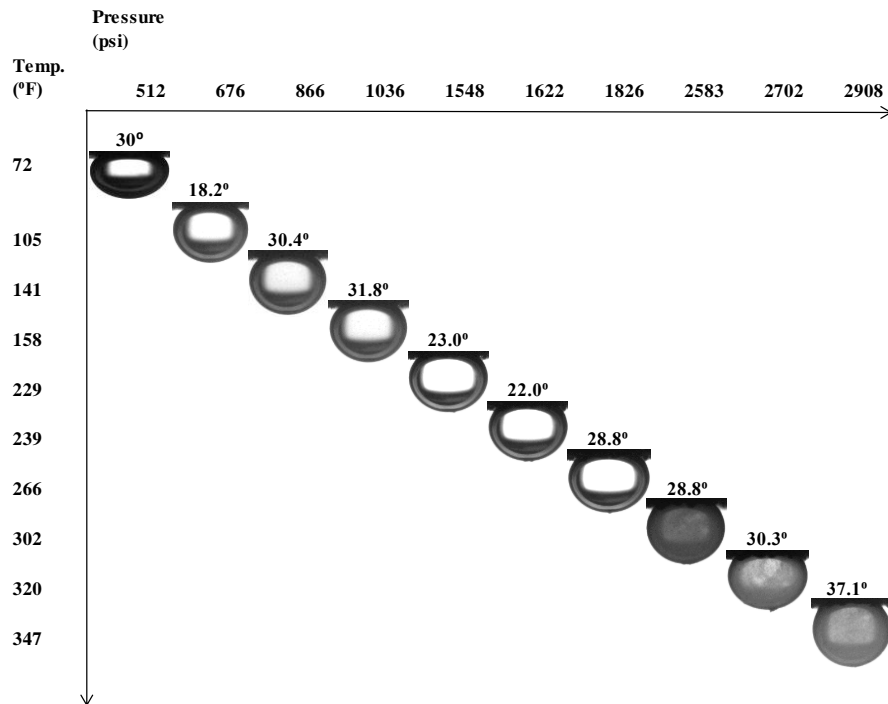


**Figure 44: HPHT contact angle data for C-2:Z-1\_1:3 0.4 wt.% surfactant in brine  
A. CA observed to be water-wet up to 355°F.**

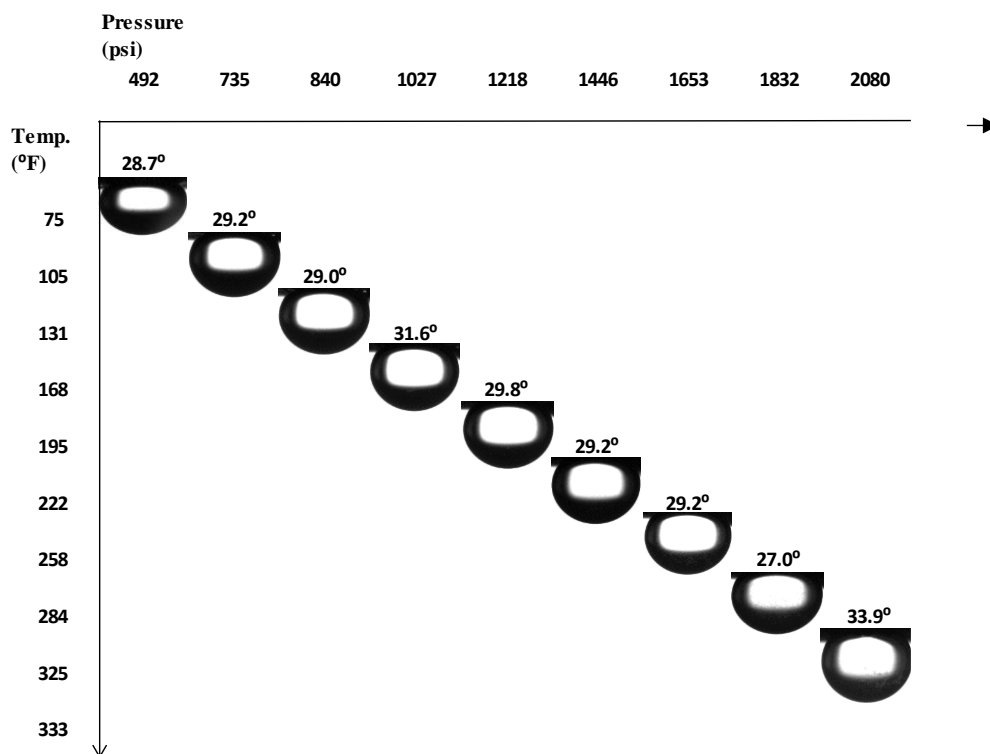


**Figure 45: Contact angle images and values for co-surfactants C-2:Z-1 at combination 2:3 at a total concentration of 0.4 wt.% in brine A at high-temperature conditions. CA observed to be water-wet up to 333°F.**

#### 5.1.5.4 *Effect of salinity on single and cosurfactant systems*

##### 5.1.5.4.1 Single surfactant systems

**Figure 46** displays the results for surfactant C-1 at a concentration of 0.2 wt.% in different salinity aqueous phases. The salinities evaluated are 0.2% (brine A), 1% (brine 1D) and 2% (brine 2D). In brine A, of the lowest salinity, the initial CA produced by the surfactant system was 43.7°. The low salinity system maintained a water-wet system with average CA values of  $34.8^\circ \pm 6.5^\circ$  up to ITL of 250°F. When the salinity of the aqueous phase is increased up to 1%, it was observed that the system had a higher ITL. The initial CA value, in this case, was strongly water-wet at 23.2°. The higher salinity system

produced a water-wet system with average CA values of  $30.5^\circ \pm 5.1^\circ$  up to ITL. Compared to the ITL in brine A, the ITL for the brine 1D system was  $312^\circ\text{F}$ , which is a significant increase from the lower salinity brine.

A similar trend was observed when salinity was increased to 2% NaCl. A lower initial CA value was produced ( $20.91^\circ$  at  $72^\circ\text{F}$ ). The system remained water-wet with average CA values of  $28.5^\circ \pm 6.5^\circ$  up to ITL. The ITL increased compared to the lower salinity cases with a value of  $324^\circ\text{F}$ . It is expected that further increases in salinity will continue to increase the ITL. However, lower salinity systems have been shown to be more favorable for improving recovery in carbonate-rich systems.

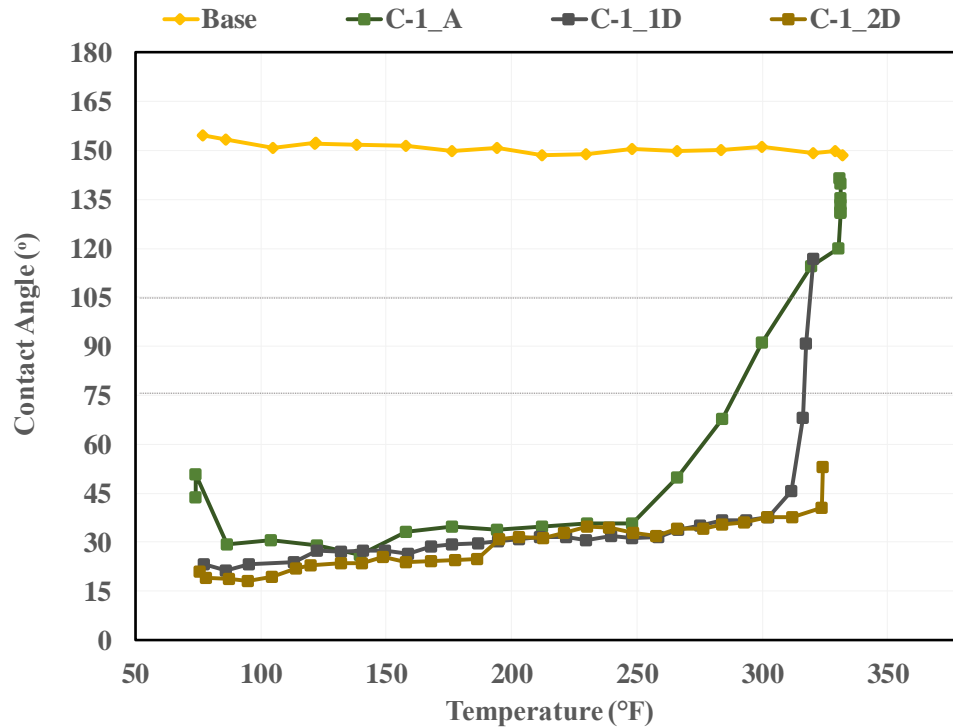


**Figure 46: Contact angle results for surfactant C-1 at a concentration of 0.2 wt.% in brine A (0.2% TDS), brine 1D (1% TDS), and brine 2D (2% TDS) evaluated at high-temperature conditions.**



#### 5.1.5.4.2 Co-surfactant systems

Higher salinity surfactant systems have been determined to be effective for higher temperature applications. Results for blend 1:3 at 0.2 wt.% are presented in **Figure 47** for three different salinity cases. The salinities evaluated are 0.2% (brine A), 1% (brine 1D) and 2% (brine 2D). While blend 1:3 at 0.2 wt.% in brine A produced average CA values of  $53.6^\circ \pm 7^\circ$  for temperatures evaluated up to 300°F, this result was improved as the salinity of the aqueous phase increased. When salinity was increased to 1% (brine 1D), a more water-wet condition was observed with an initial CA of 17.6°. In brine 1D, the system remained water-wet up to 320°F with average CA values of  $27.0^\circ \pm 8.6^\circ$ . Above 320°F, the system is observed to transition into the intermediate-wet zone, indicating that the ITL had been reached. Corresponding CA images at various temperature and pressure conditions are shown in **Figure 48**.

When the salinity of the system was further increased to 2% (brine 2D), it was observed that the system produced lower CA values at higher temperature conditions compared to the lower salinity systems previously evaluated. The initial contact angle measured was 19.8°. The system remained water-wet for temperatures up to and likely greater than 350°F with average CA values of  $21.5^\circ \pm 3.2^\circ$ .

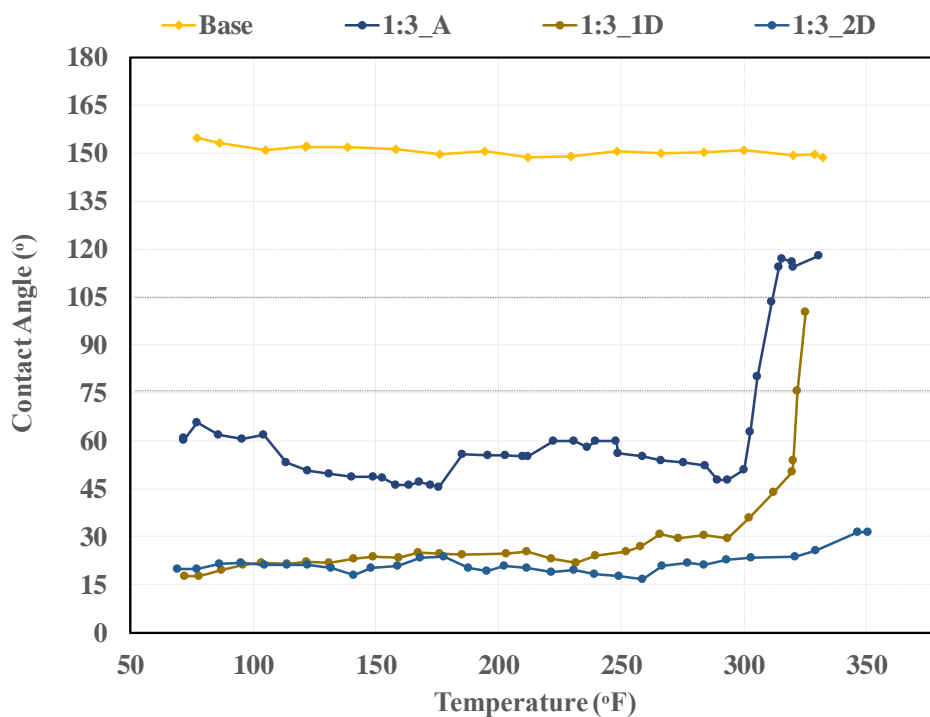


**Figure 47: Contact angle results for co-surfactants C-2:Z-1 at combination 1:3 at a total concentration of 0.2 wt.% in brine A (0.2% TDS), brine 1D (1% TDS), and brine 2D(2% TDS) evaluated at high-temperature conditions.**

#### 5.1.5.4.3 Understanding the effect of salinity

The salinity of the aqueous phase was observed to be a determinant in the behavior of the surfactant at high-temperature conditions. For the single surfactants and co-surfactant systems, their effectiveness at higher temperature conditions was observed to increase as the salinity of the aqueous phase was increased. The higher the salinity of the brine phase, the higher the ITL value produced. Hence, higher salinity systems were observed to be effective for higher temperature applications.

It was determined that the presence of a significant amount of salt ions in the aqueous phase reduces the solubility of surfactant molecules. This is because when the

aqueous phase is saturated with salt ions, fewer surfactant molecules are able to dissolve into the solution. Therefore, more surfactant molecules remain at the interface and alter the wettability. The presence of ions in the aqueous phase reduces the solubility of the surfactants, which ensures their effectiveness at high-temperature conditions.

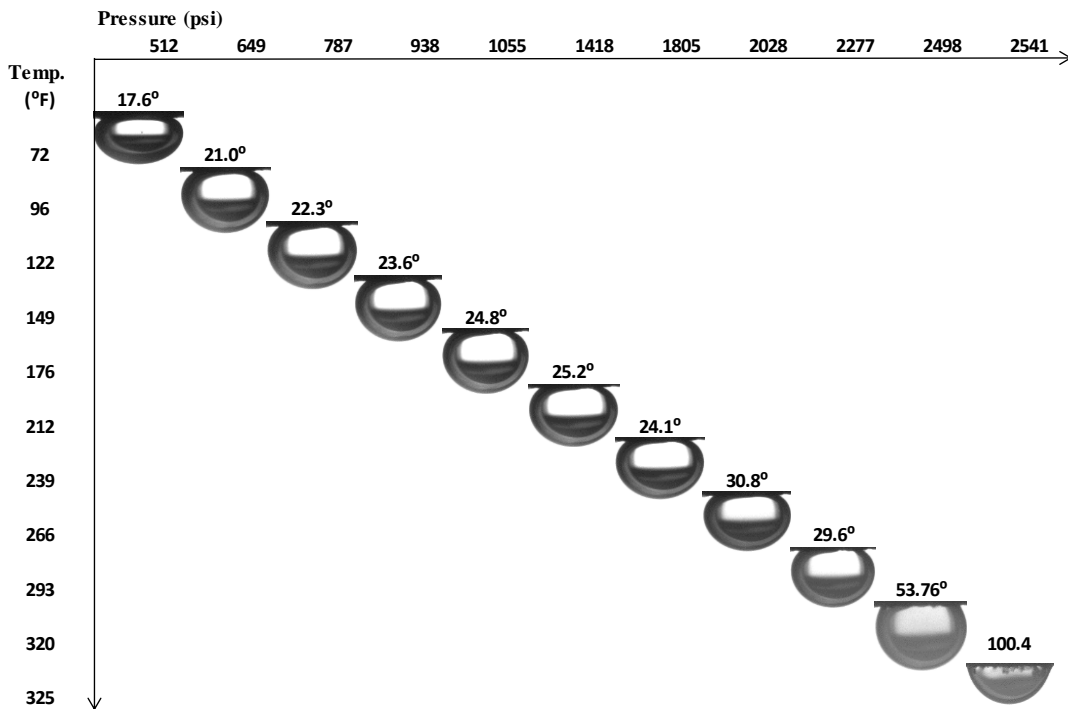


**Figure 48: Contact angle images and values for co-surfactants C-2:Z-1 at combination 1:3 at a total concentration of 0.2 wt.% in brine 1D evaluated at high-temperature conditions. Contact angles observed to be water-wet up to 320 °F.**

#### ***5.1.5.5 Summary of observations from HPHT CA Results***

The trend observed in the HPHT analysis of ionic surfactants indicates that ionic surfactants are effective only up to a certain temperature beyond which they become ineffective. This temperature is the ionic surfactant temperature limit (ITL) which is defined as the temperature beyond which the surfactant system becomes ineffective in producing a favorably water-wet system as a result of increased solubility in the aqueous phase.

For surfactants to be effective in wettability alteration, the surfactant molecules must be present at the crude oil/brine/rock interface in order to alter the behavior of the rock surface. Hence, when the surfactant molecules are not present at the interface, they can no longer work effectively in the system. Therefore, an ionic surfactant system that can create and maintain water-wet systems at lower temperatures becomes less effective at higher temperatures causing the system to transition into intermediate-wet and oil-wet zones. This is a result of the surfactant molecules going into the aqueous phase as the temperature increases due to their increased solubility with temperature. As more and more surfactant molecules go into the aqueous phase, the system becomes less and less effective in altering the wettability favorably.

To design surfactant systems for high-temperature EOR applications, the surfactant must maintain their wettability alteration properties even at high-temperature conditions. The surfactant molecules must remain at the crude oil/brine/rock interface at high temperatures instead of dissolving into the aqueous phase.

Based on the HPHT results, it was determined that the effectiveness of the surfactant systems at high-temperature conditions could be improved by:

1. Increasing the surfactant concentration,
2. Optimizing surfactant structure based on molecule solubility,
3. Using co-surfactants, and
4. Increasing the salinity of the aqueous phase.

## 5.2 Interfacial tension results

Surfactants have a significant effect on the IFT of an oil-aqueous phase system. A reduction in IFT is typically observed when surfactants are present. Lower IFT values are less favorable for enhancing recovery in reservoir systems when the goal is wettability alteration. Lower IFT values have been correlated to reduced capillary pressure, which is less favorable for spontaneous imbibition. However, low IFT values can be preferred for improved oil mobility. A moderate IFT is the objective of this study.

### 5.2.1 LPT IFT results

#### 5.2.1.1 *Single surfactant systems*

The single systems of cationic (C-1, C-2, C-3, C-4, and C-5), anionic (A-1, A-2, A-3), and zwitterionic (Z-1) surfactants were also evaluated at LPT conditions at 170°F to observe IFT behavior. **Figure 49** shows IFT results for the different surfactants at varying concentrations. Generally, anionic surfactants resulted in lower IFT values compared to cationic and zwitterionic surfactants. IFT was observed to not vary significantly with concentration. The lowest IFT values were measured with an anionic surfactant, A-1.

At LPT conditions, all ionic surfactants tested were effective in reducing the IFT value at any concentration. Initially, in the brine A system with no surfactants present, the IFT was estimated to be 11.2mN/m. The measured IFT values for the different surfactant systems are presented in **Figure 49**. Cationic surfactants lowered the IFT values at all concentrations evaluated. Surfactant C-5 resulted in the lowest IFT values of all the cationic surfactants tested. In comparison, surfactant C-3 resulted in the least IFT

reduction. As surfactant concentration increased, a slight reduction was observed in IFT values in some cases. At a concentration of 0.2 wt.%, the cationic surfactants reduced IFT to values in the range of 0.61 – 8.48 mN/m. Zwitterionic surfactant also resulted in IFT reduction.

Anionic surfactants caused the most IFT reduction. Marked reduction in IFT was observed at higher surfactant concentrations. At a low concentration of 0.2 wt.%, anionic surfactants produced low IFT values in the range of 0.03 - 0.8mN/m. These low IFT values are in the range of values typically preferred for water flooding in conventional reservoirs. Low IFT values of anionic surfactants presented limitations for HPHT CA measurements. As a result of low IFT, there was increased difficulty in preventing experiment contamination in HPHT measurements - oil drops more easily escaped the oil line disrupting the oil drop/rock system being evaluated.

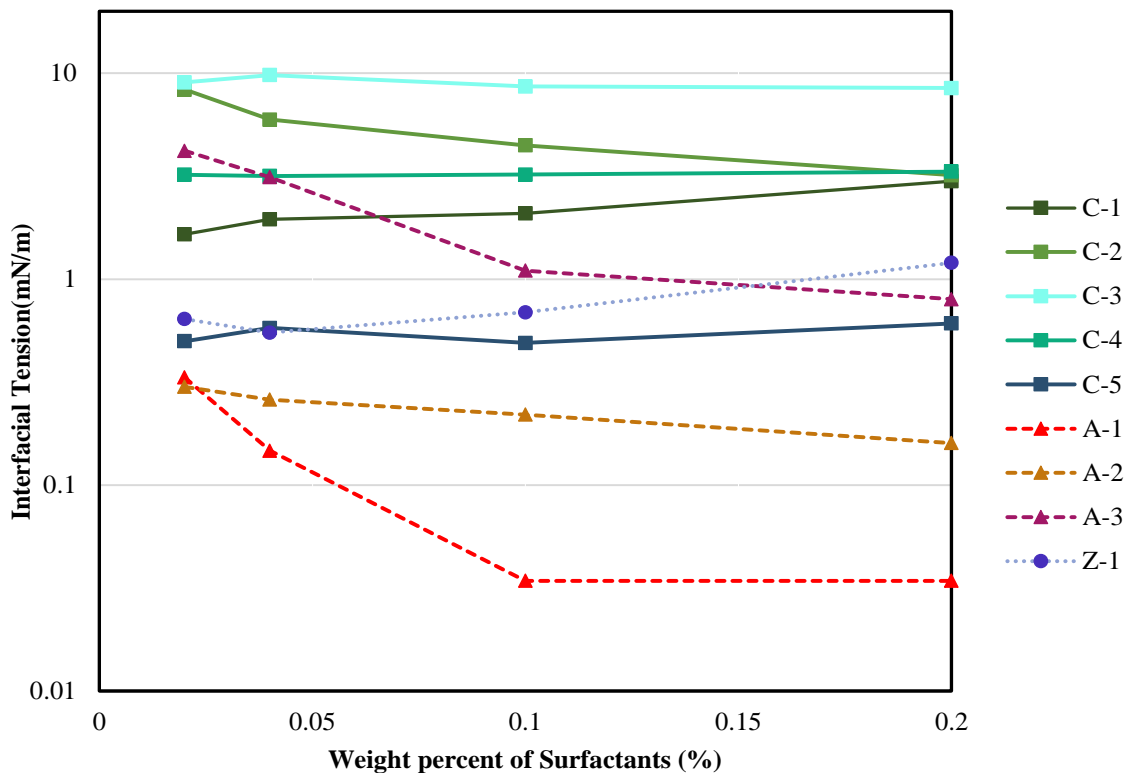


**Figure 49: IFT results for different ionic surfactants at varying concentrations evaluated at LPT conditions.**

### 5.2.1.2 Co-surfactant blends

The use of cosurfactants has been shown to have an impact on the contact angle. These co-surfactants also impact the IFT of the system. When surfactants are mixed, chemical interactions between the hydrophilic heads and hydrophobic tails result in a unique set of properties. IFT results for single surfactant systems, as well as their blends, are presented in **Figure 50**.

Surfactant C-1 had an initial IFT value of 3 mN/m, while Z-1 had a value of 1.2 mN/m. In combination (C-1:Z-1), at the different blend ratios, the measured IFT was an average of the singular systems with values in the range of 2.3 – 2.5 mN/m. Also,



surfactant C-2 had an initial IFT value of 3.2 mN/m. In combination (C-2:Z-), the different blend ratios also resulted in IFT values (2.5 -2..6 mN/m) which were in the average range of the singular systems.

There was no significant difference in IFT for the different combination ratios evaluated. Although the use of co-surfactants resulted in a range of wettability conditions, their IFT results were quite consistent. There was no correlation established between the IFT values estimated for the blends and the contact angles that they produced. LPT IFT measurements did not offer much insight into the behavior of these blends.

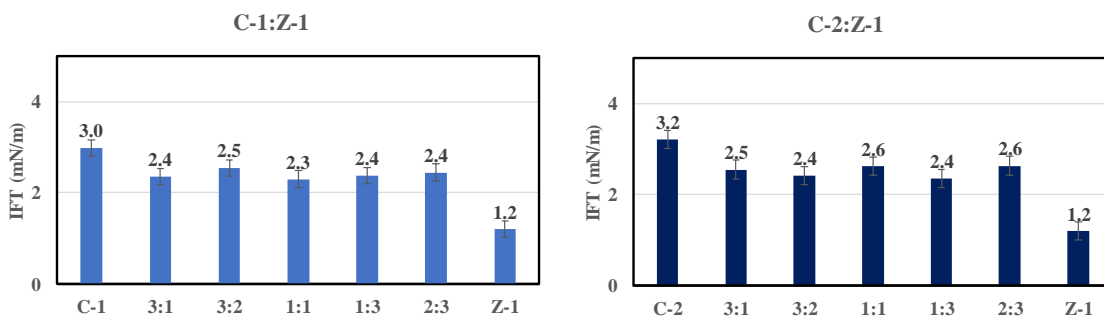


**Figure 50: IFT results for co-surfactants C-1:Z-1 and C-2:Z-1 at different combination ratios and total concentration of 0.2 wt.%.**

### 5.2.1.3 Summary of observations from LPT IFT Results

Surfactants were effective in reducing the IFT to varying degrees at LPT conditions. Cationic and zwitterionic surfactants resulted in some IFT reduction. However, the anionic surfactants evaluated resulted in significant IFT reduction compared to the other surfactants tested. For the base case without surfactants, IFT was determined to be 11.2mN/m. The presence of anionic surfactants resulted in IFT values within the range 0.03 - 0.8mN/m at a concentration of 0.2 wt.%.

IFT was also evaluated using co-surfactants at different combination ratios. The results showed that the blend of the cationic and zwitterionic surfactants resulted in intermediate IFT values of those produced by the cationic surfactant and the zwitterionic surfactant alone. The IFT values produced by the blends were in the same range irrespective of the blend combination ratio.

### 5.2.2 HPHT IFT results

Pressure and temperature are the two parameters being altered during HPHT measurements. Both factors influence the density of the fluid phases. Hence, it was important to correct for density changes of the oil and aqueous phases as a result of PVT changes in order to generate accurate IFT results. An equation was developed to correct for density using data from PVTsim (a 40+ component fluid model) derived with JMP. The corrected density values were used in the IFT calculations. The corrected IFT values are presented in this section.

**Figure 51** displays results for the IFT measured at different temperature points. When no surfactants are present (Base), the IFT of the crude oil in brine A is high with an initial value of 28 mN/m at 72°F. However, as the temperature of the system was increased, the IFT of the system was reduced. At a temperature of 325°F, IFT was reduced to 18.4 mN/m. The decrease in IFT is a result of the reduction in the oil density as the temperature was increased.

### 5.2.2.1 *Single Surfactant systems*

From **Figure 51**, the presence of surfactants in the aqueous phase resulted in lower IFT values than the base case, as expected. Corresponding images are displayed in **Figure 52**. At a concentration of 0.2 wt.%, surfactant C-5 resulted in an IFT value of 0.4 mN/m at 72°F, which was significantly lower than the IFT of the base case at the same conditions. There was a steady increase in IFT up to At 200°F, followed by a much steeper rise as the temperature increased. At 200°F, IFT was 2.0 mN/m. At the temperature of 325°F, the IFT increased to 15.3 mN/m. This is close in value to the base case at the same temperature when no surfactants are present.

A similar trend was observed when the concentration of the surfactant was increased. At a concentration of 0.4 wt.%, similar IFT values are observed as with the 0.2 wt.% concentration system. The IFT of the system increased steadily from 0.5 mN/m at 72°F up to 2.6 mN/m at 212°F, then steeply up to 13.2 mN/m at 325°F. At higher temperatures, the higher concentration 0.4 wt.% surfactant system produced lower IFT values than the 0.2 wt.% system. At surfactant concentration of 0.6 wt.%, the IFT value was observed to increase steadily from 0.3 mN/m at 72°F up to 1.5 mN/m at 250°F, then steeply up to 7.8 mN/m at 325°F. Generally, higher surfactant concentrations resulted in lower IFT values at the same temperature conditions. The contrast in IFT values with concentration was more pronounced at high-temperature conditions. The higher the surfactant concentration, the lower the value of the IFT produced, especially at high temperatures.

The general trend observed with single ionic surfactant systems shows that the presence of surfactants results in low IFT values at low temperatures. However, IFT values increase as the temperature is increased. This is further confirmation that the solubility of surfactants increases with increasing temperature. Hence, the surfactant dissolves in the aqueous phase as opposed to partitioning at the oil-brine interface. As a result, higher IFT values are observed at higher temperatures. As discussed previously, higher surfactant concentrations result in reduced solubility with temperature because an increased number of surfactant molecules can remain at the crude oil/brine/rock or oil/brine interface as a result of the increased saturation of the aqueous phase. Hence, higher concentration surfactant systems produce lower CA and IFT values.

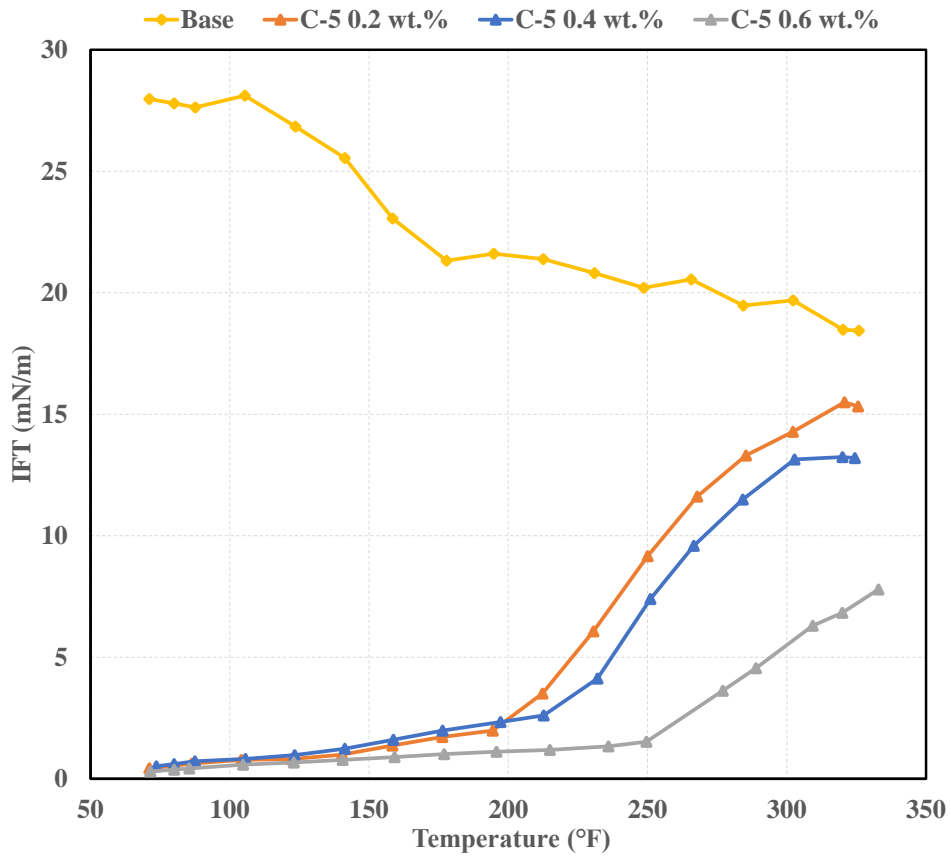


**Figure 51: IFT Results for surfactant C-5 at concentration 0.2 wt.%, 0.4 wt.%, and 0.6 wt.% evaluated in brine A at high-temperature conditions. IFT values increase with increasing temperature when surfactants are present.**

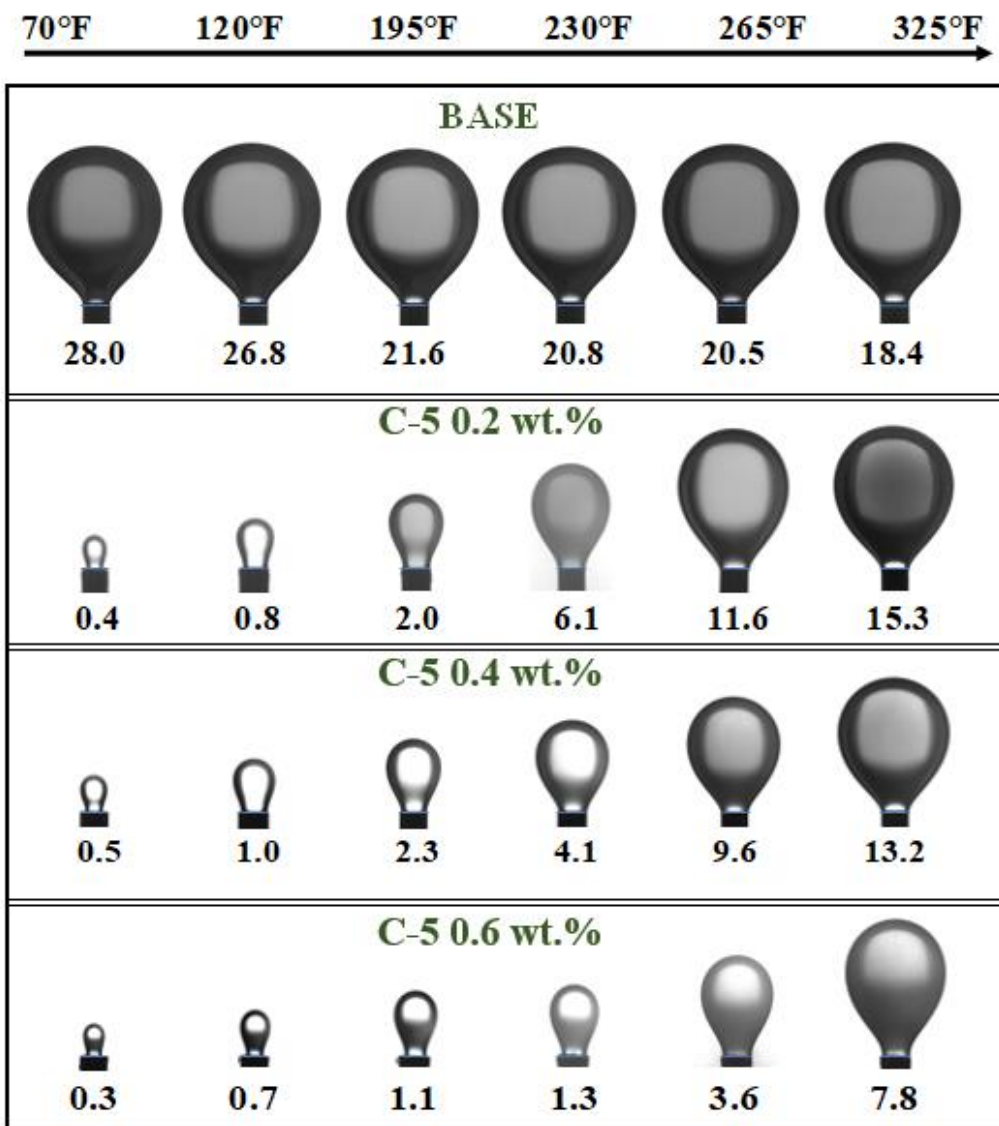


Figure 52: IFT Images and values (in mN/m) displayed with temperature. Results displayed for the base case and surfactant C-5 at concentrations of 0.2 wt.%, 0.4 wt.%, and 0.6 wt.%.

### 5.2.2.2 *Co-surfactant systems*

The effect of concentration was also investigated with the co-surfactant blend of C-2:Z-1 at a combination ratio of 1:3. The results and corresponding images are displayed in **Figure 53** and **Figure 54**, respectively. As expected, the co-surfactant blend resulted in lower IFT values compared to the base case at the concentrations evaluated. The concentration of 0.2 wt.% resulted in an IFT value of 2.1 mN/m at 72°F. As the temperature of the system was increased, further reduction in IFT was observed with a value of 0.9 mN/m at 200°F. This was subsequently followed by a steep increase in IFT as the temperature was further increased. At the temperature of 325°F, the IFT increased to 14.6 mN/m.

When the total concentration was increased to 0.4 wt.%, lower IFT values were observed. At 72°F, the IFT value was 1.6 mN/m. As the temperature was increased, the IFT values remained fairly consistent up to 285°F. Further increase in temperature resulted in a steady increase in the IFT. At 325°F, the IFT value remained as low as 2.8 mN/m. When the total concentration was increased to 0.6 wt.%, the IFT value of the system was determined to be 1.6 mN/m at 72°F. The IFT was fairly constant for a wide temperature range with a value of 1.3 mN/m at 325°F. Similar to the single surfactant system previously discussed, higher co-surfactant blend concentrations resulted in lower IFT values at the same temperature conditions.

It is important to note that while even at high concentrations, the single surfactant system resulted in increased IFT values at high-temperature conditions, co-surfactants systems maintained fairly low IFT values at these high temperatures. This is indicative

that the solubility of the co-surfactant systems is much lower compared to the single surfactant systems (this was also observed in the CA results). However, even for the high concentration co-surfactant systems, a steep increase in IFT is to be expected beyond a certain temperature limit.

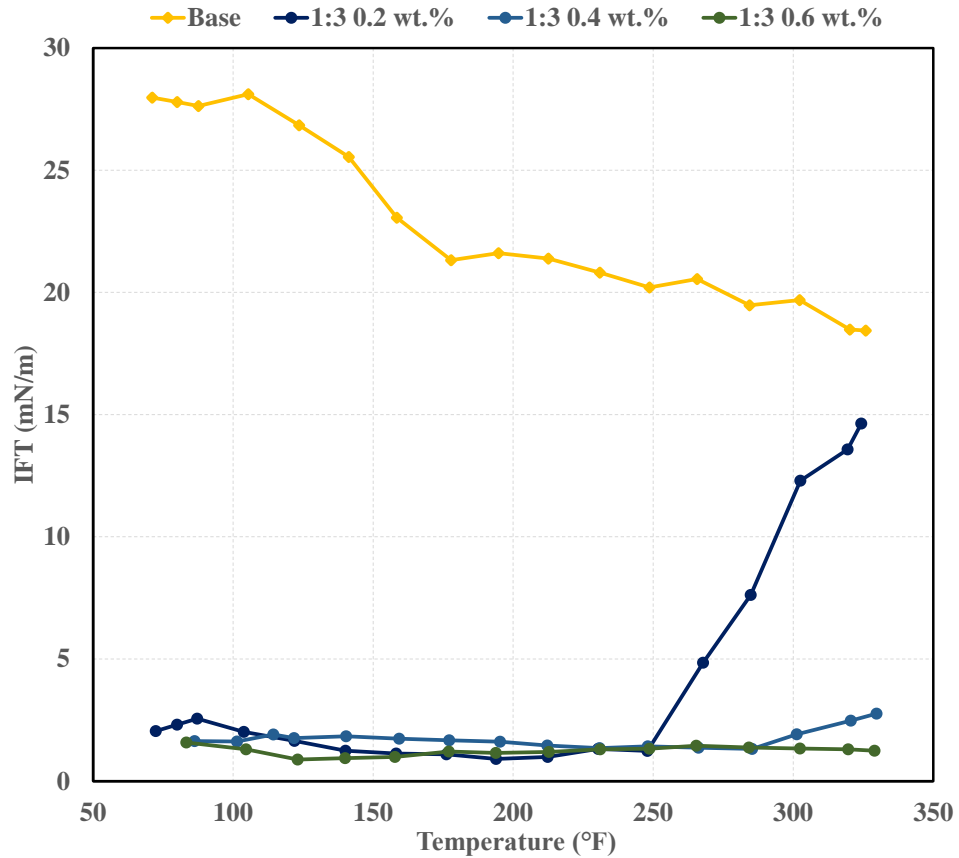


**Figure 53: IFT Results for co-surfactants C-2:Z-1 at combination ratio 1:3 at total concentration of 0.2 wt.%, 0.4 wt%, and 0.6 wt.% in brine A evaluated at high-temperature conditions.**



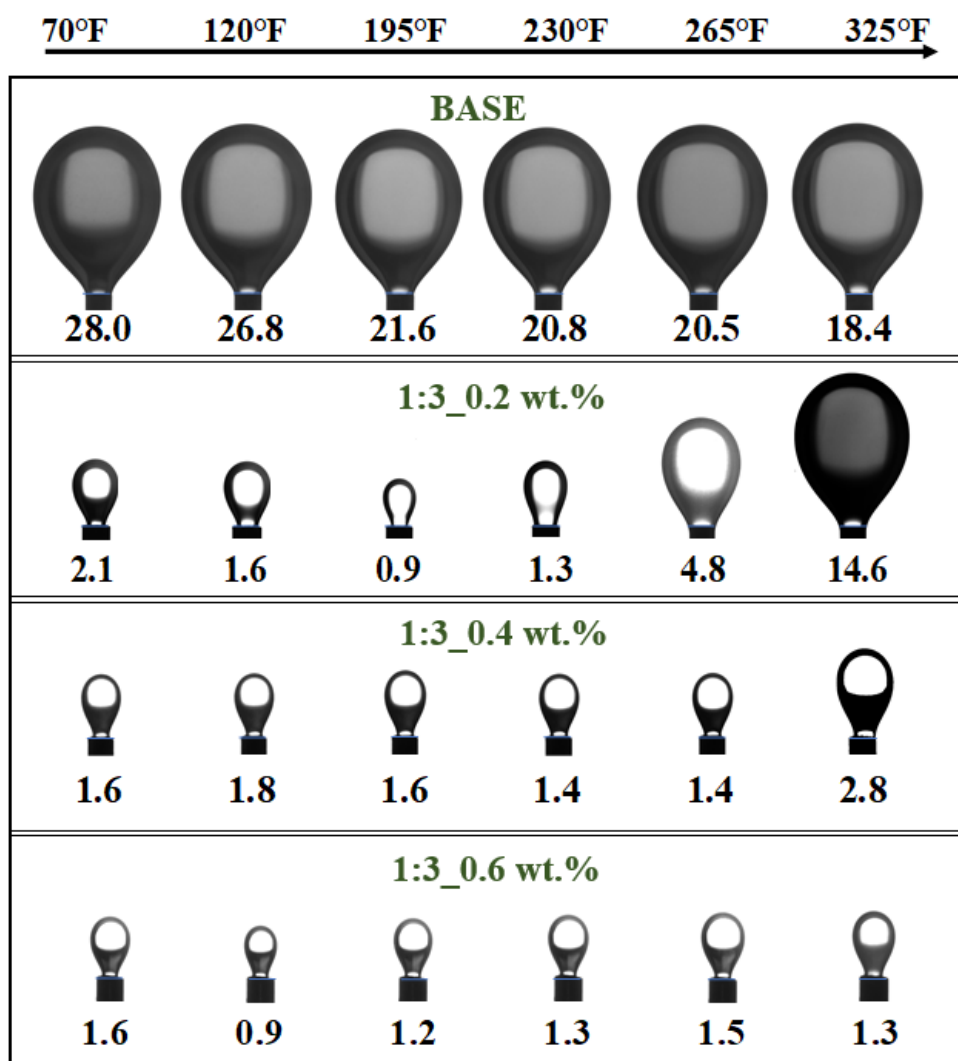


Figure 54: IFT Images and values (in mN/m) displayed with temperature. Results displayed for base case and co-surfactants C-2:Z-1 at concentrations of 0.2 wt.%, 0.4 wt.%, and 0.6 wt.%.

### 5.2.2.3 Effect of salinity on single and co-surfactant systems

Higher salinity systems were observed to result in lower IFT values. **Figure 55** and **Figure 57** show results for single system C-1 and co-surfactant system C-2:Z1(1:3),

respectively. CA values were evaluated in brine A (0.2% TDS), brine 1D (1% TDS), and brine 2D (2% TDS). **Figure 56** and **Figure 58** display the corresponding images.

As observed in the figures, at the same surfactant concentration of 0.2 wt.%, different results were observed based on the salinities of the various systems. For the single C-1 surfactant system, when salinity increased from 0.2% TDS (brine A) to 1% TDS (brine 1D), a significant difference was observed in IFT values. The contrast in the IFT values was more significant at higher temperature conditions. For the low salinity case (brine A), the IFT value was 2.2 mN/m at 72°F. The IFT value increased steadily up to 6.0 mN/m at 230°F. Onward, a steeper increase was observed. At a temperature of 325°F, the IFT value increased to 13.3 mN/m. When the salinity of the system increased to 1% TDS (brine 1D), the IFT was observed to show less variation with temperature. This is an indication that the surfactant system is more stable with less solubility. The system produced an IFT value of 1.1 mN/m at 72°F, which gradually increased up to a value of 1.8 mN/m at 230°F, with a further increase up to 3.4 mN/m at 325°F. For the higher salinity case of 2% TDS (brine 2D), a further reduction was observed in the IFT. At a low temperature of 72°F, an IFT value of 0.7 mN/m. The IFT was observed to increase steadily up to 1.5 mN/m at 230°F and to 2.6 mN/m at 325°F.

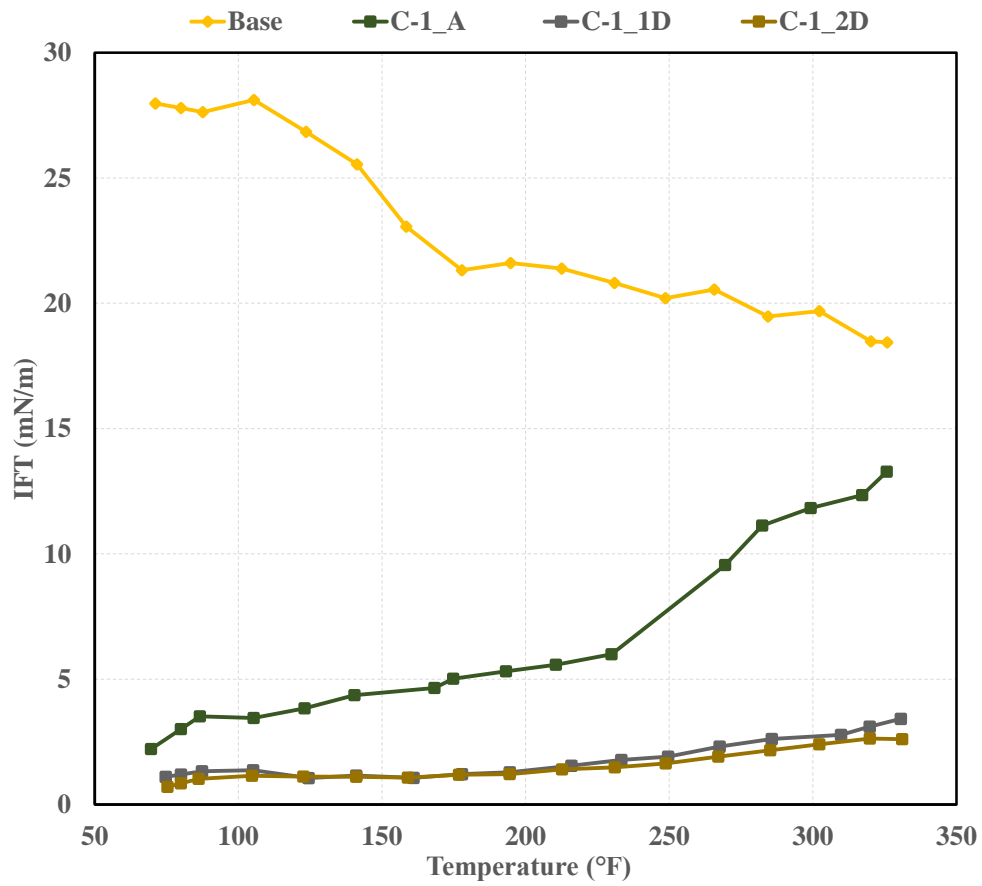


**Figure 55: IFT results for surfactant C-1 at 0.2 wt.% in brine A (0.2% TDS), brine 1D (1% NaCl), and brine 2D(2% NaCl) evaluated at high-temperature conditions.**

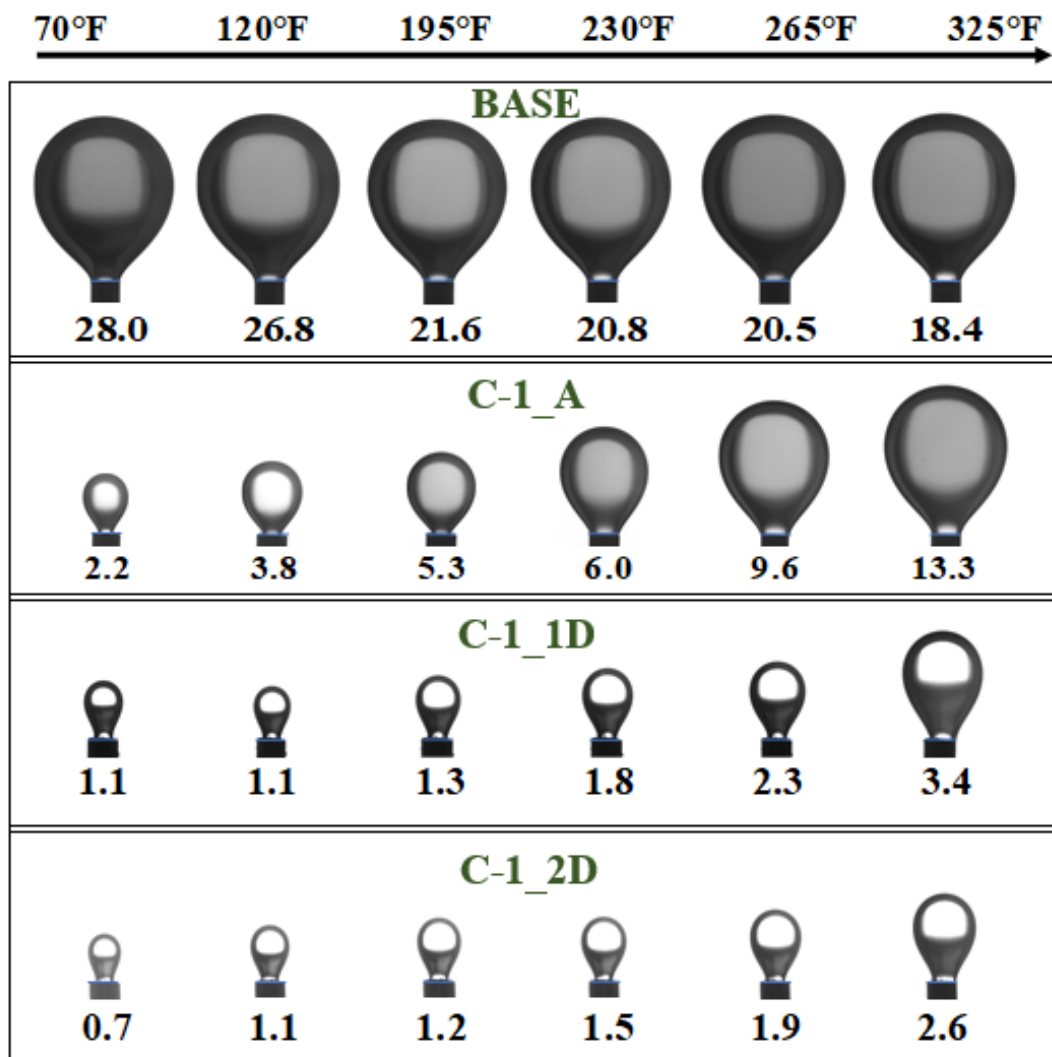


**Figure 56: IFT Images and values (in mN/m) displayed with temperature for surfactant C-1 at 0.2 wt.% in brine A, brine 1D, and brine 2D.**

Salinity also showed a unique effect on the behavior of co-surfactant systems. There was not much contrast in the IFT values produced by the different salinity systems at low-temperature conditions. Below 250°F, the varying salinity systems produced IFT values in the range of 0.9 mN/m – 2.6 mN/m. For all three salinity cases, the IFT values

were slightly reduced as the temperature was increased. For brine A, IFT was reduced from 2.1 mN/m at 72°F to 0.9 mN/m at 195°F. For brine 1D, the IFT value was at 1.6 mN/m at 72°F then lowered to 0.7 mN/m at 265°F. In the higher salinity brine 2D, IFT was reduced from 2.6 mN/m at 72°F to 1.3 mN/m at 265°F. Subsequently, beyond the temperature point where the minimum IFT value was observed, there was a steep increase in the IFT value. The higher salinity brine system produced the lowest IFT value at a high temperature of 325°F. At 325°F, brine A, 1D, and 2D produced IFT values of 14.6 mN/m, 3.2 mN/m, and 3.0 mN/m, respectively.

Generally, the results for the single surfactant system and the co-surfactant system show a similar trend of lower IFT values at higher temperatures when the salinity of the aqueous phase is increased. This is further validation of the impact of surfactant solubility with temperature on the effectiveness of the surfactant system. The presence of a significant amount of salt ions in the aqueous phase reduces the solubility of surfactant molecules. This is because when the aqueous phase is saturated with salt ions, fewer surfactant molecules can dissolve into the solution. Therefore, more surfactant molecules remain at the interface and alter the wettability. The presence of ions in the aqueous phase reduces the solubility of the surfactants, which ensures their effectiveness at high-temperature conditions.

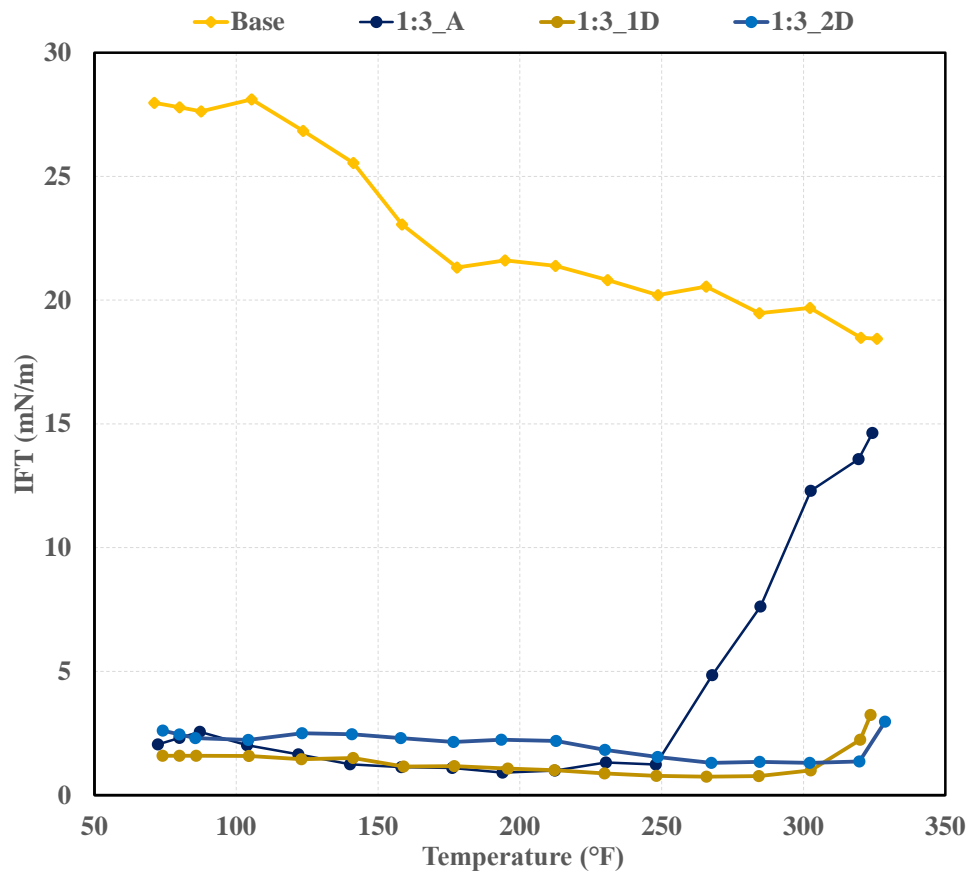


**Figure 57: HPHT IFT results for co-surfactant blends of C-2 and Z-1 at combinations 1:3 at a total concentration of 0.2 wt.% in brine A, brine 1D, and brine 2D.**

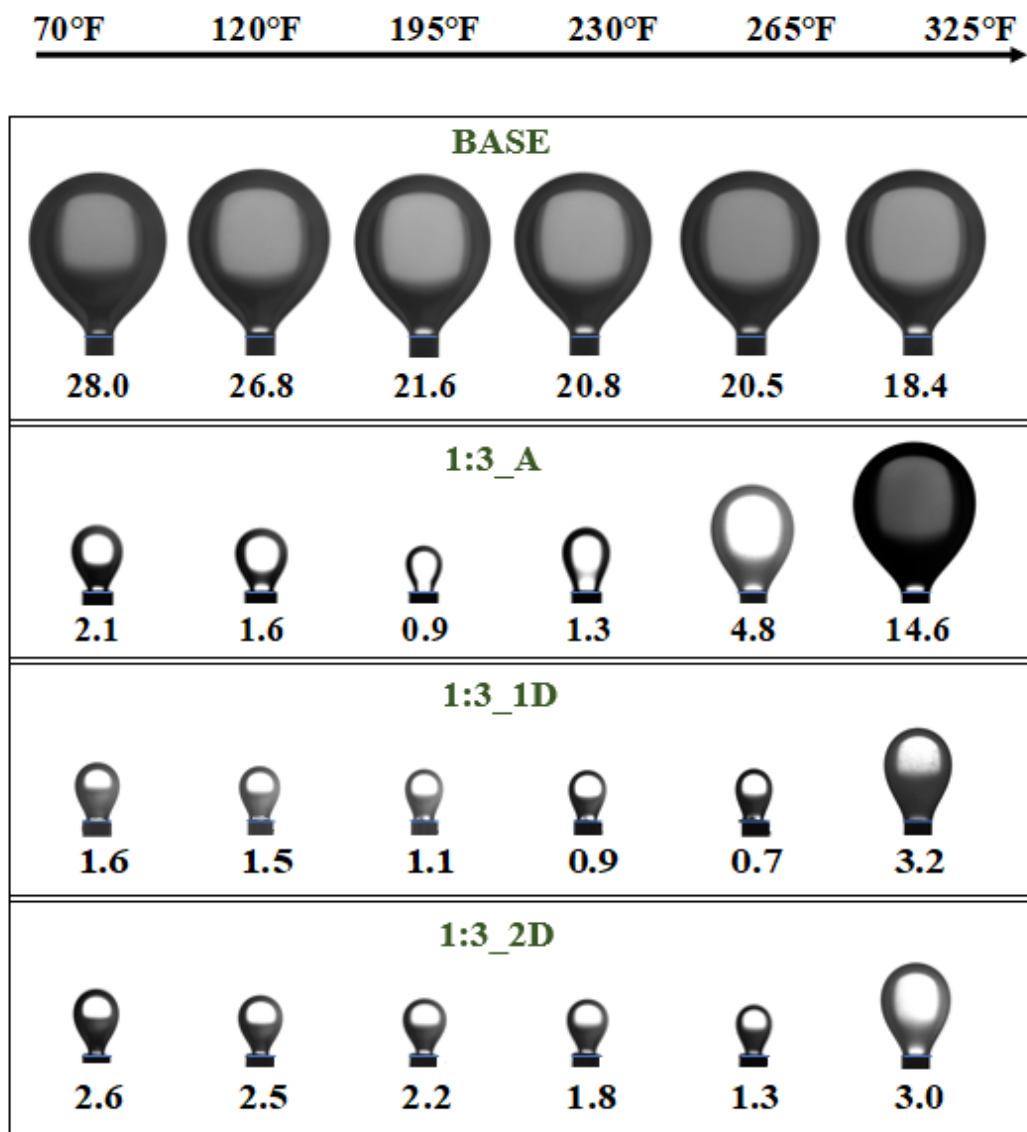


Figure 58: IFT images and values (in mN/m) for co-surfactant blends of C-2 and Z-1 at combinations 1:3 at a total concentration of 0.2 wt.% in brine A, brine 1D, and brine 2D.

#### **5.2.2.4 Additional insights into co-surfactant blends**

The co-surfactant blends being investigated so far are a combination of cationic surfactant C-2 and zwitterionic surfactant Z-1. To further understand the behavior of the blends, it was important to establish base cases for the single surfactant systems. The IFT results for single surfactant systems C-2 and Z-2 at concentrations of 0.2 wt.% are presented in **Figure 59**. The result for blends of the two surfactants at combination ratios of 1:3 and 3:1 at a total concentration of 0.2 wt.% are also presented. The corresponding IFT images are shown in **Figure 60**.

The single surfactant system C-2 produces relatively low IFT values at low temperatures. The IFT value was 6.4 mN/m at 72°F. However, the values were higher than that observed for the longer hydrophilic tail surfactant C-1 (**Figure 55**). As the temperature was increased, the IFT value was also observed to increase steadily. At 325°F, IFT had increased to 14.6 mN/m. This is a slightly different trend from that observed with the Z-1 surfactant. For the Z-1 case, the IFT produced at low-temperature conditions were significantly lower (1.1 mN/m at 72°F) and remained fairly constant for a wide range of temperature. Beyond 300°F, a notable increase in the IFT was observed. At 325°F, IFT had increased to 3.4 mN/m.

For combination ratio 1:3, at low temperatures, the blend produced low IFT values similar to the Z-1 surfactant with a range of values between 0.9 – 2.1 mN/m. However, above 250°F, a steep increase is observed in the IFT values, which mirrors a similar trend of increasing IFT values for the single C-2 surfactant. At 325°F, IFT had increased to 14.6 mN/m. A similar trend was observed with the combination ratio 3:1, where low IFT values



were produced at low temperatures with values in the range of 1.6 – 2.8 mN/m. An increase in IFT values was also observed as the temperature was increased to up to 10.8 mN/m at 325°F.

When surfactants C-2 and Z-1 were combined, the blends produced results that were intermediate of the single surfactant systems. For the blends evaluated, low IFT values were produced at low-temperature conditions, and at higher temperatures above 250°F, a significant increase in IFT was observed. Comparing results for blend 1:3, where the volume of Z-1 was higher, and blend 3:1, where the volume of C-2 was higher, showed that the blend systems behaved similarly irrespective of the combination ratio. It could be expected that when the volume of surfactant C-2 is higher in the blend combination, the blend may behave similarly to the C-2 surfactant and consequently for the Z-1 case as well. However, these blends form unique systems which are intermediate of the single surfactant systems irrespective of their combination ratios.

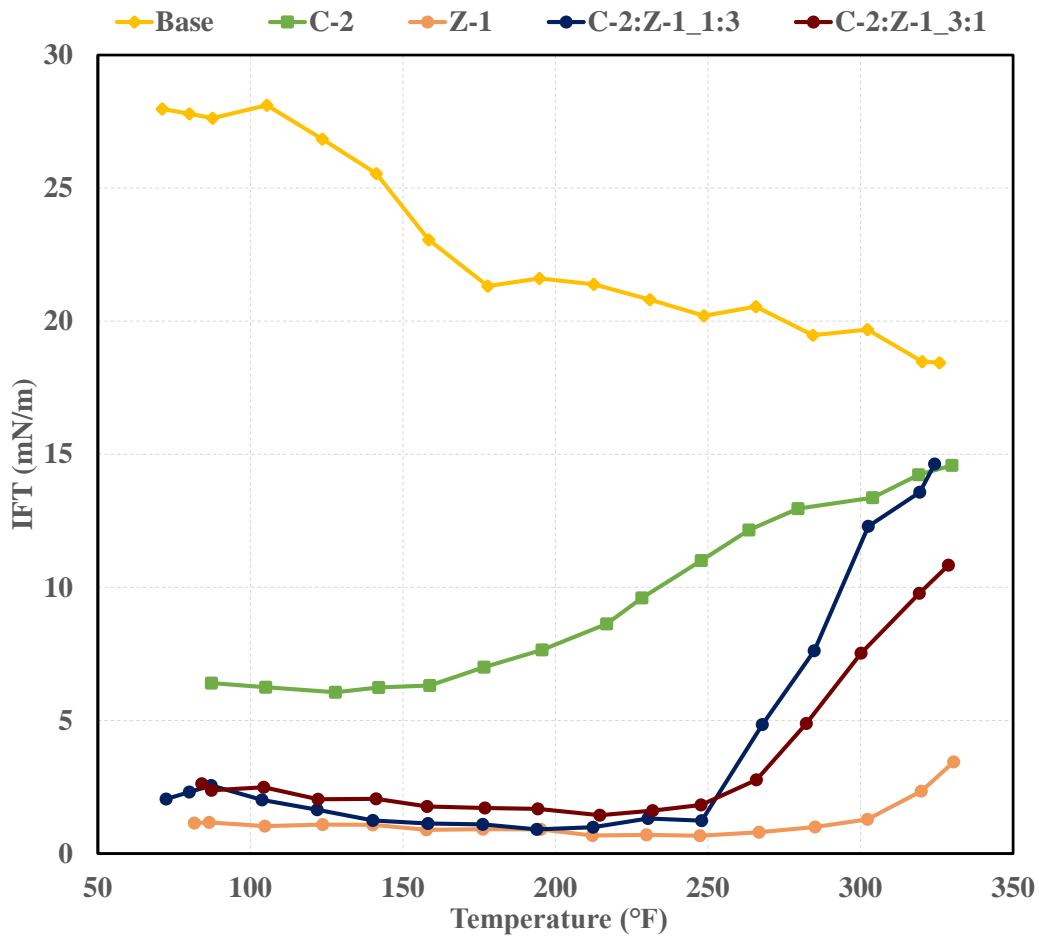


**Figure 59: IFT results for single surfactant systems C-2 and Z-1 at concentrations 0.2 wt.% and the co-surfactants C-2:Z-1 at combination ratios 1:3 and 3:1 at a total concentration of 0.2 wt.% in brine A evaluated at high-temperature conditions.**

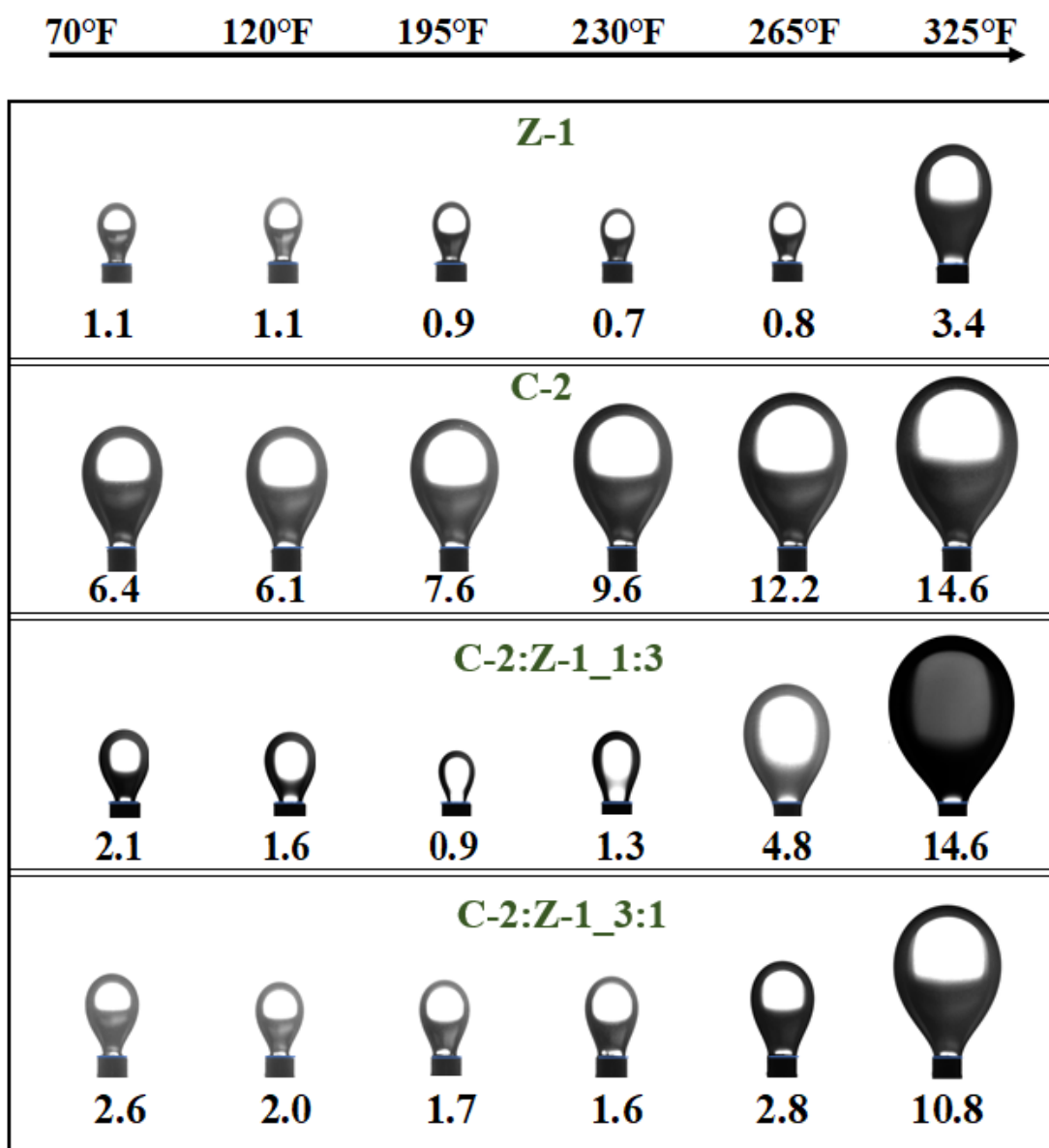


**Figure 60: IFT images and values (mN/m) for single surfactant systems C-2 and Z-1 at concentrations 0.2 wt.% and co-surfactants C-2:Z-1 at combinations 1:3 and 3:1 at total concentration of 0.2 wt.%.**

#### ***5.2.2.5 Summary of observations from HPHT IFT Results***

The presence of surfactants in the aqueous phase resulted in lower IFT values compared to the base case. The IFT reduction was greater at low-temperature conditions. However, the IFT value was observed to increase with increasing temperature. As the temperature was increased, the IFT increased steadily, up to a certain temperature point beyond which a steeper increase in IFT was observed. This is further confirmation that the solubility of surfactants increases with increasing temperature and that an ITL exists. This trend was observed for both the single and co-surfactant systems evaluated. However, the co-surfactant blends resulted in lower IFT values even up to the higher temperature conditions. This indicates that the solubility of the co-surfactant systems with temperature is significantly reduced compared to the single surfactant systems.

Generally, higher surfactant concentrations resulted in lower IFT values. At high-temperature conditions, the impact of the higher concentration system in producing lower IFT values is even more pronounced. Also, lower IFT values were observed with temperature as the salinity of the aqueous phase was increased. Hence, increasing the surfactant concentration or the salinity of the aqueous phase had a similar effect on the surfactant behavior. This results from the increased saturation of the aqueous phase in both cases, which reduces the solubility of surfactant molecules. Hence, increasing their effectiveness in producing low IFT values even at high-temperature conditions.

## 6 SPONTANEOUS IMBIBITION EXPERIMENTS

Spontaneous imbibition experiments are the final step in the workflow for the surfactant selection process for a laboratory study. In the previous section, contact angle and IFT values were estimated for the crude oil/brine/rock system. Surfactant systems that were effective in altering wettability favorably and producing moderate IFT values were identified and then further evaluated by HPHT SASI experiments. SASI experiments quantify the actual amount of oil recovered from the rock sample as a result of the presence of the surfactant molecules in the aqueous phase. It is expected the surfactant systems which produced low water-wet CA and relatively moderate IFTs will be most effective in improving recovery and increasing the recovery factor. Ultimately, the SASI experiments validate the capability of the surfactant systems being investigated in improving oil recovery from the shale core at high-temperature conditions.

The SASI experiments were carried out on Eagle Ford core plugs which were cleaned and aged for an optimal aging time. The aging process restored the original oil saturation of the core sample. The aged cores were immersed in the surfactant/brine solutions contained in the HPHT SASI cell. The HPHT SASI cell was placed in the oven at the Eagle Ford reservoir temperature of 325°F for 192h (192 hours). The amount of oil expelled from the core plugs was measured at the end of the experiment.

## 6.1 Impact of CA and IFT on Capillary Pressure ( $P_c$ )

Six (6) surfactant systems were selected for SASI studies. The selected surfactant systems are identified in

**Table 10.** The CA and IFT measurements of these systems have already been determined as detailed in the previous sections. Hence, the capillary pressure ( $P_c$ ) can be estimated using the Young-Laplace equation (**Eq 2-3**). However, this equation requires knowledge of the pore radius ( $r$ ) value of the rock sample, which is tedious to estimate. Hence, the results are presented in  $P_c / r$ , where the denominator is the unknown radius.

Tag	Surfactant System	Blend Ratio	Concentration wt. %	Brine Solution	ITL (°F)
S0	None			A	N/A
S1	C-1		0.2	2D	324
S2	C-2:Z-1	1:3	0.2	A	300
S3		1:3	0.4	A	355
S4		2:3	0.4	A	333
S5		1:3	0.2	1D	320
S6		1:3	0.2	2D	>350

**Table 10: Selected surfactant systems for SASI investigation. Systems will be referenced by their tags.**

**Figure 61** displays  $P_c / r$  results against temperature for the base case as well as the selected surfactant systems. The base case shows negative  $P_c$  values for the range of temperatures evaluated. The  $P_c$  of the base case is shown to increase as the temperature was increased. This change in  $P_c$  resulted from the reduction in the IFT of the base case with temperature, as shown in **Figure 51**. These negative capillary pressure values are

unfavorable for imbibition, and limited oil recovery is expected in this case. When surfactants are present, the capillary pressure of the system shifts to positive. The higher capillary pressure is more favorable for recovery because spontaneous imbibition is primarily driven by capillary forces.

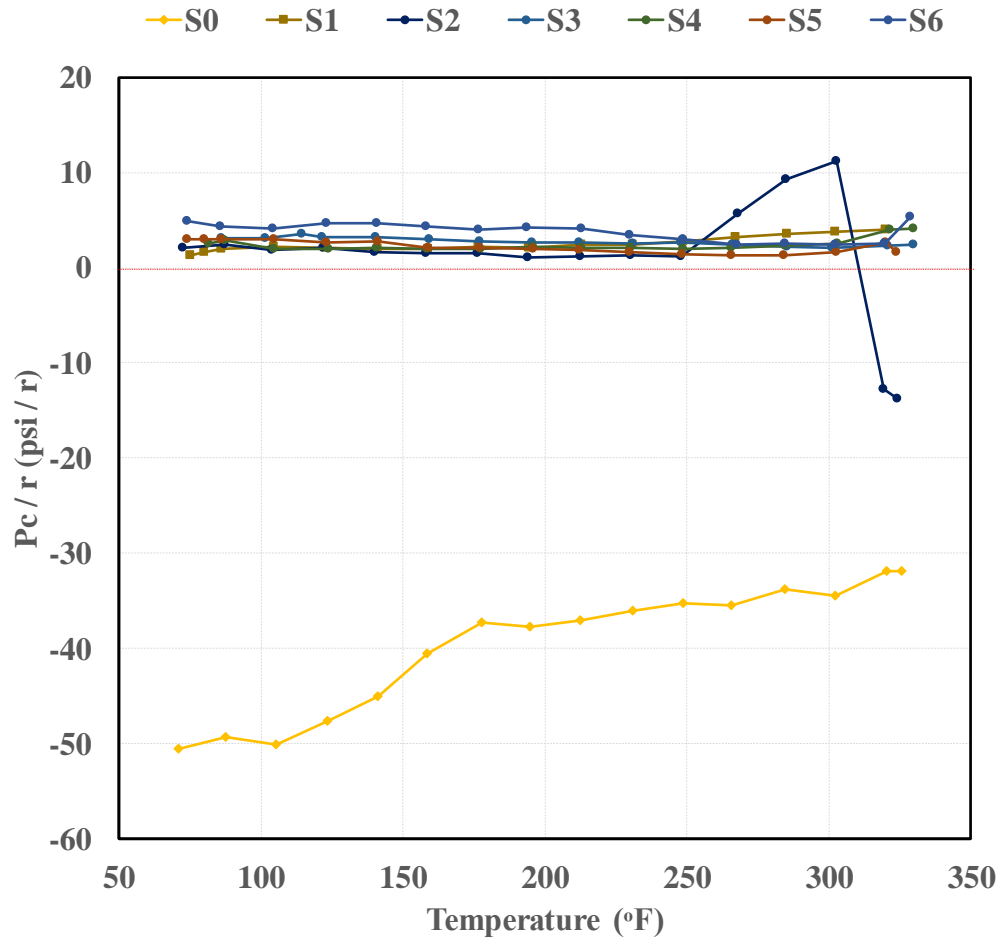


**Figure 61:  $P_c/r$  results for the selected surfactant systems.**

## 6.2 Oil recovery from SASI experiments

In order to determine the recovery factor, the volume of oil in place before the SASI experiment (OOIP) and the volume of oil produced during the SASI experiment

must be known. The OOIP was determined for the different cores from the mass difference of the core sample before and after aging and the oil density. The details on the core dimensions data and their OOIP after saturation are shown in **Table 11**. The OOIP differed for the core samples evaluated as a result of variation in porosity and mineralogy across the Eagle Ford depth, which impacts the oil saturation. An average OOIP value for the core samples evaluated is 2.80cc.

Core Sample	Diameter (in)	Length (in)	Bulk Volume (cc)	m_AC (g)	m_AA (g)	Oil Density (g/cc)	OOIP (cc)
Q0	0.985	1.970	24.547	56.004	58.363	0.779	3.029
Q1	0.946	2.049	23.527	60.115	61.752	0.779	2.102
Q2	1.024	2.167	29.205	63.505	66.417	0.779	3.739
Q3	0.985	1.891	23.565	54.595	56.843	0.779	2.879
Q4	0.985	2.049	25.529	59.170	60.974	0.779	2.316
Q5	0.985	2.916	25.275	62.994	65.329	0.779	2.998
Q6	1.024	2.049	27.612	60.334	62.229	0.779	2.433

**Table 11: Data on core samples used in SASI experiments. (m\_AC = mass of core after cleaning, m\_AA = Mass of core sample after aging).**

The fluid systems detailed in

**Table 10** were investigated by SASI analysis using the core samples in **Table 11**.

The pairing of fluid systems and the core sample used in SASI analysis are shown in **Table 12**.



	Core Sample	Fluid System
1	Q0	S0
2	Q1	S1
3	Q2	S2
4	Q3	S3
5	Q4	S4
6	Q5	S5
7	Q6	S6

**Table 12: Core Samples and Fluid Systems used in SASI analysis.**

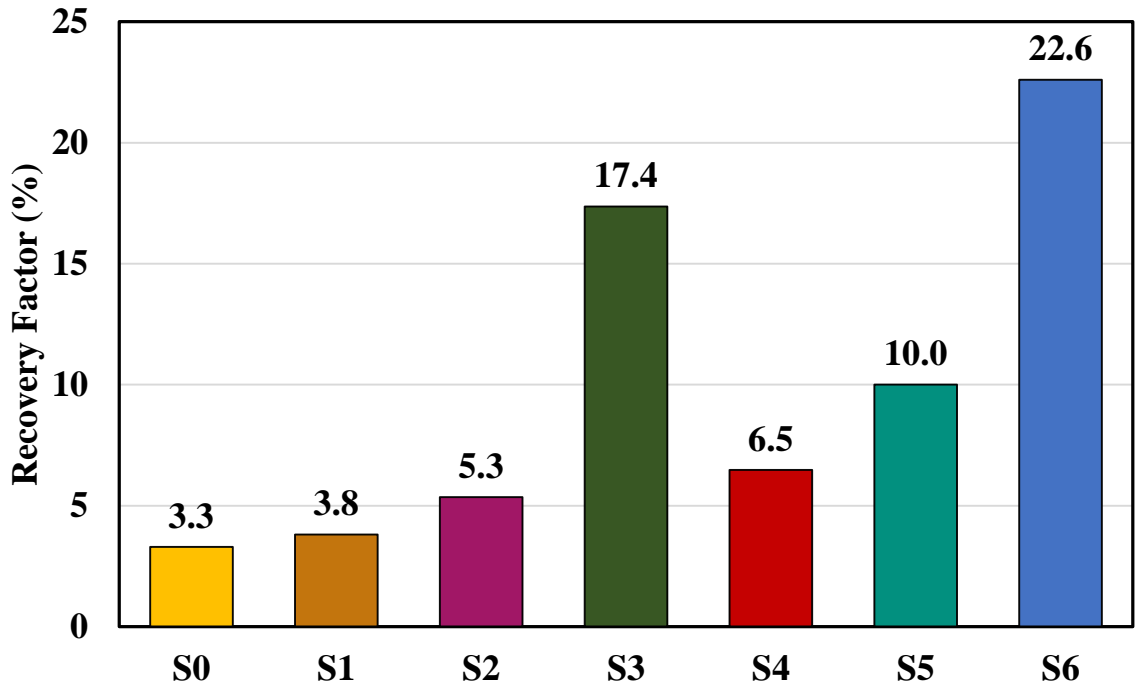


**Figure 62: Oil recovery factors for the different surfactant systems after the SASI experiments.**

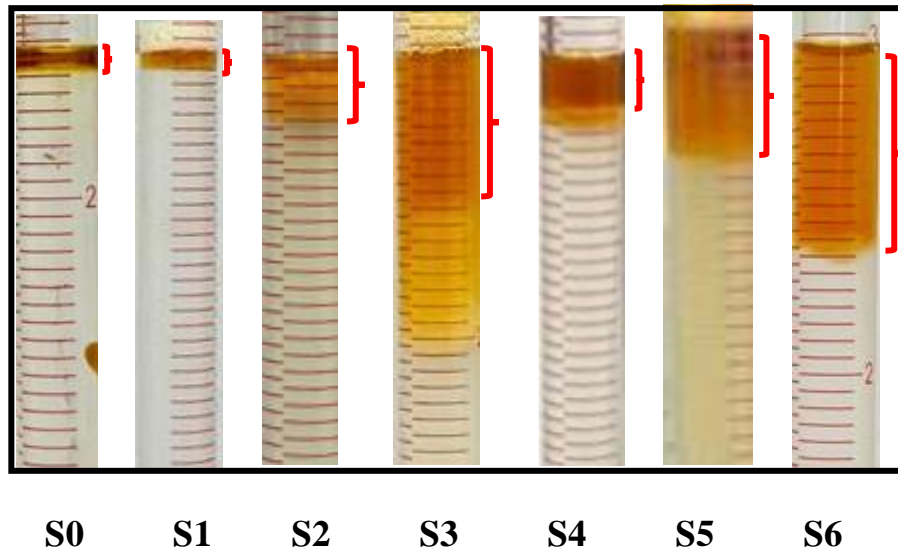


**Figure 63: Images of produced oil volume for the different surfactant systems at the end of 192h.**

The recovery factors and images of the produced oil volumes for the surfactant systems evaluated are shown in **Figure 62** and **Figure 63**, respectively. First, oil recovery for the base case without any surfactants (S0) was evaluated. At the end of the 192h time period, system S0 resulted in a 3.3% recovery factor. When surfactant molecules were present in the aqueous phase, the recovery factor was increased. For single surfactant system S1, the recovery factor obtained was 3.8% OOIP. The blend at 0.2 wt.%, i.e., S2, resulted in a recovery of 5.3% OOIP. At a higher concentration of 0.4wt.% for the same blend, i.e., S3, the recovery factor was 17.4 wt.%. Another blend at 0.4 wt.% concentration, i.e., S4, resulted in a recovery factor of 6.5% OOIP.

System S5 (salinity = 1% TDS) recovered 10% OOIP while brine S6 (salinity =2% TDS) recovered 22.6% OOIP. In comparison, surfactant system S2 (salinity = 0.2% TDS) had resulted in 5.3% RF as shown in **Figure 64(a)**. Hence, higher salinity surfactant-brine

systems produced higher recovery factors. This is an expected result since increasing the salinity of the surfactant-brine systems has been shown to result in increased ITLs and produce lower CA values.

The recovery factors produced by the co-surfactant blend systems were higher than that of the single surfactant system (S1) in all cases. At the same surfactant concentration (0.2 wt.%) and brine salinity (2% TDS), the co-surfactant blend case (S6) produced a recovery factor (22.6% OOIP) which was up to six(6) times more than that produced by the single surfactant system (S1, 3.8% OOIP). This is an expected trend since system S1 had produced higher CA values and a lower ITL at the desired temperature of 325°F. The use of co-surfactant systems is most effective for high-temperature applications.

In some cases (S3 and S4), some volume of stable emulsion was produced in addition to the produced oil. These systems can be applied for use in field applications based on their promising results. However, they will require the use of demulsifiers or emulsion breakers.

In summary, the co-surfactant systems resulted in higher RFs compared to the best case single surfactant system evaluated. Also, higher concentration surfactant systems resulted in higher oil recovery compared to the lower concentration surfactant case. Lastly, higher salinity surfactant-brine systems resulted in higher high recovery compared to the lower salinity cases.

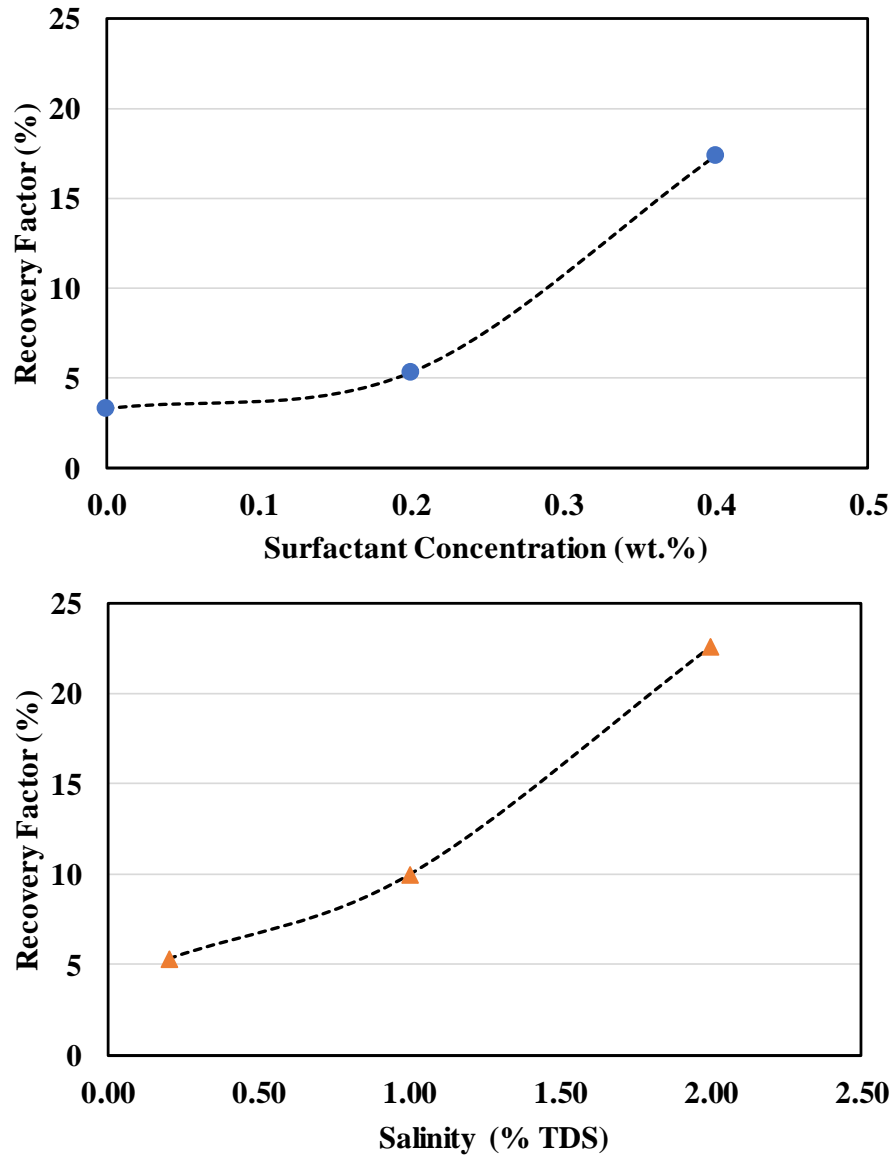


**Figure 64: Effect of (a) surfactant concentration and (b) brine salinity on recovery factor.**

### 6.3 CT Scan Images and Results

The core plugs used in the SASI experiments were scanned before and after the imbibition process using CT scanning. The CT images show the porosity distribution as

well as fluid displacement within the core. Images of a 2D cross-section slice of the core plug are compared at a  $T = 0\text{hr}$  (before experiment began) and at  $T = 192\text{ hr}$  (after experiment was completed). CT number is a function of density, and a higher CT number is indicative of a higher fluid density value. Hence, a higher CT number is correlated with a high water saturation represented with bright color. A lower CT number indicates oil saturation and is represented with darker colors (dark red and red). Hence, a color transition from dark red to green/yellow over time is indicative of an increase in water saturation as the movement of the aqueous fluid into the core plug displaces the oil from the core plug. The CT scans at 0h and 192h are presented in **Figure 65** for four (4) surfactant system cases (S3 and S6). At  $T = 0\text{h}$ , dark red color is observed pre-imbibition, which indicates the oil saturation in the core plug. Post imbibition, at  $T = 192\text{h}$ , a transition to lighter colors is observed. Hence, the CT scans show that oil has been expelled and the aqueous phase imbibed into the plug.

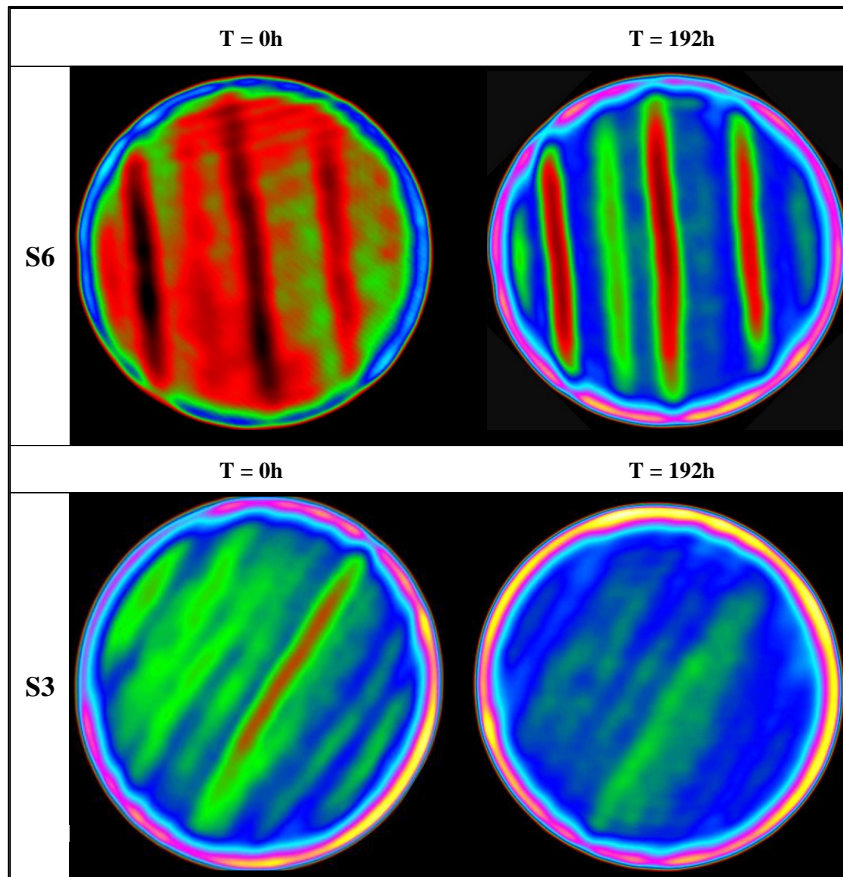


**Figure 65: CT Images of core samples before and after imbibition experiments for different surfactant cases.**

Images generated from the CT scan also provide information on the direction of fluid displacement. CT scans from before and after imbibition scans were subtracted to determine areas of higher density change which indicates areas of increased oil production. The before, after, and subtracted imbibition images of plug Q6 using surfactant system S6 are presented in **Figure 66**. For these slides, the red color represents high CT numbers, while the yellow color is indicative of higher density. In the ‘subtracted’ slides, the blue color represents areas of markedly lower change in density before and after

the imbibition experiment. It is observed that the core plug is heterogeneous and has small bedding planes. The bands in the image have higher porosity and permeability. Over the course of the experiment, the aqueous phase is drawn in from the rock matrix into the higher porosity, higher permeability bands. It is assumed that imbibition occurs in the tighter rock, thereby forcing oil into the higher conductive flow paths represented by the bands. This would be consistent with capillary pressure being greater in the smaller pore throats. Secondly, it is observed that there is a greater density contrast at one face of the rock compared to the other face. It appears that the aqueous phase is being imbibed or drawn in from one face of the rock, and consequently, the oil in place is expelled through the other face. This indicates that a co-current flow has occurred in this case.

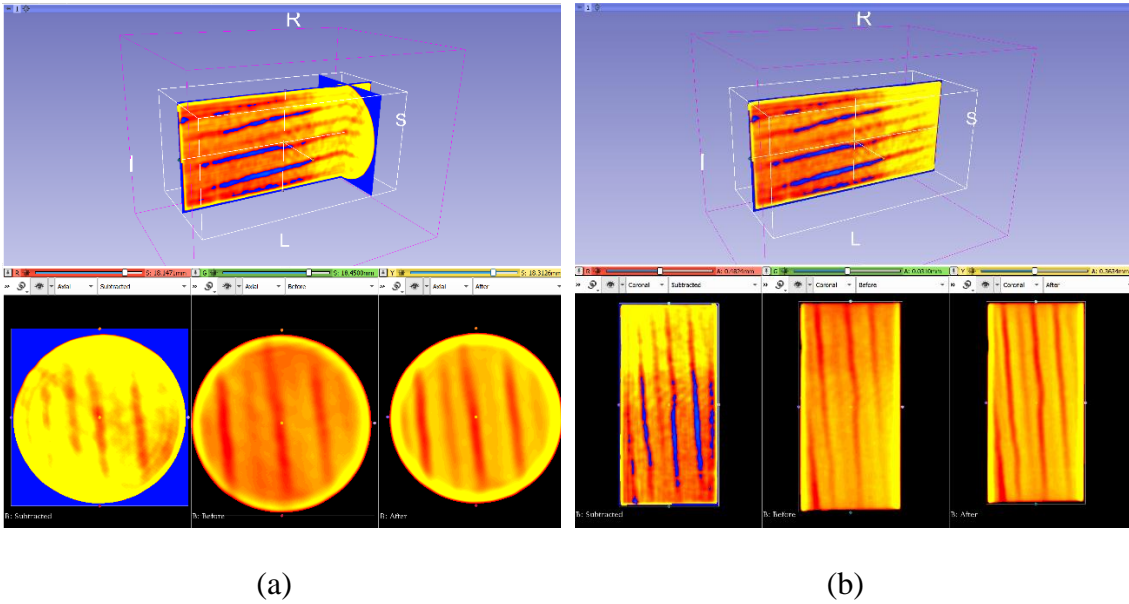


**Figure 66: Subtracted, Before, and After Imbibition scans presented for (a) 2D slice across core diameter (b) 2D slice across core length.**

## 7 CONCLUSIONS

This study provides a complete workflow for surfactant selection for high-temperature EOR applications and presents guidelines for designing surfactant systems for high-temperature conditions. The workflow consisted of investigating single surfactant systems and novel co-surfactant systems by; a) surfactant screening at LPT and HPHT conditions, b) spontaneous imbibition experiments. A summary of the conclusions drawn from this study is presented below:

1. The initial wettability of the Eagle Ford rock sample was determined by CA measurements to be oil-wet. Some anionic and cationic surfactants (A-1, A-2, A-3, C-4, and C-5) were effective in altering the rock wettability from initial oil-wet conditions to favorable water-wet conditions at low temperatures.
2. Solubility is a more critical issue for ionic surfactants compared to nonionic surfactants due to interactions between their charged heads and the charged salt ions in the aqueous phase. Surfactant solubility is affected by the degree of salinity of the aqueous phase and the types of ions present.
3. Time stability results showed that the effectiveness of ionic surfactants in altering wettability was reduced over time. Initially, surfactants are able to alter wettability to water-wet conditions. However, over time, there is an increase in the contact angle, and the system becomes intermediate- to oil-wet. This behavior is a result of the increasing surfactant solubility over time.



4. Temperature has a significant effect on surfactant behavior. Ionic surfactants have a temperature limit (ITL) above which they become ineffective in altering wettability. This behavior is driven by the increase in the solubility of the surfactant molecules in the bulk phase as the temperature is increased. This causes the surfactant molecules to be re-dissolved in the aqueous phase as opposed to partitioning preferentially at the crude oil/rock/brine interface, where they will be effective in altering wettability.
5. Single ionic surfactants showed potential in altering wettability at low-temperature conditions. However, the effectiveness of the ionic surfactant systems is limited at higher temperatures. There exists an inflection temperature (the ITL) above which the ionic surfactant becomes ineffective in altering the wettability favorably.
6. Anionic surfactants are known to have a high sensitivity to temperature. In this study, they produced very low ITL values and were less effective at increased temperatures compared to cationic surfactants. The anionic surfactants also showed less time stability. The solubility of the anionic surfactants was determined to be greater than that of the other ionic surfactants evaluated.
7. The effectiveness of surfactants at high-temperature conditions cannot be extrapolated from or predicted based on surfactant effectiveness at low-temperature conditions.
8. It was determined that the use of higher concentration surfactant systems was more effective for high-temperature applications. A higher surfactant concentration increases the ionic saturation of the aqueous phase, which reduces the solubility of

the surfactant molecules. When the saturation of the aqueous phase is increased, fewer surfactant molecules are able to re-dissolve into solution, thereby ensuring that a higher number of surfactant molecules are present at the crude oil/brine/rock interface to alter wettability.

9. Higher salinity brines (~2% TDS) for ionic surfactant systems are more effective in altering wettability at high temperatures. The presence of a significant amount of salt ions increases the aqueous phase saturation, which reduces the solubility of surfactant molecules and ensures their effectiveness at high-temperature conditions.
10. Synergism was observed with blends of cationic and zwitterionic surfactants. These co-surfactant systems were effective in altering wettability favorably, outperforming the single surfactant systems in some cases.
11. Co-surfactant systems improved the surfactant properties by reducing their solubility at high temperatures, making them more effective for high-temperature applications. The co-surfactants systems were effective in altering wettability favorably up to a temperature of 355°F.
12. The presence of surfactant molecules resulted in a reduction in IFT of the crude oil/aqueous phase system, especially at low temperatures. At increased temperatures, surfactant ability to lower IFT was greatly reduced as a result of the increased solubility of the surfactant system in the aqueous phase.
13. Higher concentration surfactant systems produced lower IFT values at high-temperature conditions. Also, higher salinity brine systems resulted in lower IFT

values at high-temperature conditions. These are a result of the reduced solubility of the surfactant molecules at these conditions.

14. Spontaneous imbibition experiments showed that the base case without surfactants produced a low recovery factor of 3.3% OOIP. The presence of surfactants resulted in increased recovery factors up to 22.6% OOIP.
15. Higher concentration surfactant systems resulted in higher recovery factors. Also, higher salinity surfactant-brine systems resulted in higher recovery factors. These are expected trends since increasing the surfactant concentration, and the salinity of the aqueous phase results in increased ITLs and produces lower CA values.
16. Co-surfactant systems resulted in higher recovery factors compared to the single surfactant system evaluated.
17. Surfactant systems were successfully designed for high-temperature shale EOR applications. This unlocks great potential for improving oil recovery in high-temperature liquid-rich unconventional reservoirs.

## REFERENCES

- Adel, I. A., Tovar, F. D., Zhang, F., & Schechter, D. S. (2018). The Impact of MMP on Recovery Factor During CO<sub>2</sub> EOR in Unconventional Liquid Reservoirs. Paper presented at the *SPE Annual Technical Conference and Exhibition*. One Petro.
- Adibhatla, B., & Mohanty, K. K. (2008). Oil Recovery From Fractured Carbonates by Surfactant-Aided Gravity Drainage: Laboratory Experiments and Mechanistic Simulations. *SPE Reservoir Evaluation & Engineering*, 11(01), 119-130. 10.2118/99773-PA.
- Alameri, W., Teklu, T. W., Graves, R. M., Kazemi, H., & AlSumaiti, A. M. (2014). *Wettability Alteration During Low-Salinity Waterflooding in Carbonate Reservoir Cores*. Adelaide, Australia: Society of Petroleum Engineers.10.2118/171529-MS Retrieved from <https://doi.org/10.2118/171529-MS>.
- Alfarge, D., Wei, M., & Bai, B. (2017). IOR methods in unconventional reservoirs of North America: comprehensive review. Paper presented at the *SPE Western Regional Meeting*. One Petro.
- Alhashim, H. W., Zhang, F., Schechter, D. S., & Chen, J. (2019). Investigation of the Effect of Pore Size Distribution on the Produced Oil from Surfactant-Assisted Spontaneous Imbibition in ULRs. Paper presented at the *SPE Annual Technical Conference and Exhibition*. One Petro.

- Alotaibi, M. B., Azmy, R., & Nasr-El-Din, H. A. (2010). Wettability challenges in carbonate reservoirs. Paper presented at the *SPE Improved Oil Recovery Symposium*. One Petro.
- AlShaikh, M., & Mahadevan, J. (2016). Impact of Brine Composition on Calcite Wettability: A Sensitivity Study. *SPE Journal*, 21(04), 1214-1226. 10.2118/172187-PA.
- Alvarez, J. O., Saputra, I. W. R., & Schechter, D. S. (2017). *The Impact of Surfactant Imbibition and Adsorption for Improving Oil Recovery in the Wolfcamp and Eagle Ford Reservoirs*. San Antonio, Texas, USA: Society of Petroleum Engineers.10.2118/187176-MS Retrieved from <https://doi.org/10.2118/187176-MS>.
- Alvarez, J. O., & Schechter, D. S. (2017). Wettability Alteration and Spontaneous Imbibition in Unconventional Liquid Reservoirs by Surfactant Additives. *SPE Reservoir Evaluation & Engineering*, 20(01), 107-117. 10.2118/177057-PA.
- Anderson, W. (1986). Wettability Literature Survey- Part 2: Wettability Measurement. *Journal of Petroleum Technology*, 38(11), 1246-1262. 10.2118/13933-PA.
- Anderson, W. G. (1986). Wettability Literature Survey- Part 1: Rock/Oil/Brine Interactions and the Effects of Core Handling on Wettability. *Journal of Petroleum Technology*, 38(10), 1125-1144. 10.2118/13932-PA.
- Austad, T., Matre, B., Milter, J., Saevareid, A., & Øyno, L. (1998). Chemical flooding of oil reservoirs 8. Spontaneous oil expulsion from oil-and water-wet low permeable chalk material by imbibition of aqueous surfactant solutions. *Colloids and Surfaces A: Physicochemical and Engineering Aspects*, 137(1-3), 117-129.

- Austad, T., & Milter, J. (1997). Spontaneous imbibition of water into low permeable chalk at different wettabilities using surfactants. Paper presented at the *International Symposium on Oilfield Chemistry*. One Petro.
- Babadagli, T., Al-Bemani, A., & Boukadi, F. (1999). *Analysis of Capillary Imbibition Recovery Considering the Simultaneous Effects of Gravity, Low IFT, and Boundary Conditions*. Kuala Lumpur, Malaysia: Society of Petroleum Engineers.10.2118/57321-MS Retrieved from <https://doi.org/10.2118/57321-MS>.
- Belhaj, A. F., Shuhli, J. A. B., Elraies, K. A., Mahmood, S. M., Maulianda, B., & Alnarabiji, M. S. (2020). Partitioning behavior of novel surfactant mixture for high reservoir temperature and high salinity conditions. *Energy*, *198*, 117319.
- Clark, A. J. (2009). Determination of recovery factor in the Bakken formation, Mountrail County, ND. Paper presented at the *SPE Annual Technical Conference and Exhibition*. One Petro.
- CRAIG, F. (1971). The reservoir engineering aspects of waterflooding. *Monograph Series, Society of Petroleum Engineers of AIME*.
- Cuiec, L. E., Bourbiaux, B., & Kalaydjian, F. (1990). Imbibition in low-permeability porous media: understanding and improvement of oil recovery. *Spe/Doe*, *20259*, 833-846.
- Das, S., Nguyen, Q., Patil, P. D., Yu, W., & Bonnecaze, R. T. (2018). Wettability alteration of calcite by nonionic surfactants. *Langmuir*, *34*(36), 10650-10658.

- Donaldson, E. C., Thomas, R. D., & Lorenz, P. B. (1969). Wettability Determination and Its Effect on Recovery Efficiency. *Society of Petroleum Engineers Journal*, 9(01), 13-20. 10.2118/2338-PA.
- Felix, U., Ayodele, T. O., & Olalekan, O. (2015). Surfactant-Polymer Flooding Schemes (A Comparative Analysis). Paper presented at the *SPE Nigeria Annual International Conference and Exhibition*. One Petro.
- Feng, L., & Xu, L. (2015). Implications of shale oil compositions on surfactant efficacy for wettability alteration. Paper presented at the *SPE Middle East Unconventional Resources Conference and Exhibition*. One Petro.
- Gamadi, T. D., Sheng, J. J., Soliman, M. Y., Menouar, H., Watson, M. C., & Emadibaladehi, H. (2014). An experimental study of cyclic CO<sub>2</sub> injection to improve shale oil recovery. Paper presented at the *SPE Improved Oil Recovery Symposium*. One Petro.
- Griffin, W. C. (1954). Calculation of HLB values of non-ionic surfactants. *J.Soc.Cosmet.Chem.*, 5, 249-256.
- Gu, T., & Sjöblom, J. (1992). Surfactant structure and its relation to the Krafft point, cloud point and micellization: some empirical relationships. *Colloids and Surfaces*, 64(1), 39-46.

- Gupta, R., & Mohanty, K. K. (2007). Temperature effects on surfactant-aided imbibition into fractured carbonates. Paper presented at the *SPE Annual Technical Conference and Exhibition*, One Petro.
- Gupta, R., & Mohanty, K. K. (2008). *Wettability Alteration of Fractured Carbonate Reservoirs*. Tulsa, Oklahoma, USA: Society of Petroleum Engineers.10.2118/113407-MS Retrieved from <https://doi.org/10.2118/113407-MS>.
- Hammond, P. S., & Unsal, E. (2009). Spontaneous and forced imbibition of aqueous wettability altering surfactant solution into an initially oil-wet capillary. *Langmuir*, 25(21), 12591-12603.
- Hammond, P. S., & Unsal, E. (2011). Spontaneous imbibition of surfactant solution into an oil-wet capillary: wettability restoration by surfactant– contaminant complexation. *Langmuir*, 27(8), 4412-4429.
- Hirasaki, G., & Zhang, D. L. (2004). Surface Chemistry of Oil Recovery From Fractured, Oil-Wet, Carbonate Formations. *SPE Journal*, 9(02), 151-162. 10.2118/88365-PA.
- Hocine, S., Cuenca, A., Magnan, A., Tay, A., & Moreau, P. (2016). An Extensive Study of the Thermal Stability of Anionic Chemical EOR Surfactants-Part 1 Stability in Aqueous Solutions. Paper presented at the *International Petroleum Technology Conference*. One Petro.
- Huibers, P. D., Shah, D. O., & Katritzky, A. R. (1997). Predicting surfactant cloud point from molecular structure. *Journal of Colloid and Interface Science*, 193(1), 132-136.



- Khalil, R. A., & Saadon, F. A. (2015). Effect of presence of benzene ring in surfactant hydrophobic chain on the transformation towards one dimensional aggregate. *Journal of Saudi Chemical Society*, 19(4), 423-428.
- Kiani, S., Rogers, S. E., Sagisaka, M., Alexander, S., & Barron, A. R. (2019). A New Class of Low Surface Energy Anionic Surfactant for Enhanced Oil Recovery. *Energy & Fuels*, 33(4), 3162-3175.
- Kumar, K., Dao, E. K., & Mohanty, K. K. (2008). Atomic force microscopy study of wettability alteration by surfactants. *Spe Journal*, 13(02), 137-145.
- Kumari, R., Kakati, A., Nagarajan, R., & Sangwai, J. S. (2018). Synergistic effect of mixed anionic and cationic surfactant systems on the interfacial tension of crude oil-water and enhanced oil recovery. *Journal of Dispersion Science and Technology*.
- Kurnia, I., Zhang, G., Han, X., & Yu, J. (2020). Zwitterionic-anionic surfactant mixture for chemical enhanced oil recovery without alkali. *Fuel*, 259, 116236.
- Leverett, M. C. (1939). Flow of oil-water mixtures through unconsolidated sands. *Transactions of the AIME*, 132(01), 149-171.
- Li, Y., Zhang, W., Kong, B., Puerto, M., Bao, X., Sha, O., . . . Gu, S. (2016). Mixtures of anionic/cationic surfactants: a new approach for enhanced oil recovery in low-salinity, high-temperature sandstone reservoir. *SPE Journal*, 21(04), 1,164-1,177.

- Li, Y., Zhang, W., Shen, Z., Jin, J., Su, Z., Yao, F., . . . Wu, X. (2020). Pilot Test of Surfactant-Polymer Flood with Mixtures of Anionic-Cationic Surfactants for High Temperature Low Permeability Sandstone Reservoir. Paper presented at the *SPE Improved Oil Recovery Conference*. OnePetro.
- Lindsay, G., Miller, G., Xu, T., Shan, D., & Baihly, J. (2018). Production performance of infill horizontal wells vs. pre-existing wells in the major US unconventional basins. Paper presented at the *SPE Hydraulic Fracturing Technology Conference and Exhibition*. OnePetro.
- Manrique, E. J., Thomas, C. P., Ravikiran, R., Izadi Kamouei, M., Lantz, M., Romero, J. L., & Alvarado, V. (2010). EOR: current status and opportunities. Paper presented at the *SPE Improved Oil Recovery Symposium*. OnePetro.
- Mattax, C. C., & Kyte, J. R. (1962). Imbibition oil recovery from fractured, water-drive reservoir. *Society of Petroleum Engineers Journal*, 2(02), 177-184.
- Menouar, H., & Knapp, R. M. (1980). Numerical simulation of the imbibition process in fractured reservoirs. Paper presented at the *SPE Annual Technical Conference and Exhibition*. OnePetro.
- Mohanty, K. K., & Chandrasekhar, S. (2013). *Wettability Alteration with Brine Composition in High Temperature Carbonate Reservoirs*. New Orleans, Louisiana, USA: Society of Petroleum Engineers.10.2118/166280-MS.

- Morrow, N. R., & Mason, G. (2001). Recovery of oil by spontaneous imbibition. *Current Opinion in Colloid & Interface Science*, 6(4), 321-337.
- Morsy, S., Sheng, J. J., & Soliman, M. Y. (2013). Waterflooding in the Eagle Ford Shale Formation: Experimental and Simulation Study. Paper presented at the *SPE Unconventional Resources Conference and Exhibition-Asia Pacific*. OnePetro.
- Nakama, Y. (2017). Surfactants. *Cosmetic Science and Technology* (pp. 231-244) Elsevier.
- Nguyen, D., Wang, D., Oladapo, A., Zhang, J., Sickorez, J., Butler, R., & Mueller, B. (2014). *Evaluation of Surfactants for Oil Recovery Potential in Shale Reservoirs*. Tulsa, Oklahoma, USA: Society of Petroleum Engineers. 10.2118/169085-MS Retrieved from <https://doi.org/10.2118/169085-MS>.
- Pinnawala, G., Nizamidin, N., Spilker, K., Linnemeyer, H., Malik, T., & Dwarakanath, V. (2020). Development of Surfactant Formulation for Harsh Environment. Paper presented at the *SPE Improved Oil Recovery Conference*. OnePetro.
- Rosen, M. J. (1989). Selection of surfactant pairs for optimization of interfacial properties. *Journal of the American Oil Chemists' Society*, 66(12), 1840-1843.
- Rosen, M. J. (1991). Synergism in mixtures containing zwitterionic surfactants. *Langmuir*, 7(5), 885-888.

- Rosen, M. J., & Kunjappu, J. T. (2012). *Surfactants and interfacial phenomena* John Wiley & Sons.
- Saxena, N., Kumar, A., & Mandal, A. (2019). Adsorption analysis of natural anionic surfactant for enhanced oil recovery: The role of mineralogy, salinity, alkalinity and nanoparticles. *Journal of Petroleum Science and Engineering*, 173, 1264-1283.
- Schechter, D. S., Zhou, D., & Orr Jr, F. M. (1994). Low IFT drainage and imbibition. *Journal of Petroleum Science and Engineering*, 11(4), 283-300.
- Schott, H. (2003). A linear relation between the cloud point and the number of oxyethylene units of water-soluble nonionic surfactants valid for the entire range of ethoxylation. *Journal of Colloid and Interface Science*, 260(1), 219-224.
- Seethepalli, A., Adibhatla, B., & Mohanty, K. K. (2004). Physicochemical interactions during surfactant flooding of fractured carbonate reservoirs. *SPE Journal*, 9(04), 411-418.
- Sharma, G., & Mohanty, K. (2013). Wettability Alteration in High-Temperature and High-Salinity Carbonate Reservoirs. *SPE Journal*, 18(04), 646-655. 10.2118/147306-PA.
- Sheng, J. J. (2011). Chapter 7-Surfactant Flooding. *Modern Chemical Enhanced Oil Recovery*. Gulf Professional Publishing, Boston, , 239-335.

Shubham, A., Martavaltzi, C., Dakik, A. R., & Gupta, A. (2012). *Wettability Alteration of Carbonates by Optimizing the Brine and Surfactant Composition*. Kuwait City, Kuwait: Society of Petroleum Engineers.10.2118/163348-MS Retrieved from <https://doi.org/10.2118/163348-MS>.

Singh, R., & Miller, J. (2021). Synergistic Surfactant Blends for Wettability Alteration in Wolfcamp and Eagle Ford Shale for Improved Oil Recovery. Paper presented at the *SPE Western Regional Meeting*. OnePetro.

Somasundaran, P., & Fuerstenau, D. W. (1973). Heat and entropy of adsorption and association of long-chain surfactants at the alumina-aqueous solution interface. *Transactions*, 254.

Somasundaran, P., & Zhang, L. (2006). Adsorption of surfactants on minerals for wettability control in improved oil recovery processes. *Journal of Petroleum Science and Engineering*, 52(1-4), 198-212.

Standnes, D. C., & Austad, T. (2000). Wettability alteration in chalk: 1. Preparation of core material and oil properties. *Journal of Petroleum Science and Engineering*, 28(3), 111-121.

Standnes, D. C., & Austad, T. (2000b). Wettability alteration in chalk: 2. Mechanism for wettability alteration from oil-wet to water-wet using surfactants. *Journal of Petroleum Science and Engineering*, 28(3), 123-143.

- Standnes, D. C., & Austad, T. (2003a). Nontoxic low-cost amines as wettability alteration chemicals in carbonates. *Journal of Petroleum Science and Engineering*, 39(3-4), 431-446.
- Standnes, D. C., & Austad, T. (2003b). Wettability alteration in carbonates: Interaction between cationic surfactant and carboxylates as a key factor in wettability alteration from oil-wet to water-wet conditions. *Colloids and Surfaces A: Physicochemical and Engineering Aspects*, 216(1-3), 243-259.
- Strand, S., Høgnesen, E. J., & Austad, T. (2006). Wettability alteration of carbonates—Effects of potential determining ions (Ca<sup>2+</sup> and SO<sub>4</sub><sup>2-</sup>) and temperature. *Colloids and Surfaces A: Physicochemical and Engineering Aspects*, 275(1-3), 1-10.
- Szlendak, S. M., Nguyen, N. M., & Nguyen, Q. P. (2013). Laboratory investigation of low-tension-gas flooding for improved oil recovery in tight formations. *SPE Journal*, 18(05), 851-866.
- Teklu, T. W., Li, X., Zhou, Z., Alharthy, N., Wang, L., & Abass, H. (2018). Low-salinity water and surfactants for hydraulic fracturing and EOR of shales. *Journal of Petroleum Science and Engineering*, 162, 367-377.
- Todd, H. B., & Evans, J. G. (2016). Improved oil recovery IOR pilot projects in the Bakken formation. Paper presented at the *SPE Low Perm Symposium*. OnePetro.
- US Energy Information Administration. (2018). US Crude Oil and Natural Gas Proved Reserves, Year-end 2018.

- Wang, D., Butler, R., Liu, H., & Ahmed, S. (2011). Flow-rate behavior and imbibition in shale. *SPE Reservoir Evaluation & Engineering*, 14(04), 485-492.
- Wang, D., Butler, R., Zhang, J., & Seright, R. (2012). Wettability survey in Bakken shale with surfactant-formulation imbibition. *SPE Reservoir Evaluation & Engineering*, 15(06), 695-705.
- Wang, D., Zhang, J., & Butler, R. (2015). Scaling Laboratory Data Surfactant Imbibition Rates to the Field in Fractured Shale Formations. Unconventional Resources Technology Conference (URTEC).
- Xiao, Z., Dexin, L., Yue, L., Lulu, L., & Jie, Y. (2021). Synergistic Effects between Anionic and Amphoteric Surfactants on Promoting Spontaneous Imbibition in ultra-low permeability reservoirs: Study of Mechanism and Formula Construction. *Colloids and Surfaces A: Physicochemical and Engineering Aspects*, 126930.
- Xie, X., Weiss, W. W., Tong, Z. J., & Morrow, N. R. (2005). Improved oil recovery from carbonate reservoirs by chemical stimulation. *SPE Journal*, 10(03), 276-285.
- Zeng, T., Miller, C., S., & Mohanty, K. (2018). *Application of Surfactants in Shale Chemical EOR at High Temperatures*. Tulsa, Oklahoma, USA: Society of Petroleum Engineers.10.2118/190318-MS Retrieved from <https://doi.org/10.2118/190318-MS>.

- Zhang, D. L., Liu, S., Puerto, M., Miller, C. A., & Hirasaki, G. J. (2006). Wettability alteration and spontaneous imbibition in oil-wet carbonate formations. *Journal of Petroleum Science and Engineering*, 52(1-4), 213-226.
- Zhang, F., Saputra, I. W. R., Adel, I. A., & Schechter, D. S. (2018). Scaling for wettability alteration induced by the addition of surfactants in completion fluids: surfactant selection for optimum performance. Paper presented at the *Unconventional Resources Technology Conference, Houston, Texas, 23-25 July 2018*, 971-987.
- Zhang, K. (2016). Experimental and numerical investigation of oil recovery from Bakken formation by miscible CO<sub>2</sub> injection. Paper presented at the *SPE Annual Technical Conference and Exhibition*. OnePetro.
- Zhang, P., & Austad, T. (2005). *The Relative Effects of Acid Number and Temperature on Chalk Wettability*. The Woodlands, Texas: Society of Petroleum Engineers.10.2118/92999-MS Retrieved from <https://doi.org/10.2118/92999-MS>.
- Zhong, Q., Zhou, Z., Zhang, Q., Ma, D., Luan, H., Zhang, L., . . . Zhang, L. (2018). Studies on interfacial tensions of ionic surfactant and alkyl sulfobetaine mixed solutions. *Energy & Fuels*, 32(8), 8202-8209.
- Ziegler, V. M., & Handy, L. L. (1981). Effect of temperature on surfactant adsorption in porous media. *Society of Petroleum Engineers Journal*, 21(02), 218-228.